

CA 906A

Spatial and Temporal Variability of some Meteorological Parameters over Tropical Indian Ocean

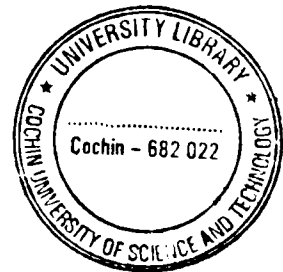
Thesis submitted to the
Cochin University of Science and Technology

In partial fulfillment of the requirement for the Degree of

Doctor of Philosophy
in
Oceanography

By

NIMMI R NAIR

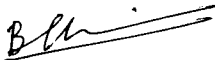


Naval Physical & Oceanographic Laboratory
Defence Research and Development Organisation
Ministry of Defence, Government of India
Thrikkakara, Kochi-682021

CERTIFICATE

This is to certify that the thesis entitled '*Spatial and Temporal Variability of some Meteorological Parameters over Tropical Indian Ocean*' is a bonafide record of research work done by Smt. Nimmi R Nair, Scientist, Naval Physical & Oceanographic Laboratory. She carried out the study reported in this thesis independently under our supervision. We also certify that the subject matter of the thesis has not formed the basis for the award of any degree or diploma of any University or Institution.

Certified that Smt Nimmi R. Nair has passed the Ph.D qualifying examination conducted by the Cochin University of Science and Technology in May 2002.



Basil Mathew

(Supervising guides)



K Mohankumar

Cochin

08 November 2004

PREFACE

The monsoon and the seasonal reversal of winds over Indian Ocean differentiate it from other oceans. A number of unique features make the Indian Ocean Monsoon (IOM) the most intense in the world. Hence a detailed knowledge of the spatial and temporal variability of the atmospheric and oceanic parameters is needed to understand and model the unique features in the Indian Ocean.

Associated with the monsoons, the surface meteorological parameters exhibit different scales of variability in the spatial and temporal domains. Because of the lack of proper data for a long period covering full Indian Ocean, not much work has been reported about the spatio-temporal variability over long time scale. In this study, an attempt has been made to understand the variability using long period data set. The objective of the present study is to understand the spatial and temporal variability of sea surface temperature (SST), precipitable water, zonal and meridional components of wind stress over the tropical Indian Ocean to understand the different scales of variability of these features of Indian Ocean. The doctoral thesis consists of 6 chapters.

Chapter 1 is introductory, explaining the unique features of Indian Ocean and the space-time variability of atmospheric and oceanic processes. Different scales of variability observed over Indian Ocean in various studies are also explained. A literature review is carried out on the spatio-temporal variability studies over Indian Ocean and included in this chapter. Significance of the study with the objectives is described here.

Chapter 2 describe the data and the methodology used for the present work. Empirical Orthogonal Function (EOF) and Wavelet analysis techniques are utilised to understand the standing oscillations and multi scale oscillations respectively. These techniques are presented. The study has been carried out over Indian Ocean (40-100⁰E, 25⁰S-25⁰N), covering Arabian Sea, Bay of Bengal, Equatorial Indian Ocean and South Indian Ocean. For the present study, NCEP/NCAR (National Center for Environmental Prediction/National Center for Atmospheric Research) reanalyzed daily fields of sea surface temperature, zonal and meridional surface wind components and precipitable water amount during 1960-1998 are used.

The principle of Empirical Orthogonal Function (EOF) analysis and the methodology used for the analysis of spatial and temporal variance modes are presented in Chapter 3. These EOF modes and the time series of expansion coefficient are computed for SST, wind and precipitable water. The spatial patterns as well as the time series of the dominant modes of these fields' surface meteorologies are included. The results drawn from these studies are presented and discussed in this chapter.

The results obtained from the study using wavelet analysis are included in chapter 4. The time series and results of spectral analysis of SST anomalies are discussed. For the present study Morlet continuous wavelet transform is used. In the 39 year (1960-1998) analysis, small scale variations (< 360 days) are not clearly detected. Hence each 10 year is considered separately to find the small scale variations. The oscillations of Madden-Julian, semi- annual, annual and those related to El Nino -Southern Oscillation (ENSO) are identified. The variations of occurrence with locations are analysed. The results of the wavelet analysis for meridional and zonal wind components and precipitable water are also presented in chapter 4.

Chapter 5 describes the propagation of the disturbance (low frequency) of SST. Longitude-time sections are made at different latitudes to see the propagation characteristics in the studied area. The results are analysed and discussed.

Chapter 6 summarises the major results from this thesis work on the temporal and spatial variability of the surface meteorological parameters. The references quoted are included at the end of the thesis in alphabetical order.

Contents

Chapter 1	Introduction	1
1.1	Introduction	1
1.2	Features of Indian Ocean	2
1.2.1	Somali current	3
1.2.2	Two-gyre system in Arabian Sea	3
1.2.3	Upwelling	3
1.2.3	East Indian current in Bay of Bengal	4
1.2.5	Planetary waves	5
1.2.6	ENSO in Indian Ocean	5
1.3	Scales of variability	6
1.4	Meteorological and oceanographic studies in the near surface fields over Tropical India Ocean	7
1.5	Objectives of the present study	11
Chapter 2	Data and Methodology	13
2.1	Data	14
2.1.1	Errors and resolution in data	15
2.2	Empirical Orthogonal function	16
2.2.1	EOF in Oceanography	16
2.2.2	Methodology	18
2.2.3	Analysis Procedure	18
2.3	Wavelet analysis	19
2.3.1	Wavelet analysis in oceanography	19
2.3.2	Wavelet transform	19
2.3.3	Methodology	20
2.3.4	Comparison of Fourier and wavelet analysis	22
2.3.5	Selection of mother wavelet	23
Chapter 3	Standing Oscillations	24
3.1	Introduction	24
3.2	Domain of study	26
3.3	EOF analysis of Sea surface temperature	26
3.4	EOF analysis of precipitation rate	31
3.5	EOF analysis of zonal wind stress component	35
3.6	EOF analysis of meridional wind stress component	38
3.7	Summary	38

Chapter 4	Time Frequency Analysis	43
4.1	Introduction	43
4.2	Station locations	44
4.3	Results	45
4.3.1	Sea surface temperature	46
4.3.1.1	<i>Time series, spectrum, autocorrelation analysis</i>	46
4.3.1.2	<i>Wavelet analysis of Sea surface temperature anomaly (SSTA)</i>	52
4.3.2	Precipitable water rate	59
4.3.2.1	<i>Time series, correlation coefficient, spectrum analysis</i>	59
4.3.2.2	<i>Wavelet analysis of precipitation rate anomaly (PWTA)</i>	63
4.3.3	Wavelet analysis of zonal wind stress component (UFLA)	65
4.3.4	Wavelet analysis of meridional wind stress component <i>anomaly</i> (VFLA)	68
4.4	Discussion	70
4.5	Conclusion	72
Chapter 5	Propagating Planetary Waves	74
5.1	Planetary waves	75
5.2	Observations of Oceanic planetary waves	76
5.3	Data	77
5.4	Results	79
5.4.1	NCEP/NCAR Sea Surface Temperature	79
5.4.2	TOPEX/POSEIDON Sea Surface Height	85
5.5	Conclusion	86
Chapter 6	Conclusion	87
References		92

Introduction

1.1 Introduction

The Tropical Indian Ocean (TIO) is unique compared to other world oceans. The dynamics of TIO is entirely different from any other oceans due to the changing wind patterns associated with summer and winter monsoon (Hastenrath and Greischer, 1993; Bauer *et al.*, 1991). Because of this and a number of associated processes (for e.g. upwelling, occurrence of warm-pool, summer cooling, monsoon depressions, cyclones etc) the characteristic features of TIO are quite different from the other tropical oceans. Associated with these dynamical processes one can expect large spatial and temporal variability of the meteorological and oceanographic parameters. For example in the Arabian Sea and Bay of Bengal, the sea surface temperature (SST) exhibits well marked bi-modal oscillation over an annual cycle with a warming phase during pre-monsoon onset and post monsoon and a cooling phase during summer and winter (Colborn, 1975). The summer cooling is a unique feature of the northern Indian Ocean compared to other oceans.

Geographically, the Indian Ocean is bounded by Asian subcontinent on the north. The Indian subcontinent divides the northern Indian Ocean into two basins the Arabian Sea and Bay of Bengal. But the physical process of Arabian Sea and Bay of Bengal are seen to be different. Before discussing the scales of variability

over Indian Ocean, let us go through the important features of Indian Ocean that make it unique and the studies on various physical processes over these regions.

1.2 Features of Indian Ocean

The TIO comprises of the Arabian Sea, Bay of Bengal and South Indian Ocean. The Arabian Sea is known for the intense annually reversing monsoon winds and high evaporation whereas Bay of Bengal for monsoon winds and for its cyclone genesis and large freshwater influx.

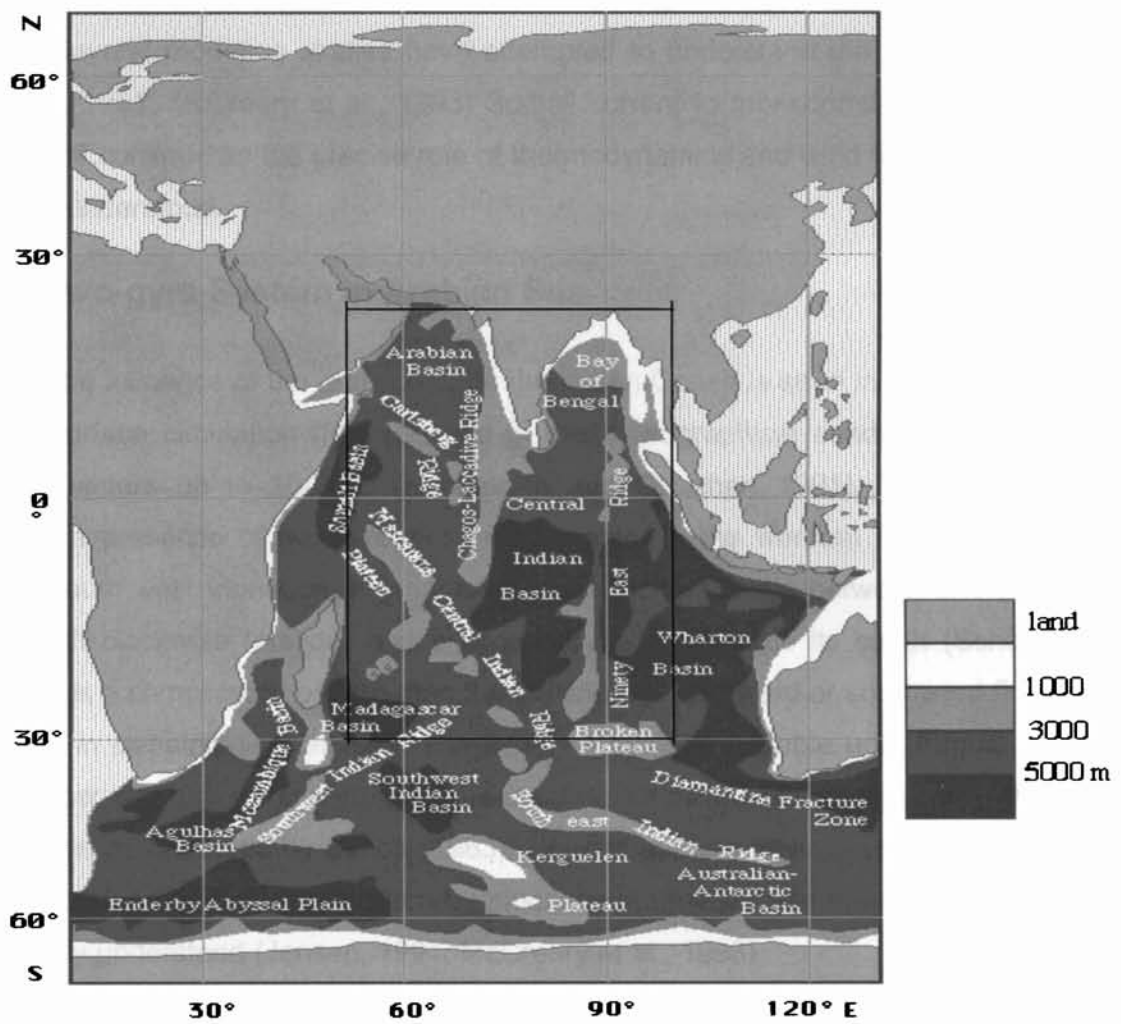


Fig 1.1 Indian Ocean – Area selected for the study

The Indian Ocean is unique with the mean wind stress change from easterly to westerly along the equator while the annual Ekman transport are ploeward on both sides of the equator (Godfrey et al., 1995). Even though the Ekman transport is less during northeast monsoon than during southwest monsoon, especially south of 10°N , the heat transport south of the Arabian Sea keeps similar amplitude as that of south-west monsoon (Wacongne and Pacanowski, 1996).

1.2.1 Somali Current

Among the western boundary currents Somali Current of Arabian Sea is unique due to its strength and the reversal during monsoon season (Schott, 1983). Several modeling studies have attempted to understand the response of (Jensen, 1991; McCreary et al., 1993) Somali current to monsoonal forcing. But the efforts continue as the precise role of thermodynamics and wind forcing is still not fully understood.

1.2.2 Two-gyre System in Arabian Sea

The influence of the monsoons on the Indian Ocean is seen in the reversal of the surface circulation (Fig 1.2) and in the hydrographical conditions of the surface waters up to $10\text{-}20^{\circ}\text{S}$ (Hastenrath and Greisher, 1991). The studies indicate a presence of two-gyre circulation system in the western Arabian Sea during south west monsoon, a great whirl in the Somali Basin between 5°N and 10°N with clockwise rotation, and a secondary eddy towards its south (Schott, 1997). It is a complicated pattern than the continuous northward or southward flow as seen in climatological atlases. The two-gyre system is stable until August or September when the southern gyre propagates northward and merges with the great whirl as observed by Schott (1983). Several authors have been successful in reproducing this two eddy pattern by modeling but the precise role of variability is not fully understood (Jensen, 1991; McCreary et al., 1993)

1.2.3 Upwelling

Another notable feature is the upwelling (Düing and Leetma, 1980) of cool subsurface waters in the Arabian Sea during the summer monsoon. This lowering of sea surface temperature (SST) during the southwest monsoon of the order of 4-

5° C in Arabian Sea is unique phenomenon compared to other parts of the world ocean where it experience warming in boreal summer. Annual mean heat flux into the Arabian Sea is associated with cooling i.e., decrease in heat content and surface temperature. The ocean circulation, characterized in boreal summer by strong coastal upwelling in the Somali Current region and southeastward Ekman flow in the interior, must therefore play a major role in exporting heat out of the Arabian Sea during the southwest monsoon. It is believed that the determination of this circulation (meridional circulation carries warm surface waters out and cool subsurface into the region) is the major goal in the Indian Ocean research (Mc Creary et al., 1993)

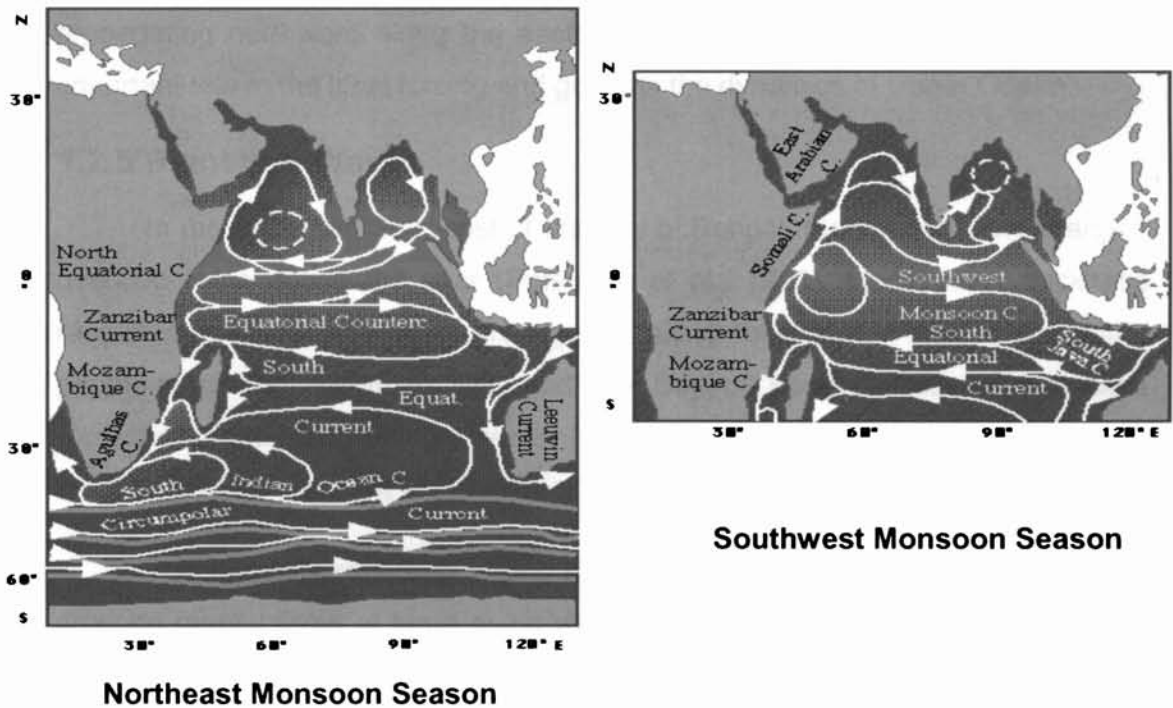


Fig 1.2 Indian Ocean circulation

1.2.4 East India Coastal Current in Bay of Bengal

Over the Bay of Bengal the upwelling occurs in the western coastal boundary upwelling (Legeckis, 1987; Shetye et al., 1996) whereas the classic coastal boundary upwelling regions are along the eastern boundary of the oceans. Like the Somali Current in the Arabian Sea, the East India Coastal Current (EICC) in the Bay of Bengal reverses direction twice a year, flowing northeastward from

February until September with a strong peak in March-April and southeastward from October to January with strongest flow in November. By late October, water from the Equatorial Jet enters the Bay in the east and cyclonic circulation is established. A remarkable feature which is still not understood properly is the fact that northward East Indian Coastal Current is seemingly an extension of the North Equatorial Current during the northeast monsoon (Mc Creary et al., 1996).

Eventhough several modelling studies have been made on the Bay of Bengal circulation (e.g.; Shankar et al., 1996; Potemera et al., 1991, McCreary et al., 1993, Haugan et al., 2002), the forcing is not fully understood. The role of freshwater from Brahmaputra and Ganges and that of coastal Kelvin waves propagating northward along the eastern boundary of the Bay of Bengal plays important role in the local forcing and governs the dynamics of Upper Ocean.

1.2.5 Planetary Waves

In the Andaman Sea, east of the Bay of Bengal, the oceanic flow changes direction twice during the year (Potemara et al., 1991). Model layer thickness reveals coastal Kelvin waves propagating along the coast, traveling the entire perimeter of the Andaman Sea and the Bay of Bengal. This wave excites westward propagating Rossby waves into the interior of the Bay. Similar results are found by McCreary et al (1993).

The annually reversing strong monsoon winds force the Indian Ocean to produce mechanisms at large scale via propagating signals (Kelvin and Rossby waves). These waves of long wavelength (500-1000 km) have different propagation characteristics. The existence of Rossby waves and Kelvin waves are reported in Indian Ocean (White, 2000).

1.2.6 ENSO in Indian Ocean

Once in few years, an El Nino (warm) event occurs, with warming of sea surface temperature in the central and eastern Pacific, accompanied by diminished easterly trade winds and an eastward shift in tropical convection. The strength of the monsoon and the occurrence of warm or cold event depend on the location and the magnitude of western Pacific SSTs and on tropical convection (Soman and Slingo, 1997). The relation between El Nino Southern Oscillation

(ENSO) and monsoon is still a very attractive field in oceanographic research. The Southern Oscillation (SO) is well-known as a standing oscillation of the surface pressure between the Indian Ocean through Indonesia and the eastern South Pacific with a changing periodicity around 40 months. The earliest work was reported by Walker (1923) and Webster and Yang (1992) reviewed the historical background of monsoon and ENSO coupling. While the correlation between the signals of various parameters in the Pacific and Indian Ocean are analysed through different methods, the mechanisms underlying the coupling of both oceans are still unknown, whether atmospheric or oceanic. Empirical orthogonal function studies of surface pressure, wind stress, SST and Ekman pumping have been carried out by many authors to understand the effects of ENSO in Indian Ocean (Hsiung and Nowell, 1983). Conceptually, any anomaly in either cycle may influence the other and lead to strong variations in the annual cycle such as El Nino in the eastern Pacific Ocean or similar events in the Indian Ocean.

The unusual characteristics such as the Somali Current, Equatorial Jets, upwelling and others in the Indian Ocean brings attention from oceanographers all over the globe to study the coastal, equatorial and subtropical ocean circulations and the interactions between them.

The research work carried out so far over Indian Ocean can be classified as the study on the regional scale at seasonal and annual time scales and on a global scale at inter-annual and longer time scales.

1.3 Scales of Variability

The scales of variability in the TIO are driven by a wide variety of factors and they exist from micro-scale to very large scale. These scales occupy periodicities right from few minutes to couple of years. The prominent periodicities, which contain significant energy, are in the low frequency band below the semi-annual periodicity.

Oceanic variability with 100 days of periodicity is mostly associated with eddies. Monsoonal and seasonal signals are apparent in the upper ocean. Multi-year variability in association with ENSO is well documented and there is

increasing evidence of other inter-annual variability in surface variables. Energetic meso-scale eddy variability, with scales of 50 to hundreds of km, is to be anticipated in most locations in the ocean. Smaller scale (tens of km) variability is typically localised around at oceanic fronts at the equator and where meridional scales are small, or in association with bottom topography and coastlines.

Sea surface temperature shows strong signals at diurnal (within 24 hour) and synoptic scales (5 to 10 days). The near surface temperature peaks up in afternoon than the bulk mixed layer temperature and by the middle of night near surface and bulk will be the same. This SST increase depends on wind and insolation. The interaction between 30-60 day waves, westerly wind bursts and ENSO remains a topic of ongoing research (Madden and Julian, 1972). Evidence has been found on the existence of 26 day wave in the western equatorial Indian Ocean similar to equatorial Pacific (Reverdin and Luyten, 1986). At mid-latitudes spectral peaks associated with each synoptic weather systems are well documented (Mc Phaden et al., 1992). Mysak and Mertz (1984) reported 40-60 day variability in temperature and velocity in the Somali Current. Duing and Schott (1978) reported 50 day oscillation in the South Equatorial Current of the Indian Ocean.

It is worth mentioning here that the work addressing a detailed study on these variability are being carried out for the other oceanic region extensively (Madden and Julian, 1994; Lie and Endoh, 1991; Levitus, 1984).

1.4 Meteorological and Oceanographic Studies in the Near Surface Fields over Tropical Indian Ocean

In this section, an attempt has been made to understand various scales of variability and their role on air-sea interaction in the TIO. It has been reported (Blanc, 1996; Webster and Yang, 1992) that there is a coupling between the Indian monsoon and southern oscillation (SO). Cadet and Diehl (1984) demonstrated the existence of SO signal of 40-60 months over Indian Ocean using power spectral estimates. They speculated that the observed variability is consistent with a 20 year cycle. The eastward propagation towards Pacific Ocean was noticed by Yasunari, (1985) who used zonal wind and velocity potential fields

and found the circulation to be on the time scale of the Southern Oscillation (40-60 month scales). It is recorded that the ENSO signal in Indian Ocean explains as much of the interannual variability in that as the ENSO signal in the Pacific (Tourre and White, 1995). However, it is an important but difficult problem to determine whether the SO and the QBO are dynamically similar phenomena in the troposphere. Yasunari (1985) noted that some studies suggest a different spatial structure of the QBO to that of the SO, while other studies treated this mode as part of the SO in a broad sense.

According to Barnett (1983), the convergence of surface winds associated with SO over Indonesia is subject to strong interannual variations in its intensity and location because of coupling of the trade winds over the Pacific and the monsoons over the Indian Ocean. Meyers (1996) showed that correlation to zonal wind anomalies are associated with thermocline variations along Java Coast, easterly wind anomalies over the equatorial Indian Ocean are associated with shallow thermocline and cold waters. Morrow and Birol (1997) using 1995-97 data noted that the interannual signal is related to warm core eddies.

The persistent anomalies in SST and wind on a seasonal cycle (Meehl, 1994) influence the air-sea interaction. The strong winds and warm SST will lead to greater evaporation and strong convection i.e., strong monsoon characteristics. The transition of SST anomalies begins by northern spring season. This transition is important for the establishment of convective heating anomalies and to contribute subsequent monsoon development.

Studies on propagating waves in the oceans have been an active area of research in recent years as they play a very crucial role in energy transport (Masumoto and Meyers, 1998; Perigaud and Delecluse, 1993; Webster and Yang, 1992). These waves are generally in the low frequency band for Rossby gravity wave with periods ranging from 3 to 5 years. Waves with periods 25-30 days referred as *Legeckis* waves are observed (Legeckis, 1987) over world's equatorial oceans. A number of studies are carried out to examine its properties (Tsai et al., 1992; Weisberg and Weingartner, 1988). Two year SST time series data at two sites in the equatorial Indian Ocean are examined for oscillations with periods 2-70 days (Meyers, and O'Brien, 1994) and revealed the evolution of 26-day

oscillation corresponding to Mixed Rossby gravity (MRG) wave also known as Yanai wave.

30-60 day variability found in tropics associated with atmospheric waves (Madden and Julian, 1972; Lau and Shen, 1988) significantly controls the variability of the dynamics of TIO. Reverdin and Luyten (1986) have found long waves in SST field in western equatorial Indian Ocean of 1000 km wavelength with 26 day periods with westward phase propagation and longer periods are reported in south of equator of Indian Ocean. Mysak and Mertz (1984) reported 40-60 day variability in temperature and velocity of Somali Current. Duing and Schott (1978) reported 50 day oscillations in the south equatorial current of Indian Ocean. Monthly and seasonal scales of 500 km and above are noted (Bauer et al., 1991). The annual variations are strong in surface variables. The seasonal cycles of SST are more pronounced with distance from equator. Along Somalia due to upwelling, surface cooling occurs within few tens to 100 km of the coast (McCreary and Kundu, 1989).

SST shows strong signals at diurnal (24 hour), synoptic 5-10days, 20-60 days, 100 days with that of eddy, monsoonal and seasonal signals, multi year with ENSO, spatial (50 to 100km) with eddy variability. Smaller scales are typically local at oceanic fronts (10 – 50 km). The space scales of SST associated with diurnal variability and synoptic variability are linked with atmospheric processes. Convectivity in the atmospheric boundary layer reflects variability in fluxes at the surface space (1-10 km) and time (few hours).

Another important mechanism governing the variability of TIO is the phenomenon of El-Nino (Cadet and Diehl, 1984; Webster and Yang 1992). The relationship between the Indian summer monsoon and the Pacific El Nino is not clearly understood. Recently discovered Indian Ocean Dipole mode event is believed to be a responsible mechanism for climate change in a wide area from the Indian Ocean to the Pacific Ocean (Saji et al., 1999; Yu and Rienecker, 1999; Webster et al., 1999; Murtugudde et al., 2000). It is understood to be a coupled air-sea interaction within the Indian Ocean. It has been identified in the years 1961, 1967, 1972, 1982, 1994 and 1997. It is identified as a pattern of inter-annual variability with anomalously low sea surface temperatures off Sumatra and high

sea surface temperatures in the Western Indian Ocean, with accompanying wind and precipitation anomalies. This air-sea interaction process is unique and inherent in the Indian Ocean and is considered to be independent of ENSO. The dipole mode causes changes in regional rainfall, with increased rainfall over eastern Africa and drought conditions over Indonesia. Indeed, there have only been three major events during the past 40 years, during 1961/62, 1993/94 and 1997/98. The two recent events are occurrences coincided with Pacific ENSO event, the first one with weak El Nino and the 1997/98 one with a strong El Nino, but the much earlier one did not coincide with El Nino. The fact that some (but not all) of the dipole mode events occur during El Nino years suggests a weak ENSO dipole mode link (Webster et al., 1999; Saji and Yamagata, 2003).

Yet another interesting phenomenon associated with the variability of monsoon reported in literature is the sunspot cycle having a periodicity of 11 year. During this event an amplitude variation of 1.5 Wm^{-2} in incoming shortwave radiation flux is reported. Interestingly, associated with this phenomenon, corresponding variability is also reported in SST field (Fris Christensen and Lassen, 1991).

From these discussions, it is clear that variability in the TIO is governed by a large number of processes in different time and space scales. The available analysis show large scale temporal and spatial anomalies exist. Understanding and quantifying these anomalies would help in the prediction of TIO down the line. Some of these processes described above are not adequately understood. This necessitates and highlights an improved understanding of the mechanisms that produce, maintain and destroy these anomalies. Understanding of the spatio-temporal evolution of these anomalies of the ocean atmosphere coupled system will not be complete without the annual cycle itself being understood as these anomalies are strongly phase-locked with the annual cycle. However, in the tropical Indian Ocean the observed inter annual (Evans and Brown, 1981; Cadet and Diehl, 1984; Rao and Goswamy, 1988) and intra seasonal variability of SST is relatively small ($1-2^{\circ}\text{C}$).

Most of these studies are limited to specific part of Indian Ocean and seasons to address some features associated with monsoons. Further there are

limitations due to inadequate data coverage. Thus Indian Ocean remains still as, not reachable, for prediction.

1.5 Objectives of the Present Study

The present work is carried out with an objective to provide a better understanding of different scales of spatio-temporal variability of oceanographic and meteorological parameters over the TIO occurring from small scale to very large scale, occupying the periodic band of a few days to years. The question that arises is that why these scales of variability are important? The energy contained in the various bands interacts with each other to drive the ocean-atmosphere system. Apart from this, there is a non-linear cascading of energy from the low to high frequency bands. It is very important to study this interaction of energy to clearly understand the dynamics of the system. The cascading of energy from the low to high frequencies is quite non-linear making things very complex. There is a need to understand this interaction of energy to study the dynamics of the system. Therefore, a comprehensive knowledge of temporal and spatial variability of oceanographic parameters is required to understand the ocean-atmosphere system which will help us in predicting the system realistically.

For other oceanic regions similar studies have been carried out to a certain extent. Climate variability in the Indian Ocean region seems to be in some aspects independent of forcing by external phenomena such as the El Nino/ Southern Oscillation. But the extent to which and how, internal coupled ocean-atmosphere dynamics determine the state of the Indian Ocean system have not been resolved. A complete study for TIO has to be carried out in detail, though there are a few fragmentary studies dealing with this aspect covering some region of the Indian Ocean. A complete understanding of this total tropical Indian Ocean is required. It is felt that a study describing the spatio-temporal variability of oceanographic and meteorological variability in the TIO will help in the long run to enhance the predictive capabilities of the system. Since these parameters are the major inputs for any forecasting models, their spatio-temporal variability has to be understood thoroughly before attempting modeling studies. The different parameters considered in this study are sea surface temperature (SST), wind

stress and precipitable water. These fields are available from satellites almost on real time basis.

In this thesis spatio-temporal variability of these fields based on a large data set (NCEP / NCAR) are examined in the framework of time and space analysis. The strength of this work lies in the exhaustive data sets and improved analysis and interpretation tools.

DATA AND METHODOLOGY

Climate variability is believed to arise from an inter-play of ocean and atmosphere. Both the ocean and the atmosphere transport energy and exchange it with each other. The dynamics of both systems are thus coupled via exchange processes at their common interface. To understand climate variability it is vital to study the spatial and temporal variability at the interface. This study on spatial and temporal variability of surface parameters of tropical Indian Ocean helps to learn more on the exchange process and hence the prediction of climate variability.

Oceanographic phenomena often contain periodic components related to forcing at a wide range of time scales hourly, diurnal, seasonal, annual cycles, ENSO, sunspot cycle, etc to name a few. Time series analysis involves the extraction of information about these periodic components from time series data of the particular parameter. Considerable use is made of regression and correlation methods in statistical data analysis in oceanography, where linear relationships are typically assumed (Nicholls,

1987; Drosowsky, 1993). This assumption is of particular concern since many potentially predictive relationships will never be discovered.

In this study on spatio- temporal variability of surface parameters of Tropical Indian Ocean (TIO), Empirical Orthogonal Function (EOF) analysis and wavelet analysis are carried out. EOF method assumes stationarity in time explicitly, but implicitly assumes that the geophysical field of interest is spatially homogeneous. On the other hand, wavelet transform is used to analyse time series that contain non-stationary power at many different frequencies (Daubechies, 1990).

2.1 Data

For the present study National Center for Environmental Prediction and National Center for Atmospheric Research (NCEP/NCAR) reanalysis (Kalnay et al., 1996) data product for the years 1960-1998 has been utilized. Each year data is available in one CD-ROM. Unlike fields reconstructed from sparser observations, this dataset has the advantage of being internally consistent (Sterl, 2001).

Each CD-ROM contains one year of selected analyses of global data of meteorological and oceanographic fields from the NCEP/NCAR Reanalysis Project, in which state-of-the-art data assimilation system is used. The PC version of "Grid Analysis and Display System" (GRADS) developed by Brian Doty of the Center for Ocean-Land-Atmosphere Studies in Calverton, Maryland provided along with the CD-ROM is used for extracting the data from the CD-ROM. The details of NCEP/NCAR 40-Year Reanalysis Project are described in Kalnay et al (1996).

As the study concentrated only on surface fields, the 'Horizontal' fields are extracted from the respective CD-ROM. Horizontal fields are of two types 144 long by 73 lat, 2.5 x 2.5 degree grid and 192 long by x 94 lat Gaussian grid. Daily fields of sea surface temperature (TMP in $^{\circ}\text{K}$), precipitation rate (PRATE in $\text{Kg m}^{-2}\text{s}^{-1}$) and momentum flux (neg. wind stress) (UFLX/VFLX in Nm^{-2}) are used for this study. The units of PRATE (total rainfall) are $\text{kg m}^{-2}\text{s}^{-1}$,

and "mm/day" units can be obtained by multiplying the values by 86400. The anomalies in the reanalysis precipitation are more similar to the observed anomalies than the reanalysis precipitation is to the total rainfall. The binary data stored in CD is extracted using GRADS and converted to ASCII for further analysis. Each parameter data is stored in a file of the particular CD-ROM which consists of 3 parts; data file, control file and index file.

Other than the NCEP/NCAR daily data TOPEX/POSEIDON Sea Surface Height (SSH) of 1993-2001 has also been used in this study. The 10-day anomaly computed after subtracting first 5-year climatological mean is used to study the nature of propagating nature of disturbances in the TIO.

2.1.1 Errors and Resolution in Data

The reanalysis gridded fields have been classified into four classes, depending on the relative influence of the observational data and the model on the gridded variable.

A indicates that the analysis variable is strongly influenced by observed data, and hence it is the most reliable class (e.g., upper air temperature and wind). The designation **B** denotes that, although there are observational data that directly affect the value of the variable, the model also has a very strong influence on the analysis value (e.g., humidity and surface temperature). The letter **C** indicates that there are no observations directly affecting the variable, so that it is derived solely from the model fields forced by the data assimilation to remain close to the atmosphere (e.g., clouds, precipitation and surface fluxes). Finally the letter **D** represents a field that is obtained from climatological values and does not depend on the model (e.g., plant resistance, land-sea mask).

The data input is pre-processed, and all the analysis output fields are monitored with a "complex QC" monitoring system, in which the statistics of the data, time tendencies, etc, are compared to climatological statistics in order to detect errors. These statistics include tendency checks.

To this point, however the quality of the NCEP /NCAR data prior to the common availability of satellite wind and precipitation information in the years before 1980's is unclear. Goswami and Sengupta (2003) reported the deviation of wind values near equator as $2-3 \text{ ms}^{-1}$ smaller compared to QuikSCAT satellite scatterometer data.

2.2 Empirical Orthogonal Function (EOF)

EOF method is the method for analyzing the variability of a single field. EOF analysis has been extensively used in oceanography to examine the variability of scalar fields. EOF method finds both spatial patterns and its time series. Hence in oceanographic studies this method finds the spatial patterns of variability, their time variation and gives a measure of the importance of each pattern as standing oscillations and not as propagating patterns.

For clarity, hereafter the spatial patterns are the *EOFs* referred as Principal Component loading patterns or principal components and *time series* as principal components of expansion coefficients referred as EOF time series or expansion coefficients or principal component time series.

2.2.1 EOF in Oceanography

Numerous studies in the last two decades have been conducted using EOF modes mainly to describe the structure and evolution of inter-annual variability and the physical processes and mechanism responsible for El Nino-Southern Oscillation (ENSO). Tourre and White (1995) performed EOF and rotated EOF (Varimax) analysis using 13-years of data to investigate the time – space evolution of ENSO in SST and heat storage of the upper 400 m of the Pacific Ocean, Indian and Atlantic Oceans and reported that the two of the dominant modes are associated with ENSO. In order to understand the dominant spatial structure and time variations of inter-annual variations in SST over Pacific Ocean, SST data has been analysed (Nitta and Yamada, 1989; Kawamura, 1994; Deser and Blackmon, 1993) for the global ocean on

the basis of empirical orthogonal functions. The dominant mode of inter-annual variability in the tropical Pacific Ocean is identified as an ENSO-related signal. Using EOF analysis for the SST data set of Advanced Very High Resolution Radiometer (AVHRR) of NOAA 6, NOAA 7 and NOAA 8, Lagerloef and Bernstein (1988) studied the front, eddy patterns in Santa Barbara Channel. Mizoguchi et al (1999) studied the multi and quasi decadal variations of SST in North Atlantic using Complex Empirical Orthogonal Function (CEOF) analysis with 46 years of COADS dataset and estimated the propagation speed of the EOF modes. The surface and subsurface structure and evolution of inter-annual variability in the tropical Pacific Ocean related to El Nino (Mizoguchi et al 1999; Zhang 1996) has been studied using yearly SST anomaly fields during 1960-90 from the estimated EOF modes. The existence of teleconnection between Atlantic Ocean and Pacific Ocean has been studied by Sterl (2001) with the help of EOF and SVD analysis on SST, Sea Level Pressure and heat flux using 52 years of NCEP/NCAR reanalysis data.

Using TOPEX altimeter (1992-1998) and SST (1982-96) the ENSO related sea level variations and surface warming has been studied (Chambers et al., 1999) by estimating dominant EOF modes over Pacific Ocean and Indian Ocean. Recently Saji et al (1999) explained that about 30% of the anomalous variation of SST with first EOF mode and 12% in the second mode, which they called as a dipole mode. Characteristic of the first mode is the uniform polarity anomalies covering the tropical Indian Ocean and that of the second mode as the reversal of SST anomaly across the basin. The dipole mode events (1961, 1967 and 1994) are studied which coincides with no ENSO, a La Nina and a weak El Nino, respectively.

The knowledge of variation of thermal structure in the Indian Ocean is most important to understand the space-time evolution of physical processes and mechanisms that govern the variation. In order to reveal the dominant structure and time variations, the surface ocean parameters are analysed on the basis of statistical methods such as EOF analysis. The present study on spatio-temporal variability of some meteorological parameters in Tropical

Indian Ocean starts with an estimation of leading patterns of standing oscillations in SST.

2.2.2 Methodology

Let us assume that we have measurements of some variable at locations $x_1, x_2, x_3, \dots, x_n$ taken at time $t_1, t_2, t_3, \dots, t_n$. For each time say t_j the measurements at different locations ($x_1, x_2, x_3, \dots, x_n$) forms a map. A matrix (F) is formed as each map into a row in F. Then each of the column of F represent a time series at a location. Then EOF analysis is performed using F (time, space) as data matrix. This matrix is then detrended to remove any trend in the data set and a covariance matrix is computed with the data.

The eigen values and eigen vectors of the covariance matrix of F is then computed. The EOFs are the eigen vectors with high eigen values. The expansion coefficients are then computed by multiplying the data matrix by the corresponding eigen vector. Now each of these EOF modes explains the mode of variability and the expansion coefficients explains the mode oscillations in time referred as time series. To get the important modes, the eigen values are sorted and variabilites are presented for the mode which contribute more than 40% variances.

2.2.3 Analysis Procedure

EOF modes can be computed ranked by their spatial as well as by their temporal variance. The EOFs are mostly computed from the eigen value decomposition of the two possible covariance matrices (R) as $F^T F$ or FF^T computed from F. The key difference between spatially and temporally ranked EOF modes lies in how the data are operated on, before the EOF decomposition is computed (Lagerloef and Bernstein, 1988). If the time series mean are first subtracted from each of the time series, the resultant mode eigen values sum the temporal variance. Conversely, if all data sampled at the same time have the spatial average removed, the modes decompose the spatial variance. If the data are analysed without prior modification, the modes

will be ranked by their total of joint space-time energy. In this study the temporal EOF is used for the analysis.

The spatial patterns of EOF modes can be presented in several ways. One possibility is to plot the values of eigen vectors itself with amplitudes as contours.

2.3 Wavelet Analysis

A physical process can generally be described by the values of some parameter x that varies with time, $x=x(t)$. We refer to this representation as the *time domain*. An alternative and equivalent representation of the same signal would be to express it as its amplitude, X , as a function of frequency, f . $X=X(f)$. We refer to this representation as the *frequency domain*. To extract the periodic components the time domain function is required to represent in frequency domain.

2.3.1 Wavelet Analysis in Oceanography

The wavelet transform has been used for numerous studies for tropical convection (Weng and Lau, 1994), the ENSO (Gu and Philander, 1995; Wang and Wang, 1996) dispersion of ocean waves (Meyers et al., 1993), wave growth and breaking (Liu, 1994). In Meyers et al (1993), wavelet analysis is used to study the propagation of mixed Rossby-gravity waves in an idealized numerical model of the Indian Ocean. They reported that at 3°S latitude, 56°E the wave in 1987 have roughly half the amplitude as the 1988 waves (Meyers and O'Brien, 1994). Interdecadal variations of El Nino/Southern Oscillation signals and annual cycles in Sea Surface Rainfall (SSR) and zonal wind in the equatorial Pacific Ocean are studied by wavelet and EOF by Setoh and Imawaki (1999). It is estimated that the typical time scale of ENSO before late 1970's as 40 months and after this period as 48-52 months.

2.3.2 Wavelet Transform (WT)

Wavelet transform is an analysis tool well suited to study multi-scale, non stationary processes occurring over finite spatial and temporal domain. Thus wavelet transform can be used to analyse time series data of oceanographic parameters that contain non-stationary power at many different frequencies. Hence by decomposing such a time series in time-frequency space using wavelet analysis, it is possible to determine both the dominant modes of variability and how those modes vary in time.

2.3.3 Methodology

To extract frequency information the time series analysis can be carried out in a number of ways using different mathematical tools. The widely used are the Fourier methods. The classical Fourier analysis makes use of sine and cosine functions to represent the signal and it is not suited for non-periodic time varying signals. To overcome this, Short Time Fourier Transform (STFT) techniques are used, in which different windowing techniques are used. But STFT has got the limitation of same resolution in time frequency domain once after selecting the window. An alternative method is to use wavelet.

A general transform equation (Rioul and Vetterli, 1991) for a time domain $x(t)$ to frequency domain conversion can be written as

$$X(a, b) = \int_{-\infty}^{+\infty} x(t) \Psi_{a,b}(t) dt \quad \dots(1)$$

Different transform can be obtained by choosing different $\Psi_{a,b}(t)$ function.

In Fourier transform

$$\Psi_{a,b}(t) = e^{-j2\pi ft} \quad \dots(2)$$

Here the length of the window is finite and basis functions are sine and cosine functions

In STFT

$$\Psi_{a,b}(t) = e^{-j2\pi at} \Psi(t-b) \quad \dots(3)$$

where a is frequency $\Psi(\tau)$ is window of finite width and b is window translation parameter.

In wavelet transform

$$\Psi_{a,b}(t) = \frac{1}{\sqrt{a}} \Psi\left(\frac{t-b}{a}\right) \quad \dots(4)$$

and called mother wavelet here $\Psi_{a,b}(t)$ is a window of finite length.

Substituting (4) in (1) we get continuous wavelet transform

$$X_{a,b}(t) = \int_{-\infty}^{+\infty} x(t) \Psi\left(\frac{t-b}{a}\right) dt \quad \dots(5)$$

A wavelet transform uses generalized local base functions that can be stretched and translated with a flexible resolution in both frequency and time. The flexible windows are adaptive to the entire time-frequency domain, known as the wavelet domain, which narrows while focusing on high frequency signals and widens while searching the low frequency background. As a result, high precision in time localization in the high frequency band can be achieved at the reduced frequency resolution, and vice versa for low frequency components. A wavelet transform allows the wavelets to be scaled to match most of the high and low frequency signals so as to achieve the optimal resolution with the least number of base functions.

In wavelet analysis a prototype function called mother wavelet is adopted at first. Then the temporal analysis is performed with high frequency version of the prototype wavelet while frequency analysis is performed with a dilated low-frequency version of the same wavelet.

2.3.4 Comparison of Fourier and Wavelet Analysis

In Fourier analysis there is no flexibility on basis functions than using sine and cosine functions while in wavelet analysis even the chosen mother wavelet can have dilation and contraction. In Fourier analysis as the functions are global in nature these are not suited to represent highly localized functions such as spikes. In STFT a window of limited time extent is used which maps the signal into a two-dimensional function in a time-frequency plane. Once a window has been chosen in STFT then the time-frequency resolution is fixed over the entire time-frequency plane. In STFT, a time series is examined in the time and frequency domains, and hence over represents high frequency components and under represents low frequency components.

In wavelet transform (WT) the length of the window can be varied. In order to analyse a signal, both short and long basis functions are required. This is readily provided by the wavelet transform analysis where the time frequency plane can be conveniently covered by windows of different and appropriate lengths of the mother wavelet. ie., wavelet analysis process data at different scales or resolutions. For gross features a large window is used while for small features a small window is used. Hence Wavelet analysis is well-suited for approximating data with sharp discontinuities of non-stationary signals.

The difference to STFT is that WT uses short windows at high frequencies and long windows at low frequencies while STFT uses a single analysis window. To overcome resolution limitation of STFT in time-frequency plane a multi resolution analysis is advised generally in STFT. While Fourier analysis yields an average amplitude and phase for each harmonic in a dataset, the wavelet transform produces an instantaneous estimate or local value for the amplitude and phase of each harmonic give time-dependent signal characteristics.

2.3.5 Selection of Mother Wavelet

There are several types of WTs. Choice of the wavelet function depends on the purpose of application. Generally the wavelet function refers to either orthogonal or non-orthogonal wavelets. Wavelet basis refers only to orthogonal set of functions. The use of orthogonal basis implies generally for discrete wavelet transform (DWT). Generally used orthogonal wavelet functions are Haar and Daubechies. While a non-orthogonal wavelet function can be continuous (CWT) like Morlet and Mexican Hat or discrete wavelet transform. The orthogonal wavelet may not always yield the most physically meaningful scale analysis because the scales are analyzed only at the octaves (powers of 2) not at the voices (fractional powers of 2)(Lau and Weng, 1995). The non-orthogonal transform is useful for time series analysis, where smooth continuous variations in wavelet amplitude are expected (Torrence and Compo, 1998). A non-orthogonal analysis is said to be highly redundant at large scale, where the wavelet spectrum at adjacent times is highly correlated.

The wavelet function can be real or complex. The difference between complex and real wavelet function is that a complex wavelet function returns information about both amplitude and phase and hence useful for capturing the oscillatory behavior while a real wavelet function is used for isolating peaks and discontinuities. The Morlet and Paul are complex while Mexican hat is real a wavelet function.

For a continuous input signal the time and scale parameters can be continuous leading to CWT. The redundancy of the continuous wavelets yields enhanced information on the time scale localization.

In this study, Morlet wavelet function is used, which is a non-orthogonal complex continuous wavelet function. Morlet wavelet is a plane wave modified by a Gaussian envelope and Mexican hat is the second derivative of the Gaussian function. As a complex continuous wavelet function Morlet has advantage in oceanographic time series data analysis, in detecting both time-dependent amplitude and phase.

Standing Oscillations

To understand the spatial and temporal variability of the surface parameters over tropical Indian Ocean region, an EOF analysis described in chapter 2 has been carried out for various surface parameters such as Sea Surface Temperature, surface wind stress and precipitation rate. For this, daily data from NCEP/NCAR reanalysis dataset of 1960-1998 of these parameters is used.

3.1 Introduction

The warmest region of the tropical oceans is the western Pacific and the northern Indian Ocean where temperature often peak near 30°C. Small changes in this warm pool SST create major perturbations in the tropical circulation and climate far removed from the tropics (Palmer and Mansfield, 1984). The sensitivity of climate to the warm pool with SST is related to the non-linear increase of vapor pressure with SST, such that small changes in the SST near its maximum values invoke longer changes in evaporation and the subsequent release of latent heat than that produced by similar perturbations where the SST is cooler (Webster, 1994; Loschnigg and Webster, 2000). The mean SST of the

Indian Ocean between equator and 20⁰N falls to about 27⁰C, although the equatorial regions (10⁰S to 10⁰N) the mean SST remains greater than 28⁰C for the entire year (Loschnigg and Webster, 2000). During the northern spring and early summer the northern Indian Ocean becomes the warmest body of open water in the tropics. After the onset of the summer monsoon, the northern Indian Ocean cools as a result of strong upwelling and evaporation (Knox, 1986). A secondary spell of heating takes place in the tropical Indian Ocean during post monsoon (Colborn, 1975) followed by cooling during winter.

Though these patterns are repeated every year, there are interannual variations in the values of SST in the tropical Indian ocean. This results in interannual variations in climate all over the places surrounding the Indian Ocean. EOF analysis of SST and related wind and precipitable water can bring out the standing oscillations which cause perturbations in these parameters.

EOF analysis of global SST variability has been carried out by Kawamura (1994) giving major emphasis to Pacific SST anomaly field. A detailed review of large scale air-sea interaction and SST anomalies are documented. Hsiung and Nowell (1983) made the first application of EOF analysis to the observed SST field and described overall features of leading modes over the entire oceans. Later similar analysis was done by Parker and Folland (1988) and Nitta and Yamada (1989). It has been found that the first mode tends to be distributed all over the globe, which is associated with ENSO phenomenon. The leading modes are characterised by interdecadal variability accompanying the warming of tropical oceans (Nitta and Yamada, 1989). Recent studies in the Indian Ocean (Saji et al 1999; Webster et al 1999; Murtugudde et al., 2000) showed that a unique dipole pattern exists in the Indian Ocean which contribute to large scale climate anomalies. Saji et al., (1999) named it as the Indian Ocean dipole mode (IOD) a pattern of internal variability with anomalously low SST off Sumatra and high SST in the western Indian Ocean which accounts for about 12% of SST variability in the Indian Ocean. Reason and Mulenge (1999) have shown a significant correlation between SST anomalies in the southwestern subtropical Indian Ocean and rainfall over southeastern Africa. Behera and Yamagata

(2003) postulated a subtropical dipole pattern in the subtropical south Indian Ocean, which usually develops in Dec/Jan, peaks in Feb and dies down by May/June. The positive dipole phase is characterised by cold SST off Australia and warm SST southeast of Madagascar. Time series of the first EOF suggest that this mode may be independent of both ENSO and IOD. This aspect needs more statistical evidence

3.2 Domain of study

EOF analysis for spatial and temporal variability has been carried out over tropical Indian Ocean. The domain of the study is 50-100⁰E and 30⁰S-22⁰N. This region essentially covers the Arabian Sea, Bay of Bengal, Tropical Indian Ocean and south Indian Ocean. EOF analysis can be performed by removing column mean or row mean as explained in 2.2.2. Generally in oceanographic data analysis this covariance matrix R is used as the input data matrix. Removing the mean just allows to interpret R.

For the present study monthly averages are taken for each parameter at the NCAR grid points. Hence 1204 grid points covered the selected area. The mean monthly anomalies are computed for each grid point by subtracting the respective monthly climatological mean from each individual monthly mean. The spatial EOF modes are computed for this composite data set after removing the linear trend. This data matrix of 468 x 1204 of monthly SST anomaly is used as the input for EOF computation. The Eigen values for spatial EOF modes are computed. The results of EOF analysis start with SST followed by other parameters.

3.3 EOF Analysis of Sea Surface Temperature

The spatial patterns of the first of the first three EOF modes(explaining more than 40% variability) of monthly SST anomalies based on NCEP/NCAR 1960-1998 data is presented in Fig. 3.1 (a, b and c). They respectively account for 29%, 12% and 9% of the variance. The first EOF mode indicates (Fig 3.1 a) positive loading almost in the entire Indian Ocean with higher values in the Arabian Sea, equatorial and southwestern and central Indian Ocean and lower in

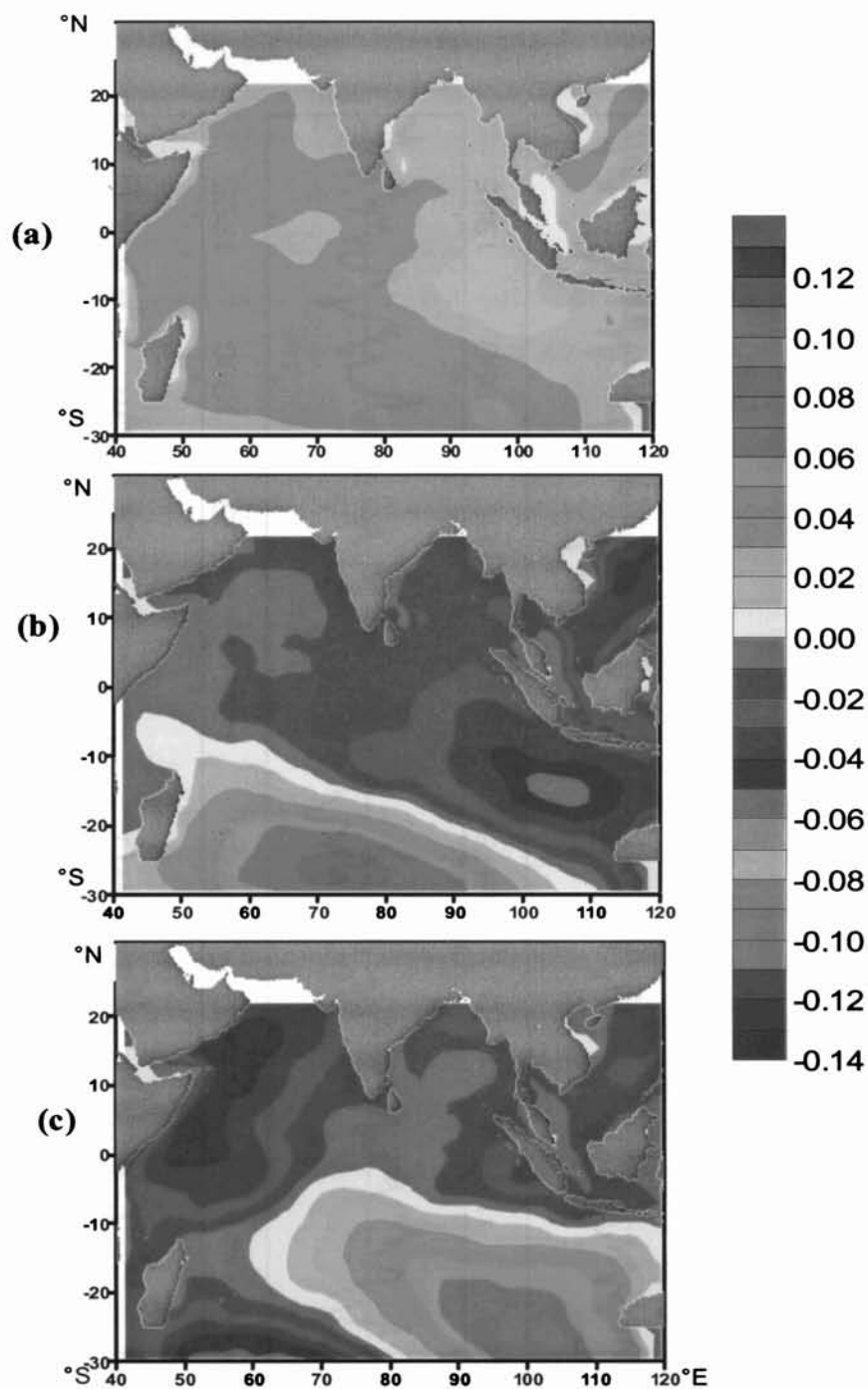


Fig 3.1 Spatial patterns of the first leading EOF modes for the monthly SST anomalies over the Indian Ocean for the 39 year period 1960-1998 (a) EOF1, (b) EOF2 and (c) EOF3

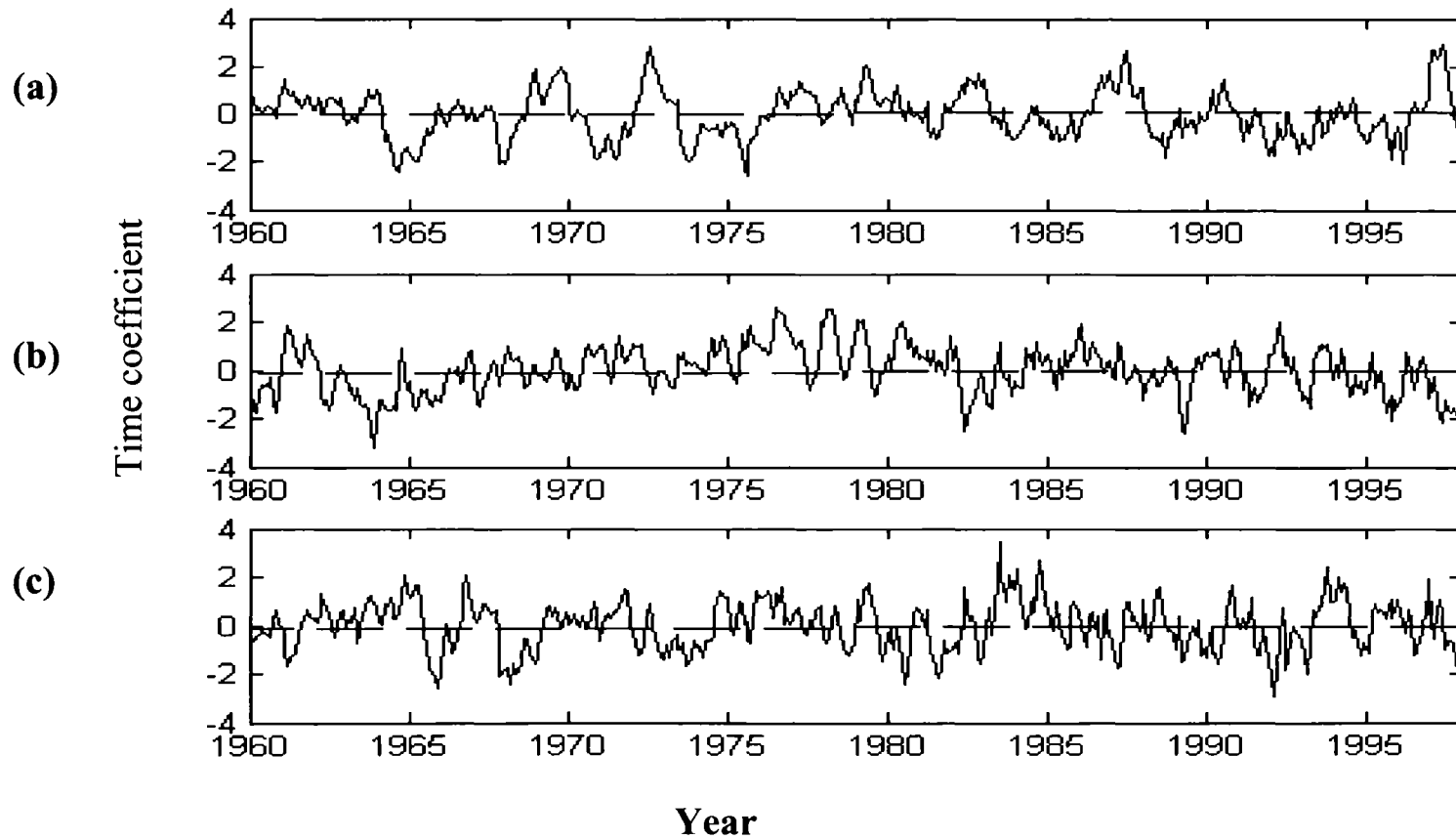


Fig 3.2 Time sequence of the first three EOF modes for monthly SST anomalies over Indian Ocean for the 39 years period from Jan 1960-December 1998 (a) EOF1, (b) EOF2 and (c) EOF3

the Bay of Bengal and eastern Indian Ocean. The corresponding time coefficients of the first three leading EOF modes are shown in Fig. 3.2 a, b and c respectively. The time sequence of the first EOF mode of SST explaining 29% of the total variance displays major peaks in 1969, 1973, 1983, 1987 and 1997. The EOF analysis of Tourre and White (1995) for a much shorter data set (1979-1991) indicated that the first EOF mode explains 31% of the total SST variability which is close to the 29% variance from the present analysis. Fast Fourier Transform (FFT) analysis of the time series of the first EOF mode showed a periodicity of 2.7 years. Earlier analysis of Kawamura (1994) indicated that the temporal variability of EOF-1 of global SST has a quasi periodicity of 2-5 years and coincides quite well with the occurrence of ENSO event; and hence this mode can be identified with ENSO mode and distinguished from the modes dominated by other periodicities. This was further confirmed by Tourre and White (1995), though they found that the ENSO signal is dominant only in the Pacific and Indian Oceans but not in the Atlantic. However they found that the evolution of ENSO signal in the Indian Ocean is different from that in the Pacific. The first peak in the Indian Ocean SST lags approximately by 6 months the first peak in the Pacific (Tourre and White, 1995) associated with ENSO. The El Nino occurred in 1965 - 1966, 1969 - 1970, 1972 - 1973, 1976 - 1977, 1982 - 1983, 1986 - 87 and 1997 - 98 within the study period. The significant warming in the Indian Ocean took place in 1969, 1973, 1977, 1979, 1983, 1987, 1991 and 1998. Out of these except 1979 and 1991 the warming of the Indian Ocean is in phase with the occurrence of El Nino. Incidentally during the El Nino of 1965-1966 and 1992-93 cooling instead of warming took place in the Indian Ocean, which indicate the influence of other forcing mechanisms in regulating SST in the first EOF mode. However, presently it is not clear the mechanism, which offsets the influence of El Nino in these years.

The first EOF mode showed significant cooling of the Indian Ocean during 1964-65, 1968, 1971, 1974-76, 1988 and moderate cooling during the early 1990's. The cooling during this period either coincided with La Nina or preceded El Nino except in the early 1990's. The warming in the Indian Ocean during 1998 was abnormally high (Chambers et al., 1999, Liu and Huang 2000). Incidentally 1997-98 was an El Nino year and also a year of IOD. However significant

warming is only seen in the first mode of EOF (Fig.3.1 (a)) which suggest that the warming could be attributed to be induced by El Nino.

The second EOF mode shows positive loadings in the southwestern and southern regions of the Indian Ocean while strong negative loadings are seen in the northern and eastern equatorial Indian Ocean. The Bay of Bengal is characterized by moderate negative loading while marginal negative loading is noticed in the Arabian Sea. This mode explains about 12% of the total SST variance. An earlier analysis (Tourre and White 1995) showed that the second EOF mode explains 14% of the total SST variability in the Indian Ocean, which is close to the present analysis.

The corresponding time coefficient (Fig.3.2 (b)) indicate that EOF mode indicate longer fluctuations in the analysis period. This shows a periodicity of about 500 days. In the Indian Ocean the second EOF mode is known to have a periodicity of 9-15 months (Tourre and White, 1995) during 1979-1991. During that period the second EOF mode showed warming during EL Nino years which is consistent with Pacific Ocean warming (Tourre and White, 1995). However this is not clear in the present analysis with exception during 1977, 1983 and 1987 and probably 1997.

Recent analysis showed that there are scales of variability unique to the Indian Ocean which caused abnormal weather in the Indian Ocean especially during 1961-1962 (Kapala et al 1994), 1993-1994 (Saji et al., 1999), 1997-98 (Webster et al., 1999, Murtugudde et al.,2000). Saji et al.,(1999) postulated that there exists a dipole mode of variability in the Indian Ocean where generally cold SST prevail in the western equatorial Indian Ocean while warm SST is observed in the eastern equatorial Indian Ocean. However in some years (eg. 1961 - 1962, 1993 – 1994, 1997 - 98) abnormally cold SST formed in the eastern equatorial Indian Ocean while warmer SST occurred in the western equatorial Indian Ocean which caused drought conditions over Indonesia while flood occurred over eastern Africa. Though presently it appears that this dipole mode may not have much impact on the Indian monsoon but is known to have immense influence on rainfall over eastern Africa and Indonesia (Webster et al., 1999; Saji et al., 1999; Murtugudde et al., 2000).

The third EOF mode explains about 9% of the total SST variability in the India Ocean. The third mode of EOF shows strong negative loadings over western Arabian Sea, eastern equatorial Indian Ocean and south western Indian Ocean while strong positive loading is confined to the south eastern regions of the Indian Ocean. FFT analysis of the corresponding time series reveals an oscillatory behaviour of the anomalies. Figure 3.2(c) shows the plot of the respective time series of third mode.

The time series indicate decadal periodicity which could be due to sunspot activity. Pacific Decadal Oscillations (PDO) are well documented (Mantua, 2001) and 1998 warming in Pacific is due to the sign change in PDO. The anomalous warming in IO also occurred during 1997-98 and moderately observed in time series of EOF3.

3.4 EOF Analysis of Precipitation Rate

Numerous studies have documented the link between ENSO and rainfall in many regions of the globe, associating the warm phase with drought conditions in some cases, unusually abundant precipitation in others. The most extensive and detailed study of this kind is Rapeswki and Halpert (1987, 1989) in which the change in the rainfall sampled over land and island stations within several regions around the globe is carefully analyzed depending on the prevailing ENSO conditions and found consistent correlation between rain anomaly and the ENSO.

Dai and Wigley (2000) using 1900-1978 data of land and island stations data carried out EOF analysis for ENSO induced precipitation anomalies and reported that changes in global precipitation anomaly patters are due to the Walker circulation generally and due to Hadley circulation over Indian Ocean.

In this study an EOF analysis has been carried out for the monthly precipitation rate anomaly and the spatial distribution of the leading three EOF modes are presented in Fig 3.3. All the three modes show positive and negative loadings. The first mode of EOF of PWT explains only 6% of the total variance

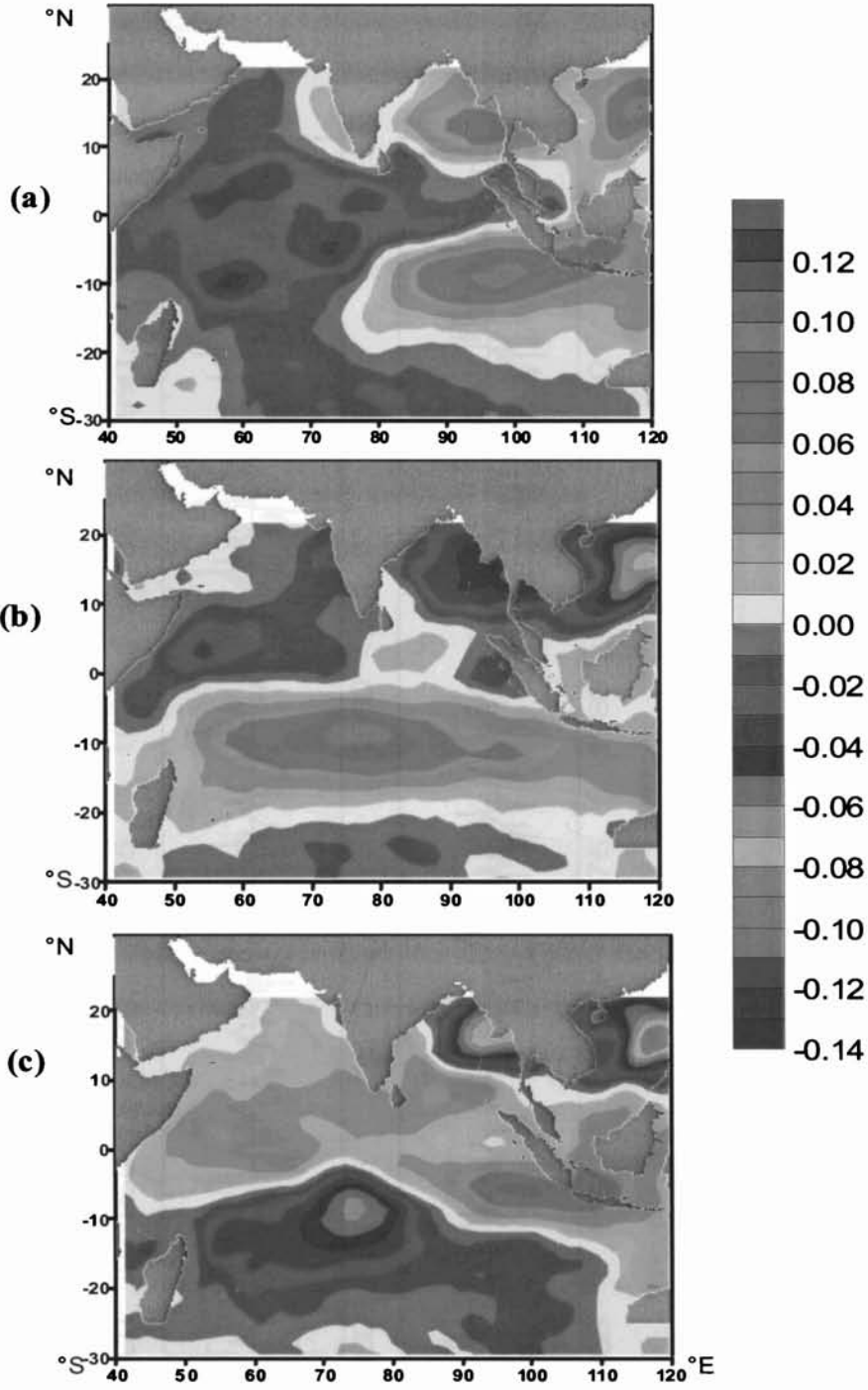


Fig 3.3 Spatial patterns of the first leading EOF modes for the monthly PWT anomalies over the Indian Ocean for the 39 year period 1960-1998 (a) EOF1, (b) EOF2 and (c) EOF3

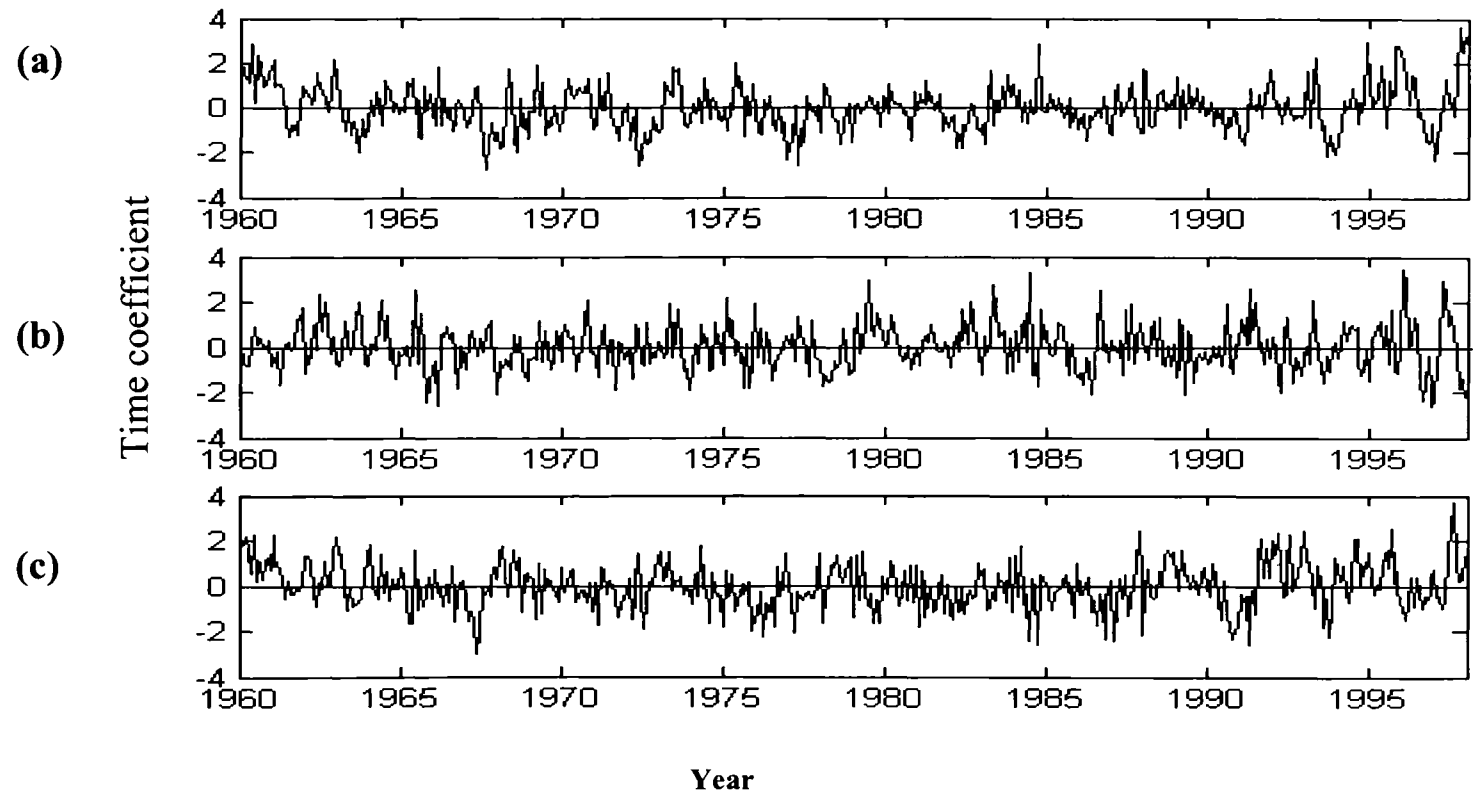


Fig 3.4 Time sequence of the first three EOF modes for monthly PWT anomalies over Indian Ocean for the 39 years period from Jan 1960-December 1998 (a) EOF1, (b) EOF2 and (c) EOF3

indicating that the variance in PWT in the Indian Ocean affected by a number of factors. This first EOF mode for the world ocean for 1997-2001 explains 13.5% of total variance (Haddad et al, 2004) compared to only 6% in the Indian Ocean. The first mode indicate strong positive loadings in the eastern Indian Ocean south of the equator and also in the eastern Bay of Bengal where as mostly negative loadings in the central and western Indian Ocean. The corresponding time series is also very heterogeneous (Fig 3.4). FFT analysis shows that the first EOF mode has a periodicity of about 500 days. And the secondary peak occurs similar to first mode of EOF for SST corresponding to El Nino.

The global monthly rainfall data from 1998-2002 using Tropical Rainfall Monitoring Mission (TRMM) showed that the first EOF mode is closely linked to El Nino (Haddad et al, 2004) though there can be regional differences. Dai et al., (2001) analysed global rainfall of 1900-1978 using EOF analysis and reported ENSO as the important factor. The results are based on land/island rain gauge data which leave vast areas of ocean unrepresented and hence a direct Precipitable water rate EOF comparison cannot be made with the present study. The first mode precipitation anomaly loading gradient over Indian region in this study is similar to the climatology from observational dataset of Legates and Willmott (1990).

The second mode of EOF of PWT (Fig 3.3 (b)) explains 5% of the total variance in the Indian Ocean compared to 5.6% for the world ocean rainfall (Haddad et al, 2004). The maximum positive loadings are observed in the central Indian Ocean south of the equator whereas negative loadings are observed in the Bay of Bengal, Arabian Sea and western equatorial Indian Ocean. The corresponding time series has a periodicity of about one year indicating the annual variance. Using 1956-1997 NCEP/NCAR data, Ajaymohan and Goswami (2000) reported that intra seasonal oscillation is the dominant contribution to the inter-annual variability in Indian rainfall and not directly to ENSO. Their study relate these intra seasonal and inter annual monsoon variability as governed by a common mode of spatial variability (mainly due to inter tropical convergence zone location).

The EOF3 of precipitation rate anomaly shows that positive loadings north of 5°S covering north Indian Ocean except the eastern part of Bay of Bengal and

negative loading to the South Indian Ocean areas which explains 4% of total variability.

Analysing the time coefficient, the ENSO years are 1965-66, 1972-73, 1976-77, 1982-83 1986-87 and 1997-98, it is found that excess rainfall is not pronounced from time series of these modes except for 1997-98 in EOF1 and EOF3.

Good monsoon years based on Indian Summer Monsoon Rainfall (ISMR) of Indian Meteorological Department are 1961, 1970, 1975, 1983 and 1994. Analysing time coefficient the excess can be seen in EOF2 generally, except in 1961. Bad monsoon (dry) years based on ISMR are 1965, 1966, 1968, 1972, 1979, 1982 and 1987. The time coefficient of EOF2 correspondingly shows deficit generally in EOF2.

According to the definitions of and weak monsoon based on intra - seasonal oscillations (Ajaymohan and Goswami, 2000), strong monsoon years are 1970, 1975, 1983 and 1988. In which EOF2 mode generally follows the excess rainfall but not so pronounced for 1988. The weak monsoon years are 1965, 1966, 1968, 1972, 1974, 1979, 1982 and 1985 and the time coefficient of second mode also shows negative peaks correspondingly but not so pronounced during 1979 and 1985.

3.5 EOF Analysis of Zonal Wind Stress Component

The spatial distribution patterns of leading EOF modes of zonal wind stress component are shown in Fig 3.5 and associated amplitude functions in Fig 3.6. The first mode of EOF shows positive loadings in the southern Indian Ocean while negative loadings most of other regions of Indian Ocean. The first mode of EOF explains 15% of the total variance. The FFT analysis of time series indicates a periodicity of one year suggesting annual variance.

The second mode of EOF explaining 9% of the total variance with maximum positive loadings in the south central Indian Ocean, and weak negative/positive loadings in the Arabian Sea and Bay of Bengal. FFT of time series of second EOF mode is also is dominated by annual periodicity.

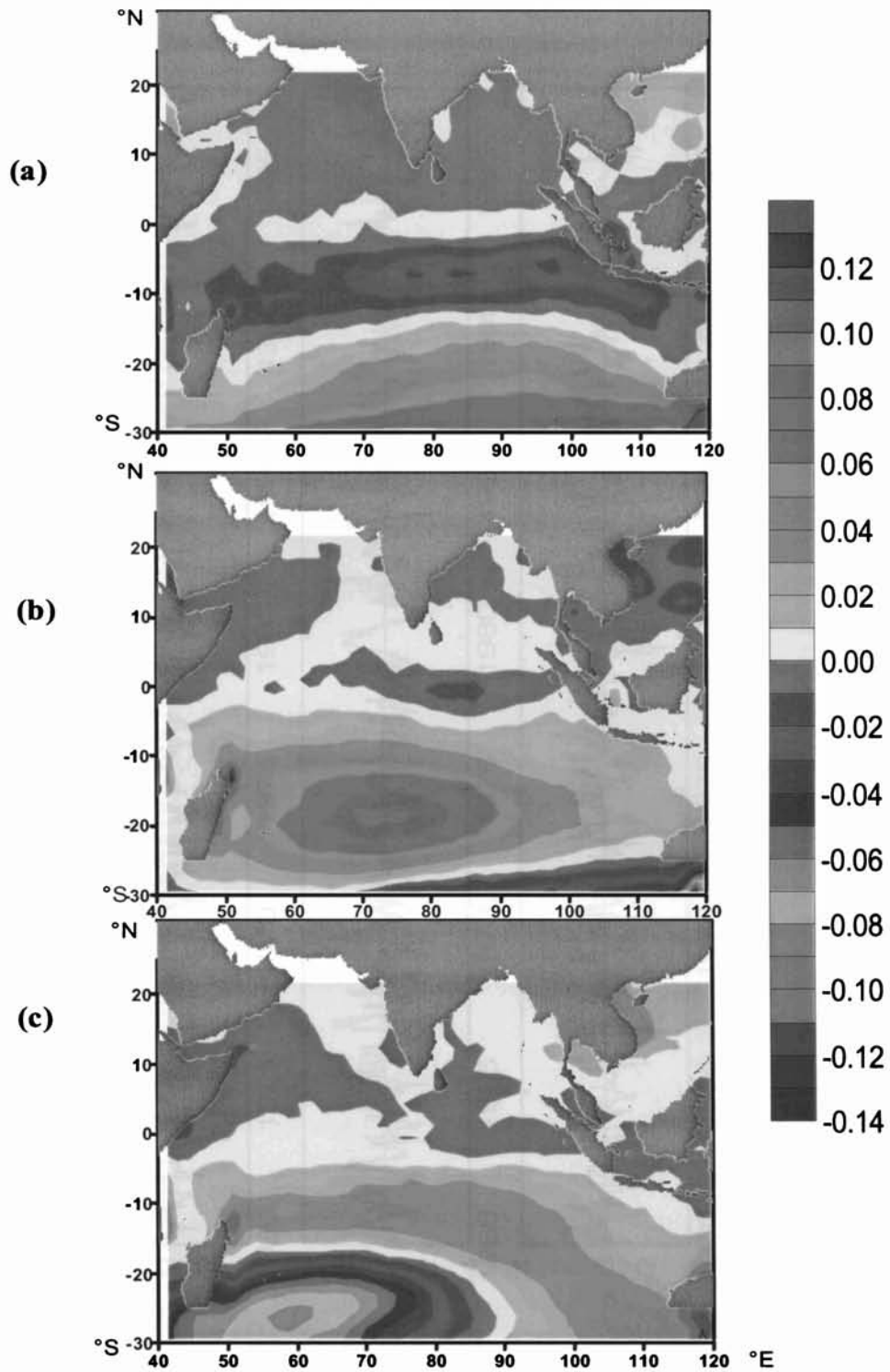


Fig 3.5 Spatial patterns of the first leading EOF modes for the monthly zonal wind stress anomalies over the Indian Ocean for the 39 year period 1960-1998 (a) EOF1, (b) EOF2 and (c) EOF3

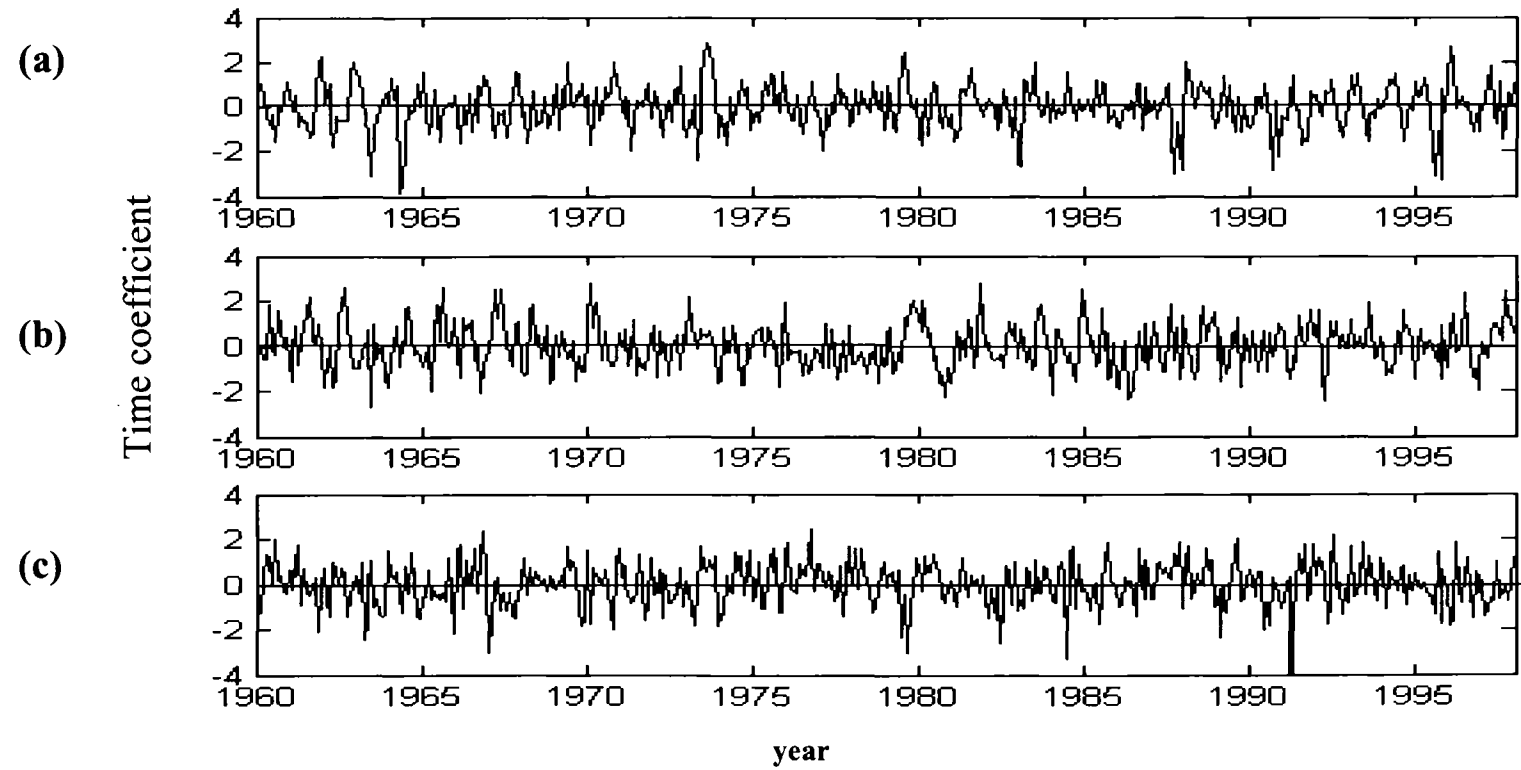


Fig 3.6 Time sequence of the first three EOF modes for monthly zonal wind stress Anomalies over Indian Ocean for the 39 years period from Jan 1960-December 1998
 (a) EOF1, (b) EOF2 and (c) EOF3

The third mode shows negative loading concentrated on the southwestern Indian Ocean, which accounts for 6% of variance. The loading pattern is such a way that both sides of the positive loading in the southeast to northwest direction covered with negative pattern.

3.6 EOF Analysis of Meridional Wind Stress Component

The first EOF mode shows negative loadings only at the southern Indian Ocean of the studied area while positive loadings most of other regions of Indian Ocean. The first mode of EOF explains 12% of the total variance. The frequency analysis of time series indicates a periodicity of one year suggesting annual variance.

The second mode of EOF explain 10% of the total variance and the spatial patterns are similar to the first mode. The FFT of time series of second EOF mode is also is dominated by annual periodicity.

The third mode shows negative loading concentrated on the southern Indian peninsula. Generally all loading patterns are such a way that it increases towards southern hemisphere without much differences in between.

3.7 Summary

First mode of EOF analysis in SST indicated positive loading in almost the Indian Ocean with higher values in the Arabian Sea, equatorial and southwestern and central Indian Ocean and lower values in the Bay of Bengal and eastern Indian Ocean. The second EOF mode shows positive loadings in the southwestern and southern regions of the Indian Ocean while strong negative loadings are seen in the eastern and northern equatorial Indian Ocean. The Bay of Bengal is characterized by moderate negative loading while marginal negative loading is noticed in the Arabian Sea. The third mode of EOF showed strong negative loadings over western Arabian Sea, eastern equatorial Indian Ocean and south western Indian Ocean while strong positive loading is confined to the southeastern regions of the Indian Ocean. They respectively account for 29%, 12% and 9% of the variance. Frequency analysis of the time series of the first of these three modes showed periodicity of 2.7 years, 500 days and

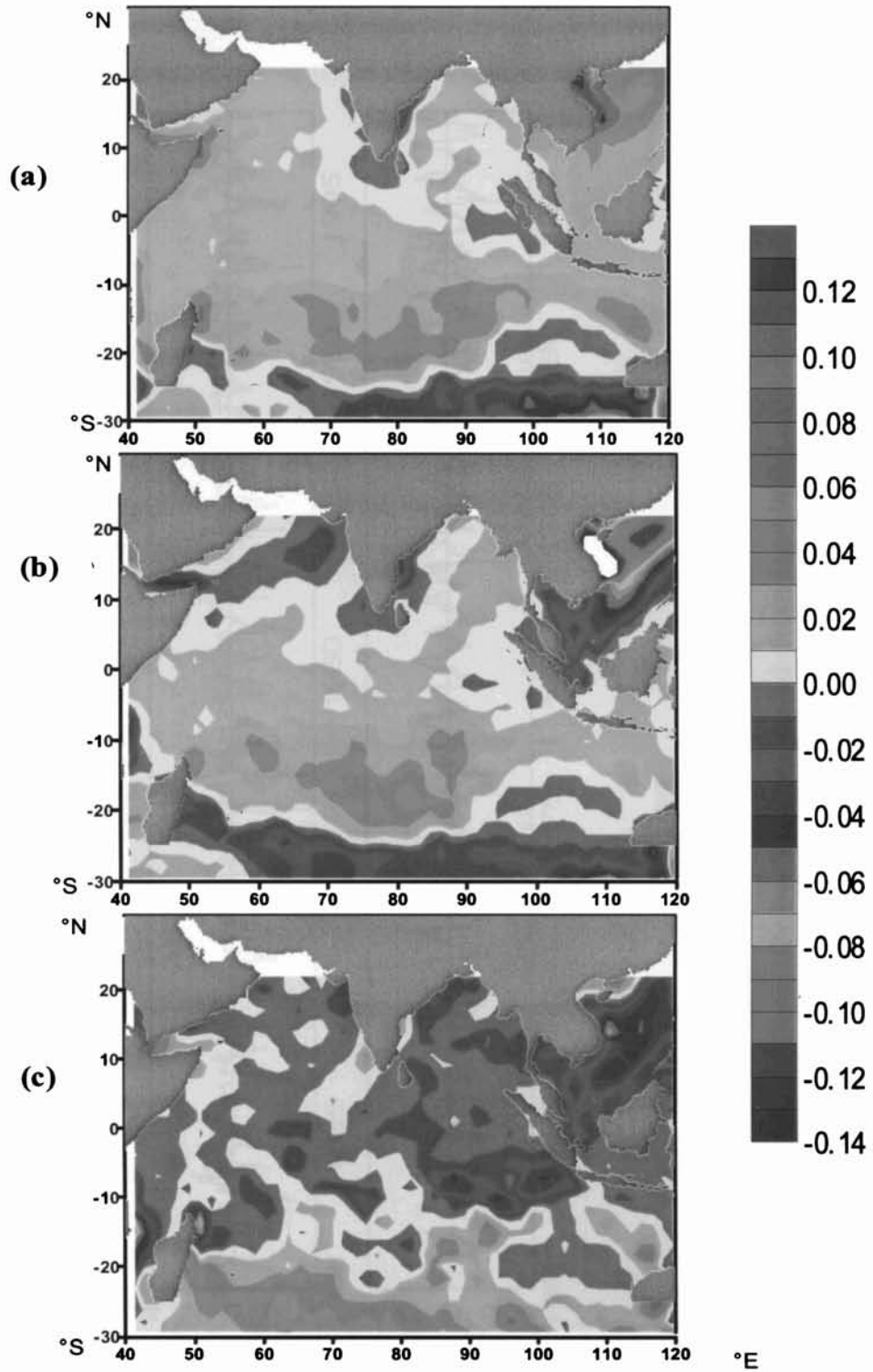


Fig 3.7 Spatial patterns of the first leading EOF modes for the monthly meridional wind stress anomalies over the Indian Ocean for the 39 year period 1960-1998 (a) EOF1, (b) EOF2 and (c) EOF3

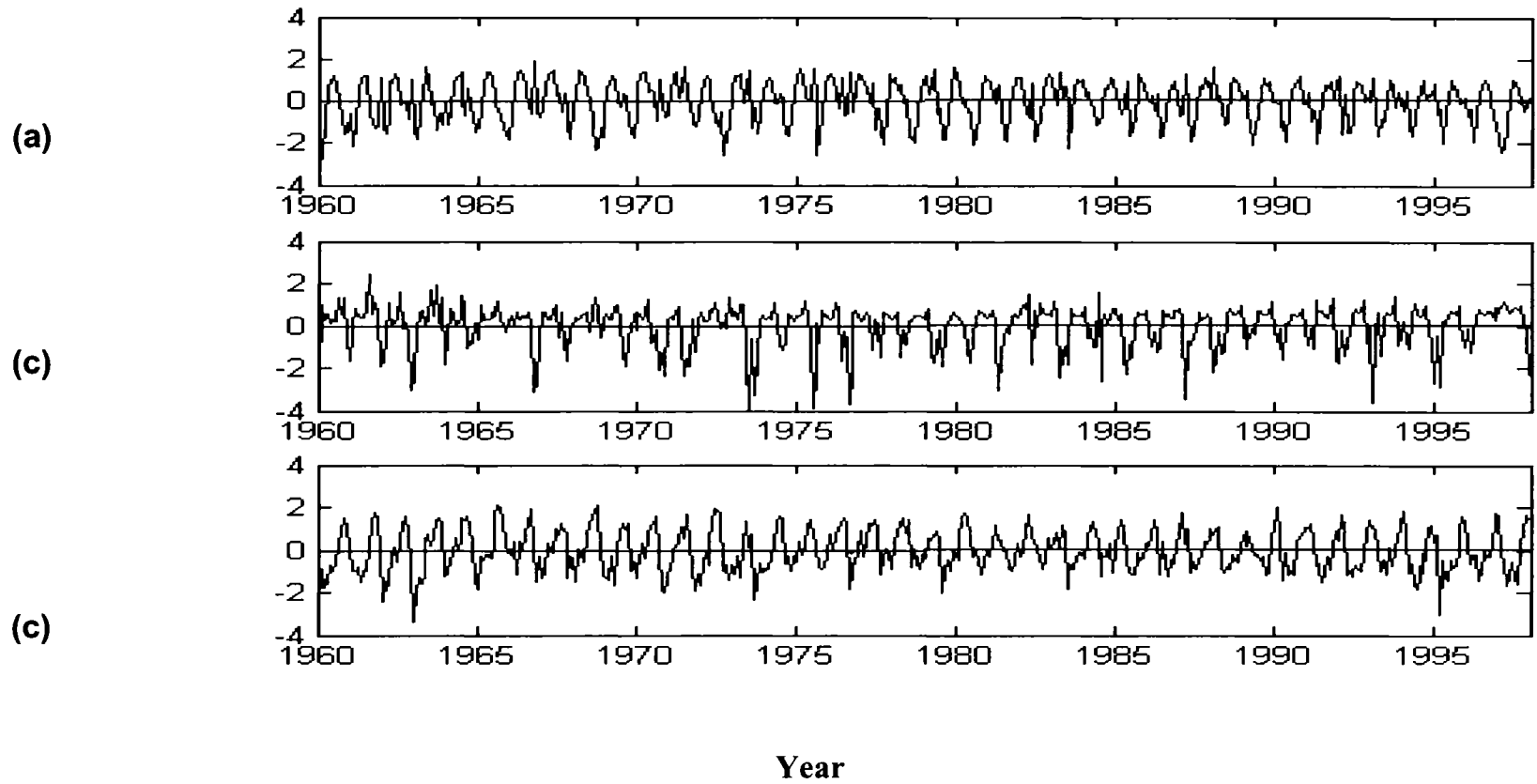


Fig 3.8 Time sequence of the first three EOF modes for monthly meridional wind stress anomalies over Indian Ocean for the 39 years period from Jan 1960-December 1998 ;
(a) EOF1, (b) EOF2 and (c) EOF3

10 years respectively. Hence the first EOF mode can be identified as ENSO mode and third with decadal oscillations

The El Nino occurred in 1965 - 1966, 1969 - 1970, 1972 - 1973, 1976 - 1977, 1982 - 1983, 1986 - 1987 and 1997 - 1998 within the study period. The significant warming in the Indian Ocean took place in 1969, 1973, 1977, 1979, 1983, 1987, 1991 and 1998. Out of these except 1979 and 1991 the warming of the Indian Ocean is in phase with the occurrence of El Nino. Incidentally during the El Nino of 1965-1966 and 1992-93 cooling instead of warming took place in the Indian Ocean, which indicate the influence of other forcing mechanisms in regulating SST in the first EOF mode. However, presently it is not clear the mechanism which offset the influence of El Nino in these years. The first EOF mode showed significant cooling of the Indian Ocean during 1964-65, 1968, 1971, 1974-76, 1988 and modulate cooling during the early 1990's. The cooling during this period either coincided with La Nina or preceded El Nino except in the early 1990's. The warming in the Indian Ocean during 1998 was abnormally high where the first and third modes of EOF contributed warming.

The first, second and third EOF mode of precipitation rate explain 6%, 5% and 4% of the variability respectively indicating that the variance in PWT in the Indian Ocean affected by a number of factors. The first mode indicates strong positive loadings in the eastern Indian Ocean south of equator and Bay of Bengal whereas negative loadings are seen on central and western Indian Ocean. The maximum positive loadings in EOF2 of precipitation rate are observed in the central Indian Ocean south of the equator whereas negative loadings are observed in the Bay of Bengal, Arabian Sea and western equatorial Indian Ocean. The EOF3 of precipitation rate anomaly shows that positive loadings north of 5°S covering north Indian Ocean except the eastern part of Bay of Bengal and negative loading to the South Indian ocean areas. The frequency analysis of respective time series shows major peaks at 500 days in EOF1 and one year in EOF2. Analysis of the EOF2 time coefficient of precipitation rate shows that it has similarity to Indian rainfall to a certain extend and the differences can be due to land - ocean differences.

The first mode of EOF of zonal wind stress shows positive loadings in the southern Indian Ocean while negative loadings most of other regions of Indian Ocean. The second mode of EOF shows maximum positive loadings in the south central Indian Ocean, and weak negative/positive loadings in the Arabian Sea and Bay of Bengal. This spatial loading pattern looks similar to EOF2 mode of precipitation rate. The third mode shows negative loading concentrated on the southwestern Indian Ocean. The loading pattern is such a way that both sides of the positive loading in the south east to north west direction is covered with negative pattern. They explain 12%, 10% and 6% of the total variance. The frequency analysis of EOF1 and EOF2 time series indicates a periodicity of one year suggesting annual variance.

First mode of meridional wind stress accounts for 12% and EOF2 accounts for 10% of variability. The first and second EOF mode shows negative loadings only at the southern Indian Ocean of the studied area while positive loadings most of other regions of Indian Ocean. The third mode shows negative loading concentrated on the southwestern Indian Ocean. Generally the loading pattern are such a way that it increases towards southern hemisphere without much differences in between. The frequency analysis of EOF1 and EOF2 time series indicates a periodicity of one year suggesting annual variance.

Time Frequency Analysis

4.1 Introduction

In the preceding chapter 3, the spatio-temporal variability of the sea surface fields are studied as standing wave oscillations using EOF analysis. In which the modes are considered as independent. Based on the variance of respective modes, the characteristic of the studied parameter's variability in each mode is understood. But the variability in periodicity observed in these fields is less understood and they are considered as different scales separately. In this chapter an attempt has been made to extract the period of oscillations inherent in these fields with respect to time using wavelet analysis. As these periodicities may differ from position to position, different locations are selected for study to reveal their spatial variability.

The time series plot directly gives an idea of the amplitude variations of SST field during 1960-1998. The Fourier spectrum gives the energy density for each oscillation which explains the dominant periodicity at each location. The Fourier transform in spectral analysis maps a signal from time to frequency domain, providing a time –mean power spectrum. It fails to reveal possible variations in oscillation characteristics with time. Since some of the oceanographic phenomena are localized in time the Wavelet Transform (WT)

method is highly suitable to study such phenomena as the time information is lost in Fourier analysis. These studies are helpful to understand the temporal component of the air-sea interaction processes at different time scales. By using this relatively new method, this study also aims at investigating relationships among variations on the inter-decadal to 30 days time scales. The overall spatial structure of these fields is studied in the previous chapter by applying conventional EOF method.

4.2 Station Locations

The Morlet wavelet analysis described in chapter 2 has been carried out for sea surface temperature, u-stress, v-stress and precipitation rate from NCEP/NCAR daily dataset.

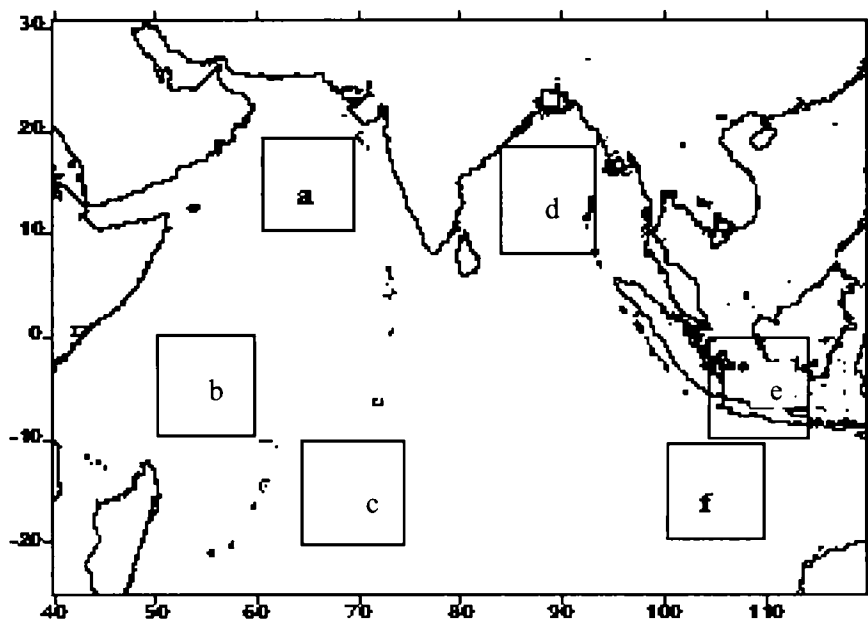


Fig 4.1 Station locations map (a) Arabian Sea (AS), (b) western EIO (WEIO), (c) western SIO (WSIO), (d) Bay of Bengal (BB) , (e) eastern EIO (EEIO) and (f) eastern SIO (ESIO)

In the present work other wavelet bases, such as Mexican hat and Daubechies have been tried out. These analyses have given a qualitative picture of variability in different surface parameters. For this purpose, time series data at 6 locations (fig 4.1) over Indian Ocean are selected covering Arabian Sea, Bay of Bengal, Equatorial Indian Ocean (EIO) and South Indian Ocean (SIO). Each

box selected for the study has a spatial resolution of $10^{\circ} \times 10^{\circ}$. The domains selected for this study essentially covers the regions influenced by the summer monsoon.

The Indian Ocean is the only ocean with climatological westerly winds on the equator. It is also unique due to the fact that it undergoes cooling the northern summer, a phenomenon known as summer monsoon cooling (Krishnamurthy et al., 1989). The shear between westerlies and the southeasterly trades results in an open-ocean upwelling band just south of equator. Hence the locations EIO are taken just south of equator. Spatial averages are computed for each location using NCEP gridded data available in the respective boxes (Table 4.1).

Table 4.1

Location details of Morlet wavelet analysis

Grid	Latitude	Longitude	label
Arabian Sea	$10^{\circ} \text{ N} - 20^{\circ} \text{ N}$	$60^{\circ} \text{ E} - 70^{\circ} \text{ E}$	a
Bay of Bengal	$10^{\circ} \text{ N} - 20^{\circ} \text{ N}$	$85^{\circ} \text{ E} - 95^{\circ} \text{ E}$	d
Eastern EIO	$0^{\circ} - 10^{\circ} \text{ S}$	$105^{\circ} \text{ E} - 115^{\circ} \text{ E}$	e
Western EIO	$0^{\circ} - 10^{\circ} \text{ S}$	$50^{\circ} \text{ E} - 60^{\circ} \text{ E}$	b
Eastern SIO	$20^{\circ} \text{ S} - 10^{\circ} \text{ S}$	$100^{\circ} \text{ E} - 110^{\circ} \text{ E}$	f
Western SIO	$20^{\circ} \text{ S} - 30^{\circ} \text{ S}$	$65^{\circ} \text{ E} - 75^{\circ} \text{ E}$	c

Daily data set of NCEP/NCAR for a period of 1960-1998 is used for the Morlet wavelet analysis. Five day average of each parameter has been computed. Thereafter, anomalies for each 5 day have been computed by subtracting the climatological 5 day mean from the 5 day data set. As described in Torrence and Compo, (1998) the minimum resolution we can achieve is 1/5 days which is equal to 0.2 day^{-1} . The wavelet scale selected for the present study is 0.4 (2×0.2) to 1024 with 0.2 step which explains periodicity up to 14 years which covers inter-decadal periodicity. As the small scale features are not discernable in the signal two more sets of Wavelet Trasforms (WT) with 256 and 64 data points are also carried out. The first set describes variability with a

periodicity up to 1280 days whereas oscillations up to a period of 320 days could be resolved when second dataset is used. When maximum scale is chosen as 64, the study was carried out only for a short period of 3 years (1996 – 98).

The data at each grid point is padded at the beginning by the half of the same data set and at the end by the second half of the data set. This process has doubled the size of data compared to original length and then wavelet analysis has been carried out. A comparison between the padded and the unpadded has been carried out before analysis. This gives us an idea of error if any in WT estimates at the beginning and at the end of data series (cone of influence). It is observed that the process of padding has not affected the results. Hence, the data set without padding are used for computation.

4.3 Results

4.3.1 Sea Surface temperature (SST)

SST and its anomaly are thought to be important symbols of the ocean thermodynamic parameters governing the air-sea interaction processes. The temporal variability of SST during 1960-1998 has been studied using time series plot, spectral and wavelet analysis. The temperature structure itself and the process interacting with it are multi-scale and hence this type of analysis is highly useful.

4.3.1.1 Time series, Spectrum, Autocorrelation Analysis

The time series of SSTA at different locations used in this study is presented in Fig 4.2. It is seen that the anomalies are in the range of the order of -1.5 to 1.5° C for the entire Indian Ocean. Another interesting observation is that they are weak (less than $\pm 1^\circ$ C) up to 1980 and increased thereafter. It is observed that SST has not much deviated from the normal value except during 1964-65 in Arabian Sea. In this period, a higher cooling than the normal is indicated. During 1970 -1980, there are three cooling episodes with 2 to 3 years duration and comparatively warming trend is noticed in 1983 and 1987. At the end of 1980-90 continuous positive anomalies are seen for 2 years which shows warming. A warming trend is seen towards end of last decade of the data set.

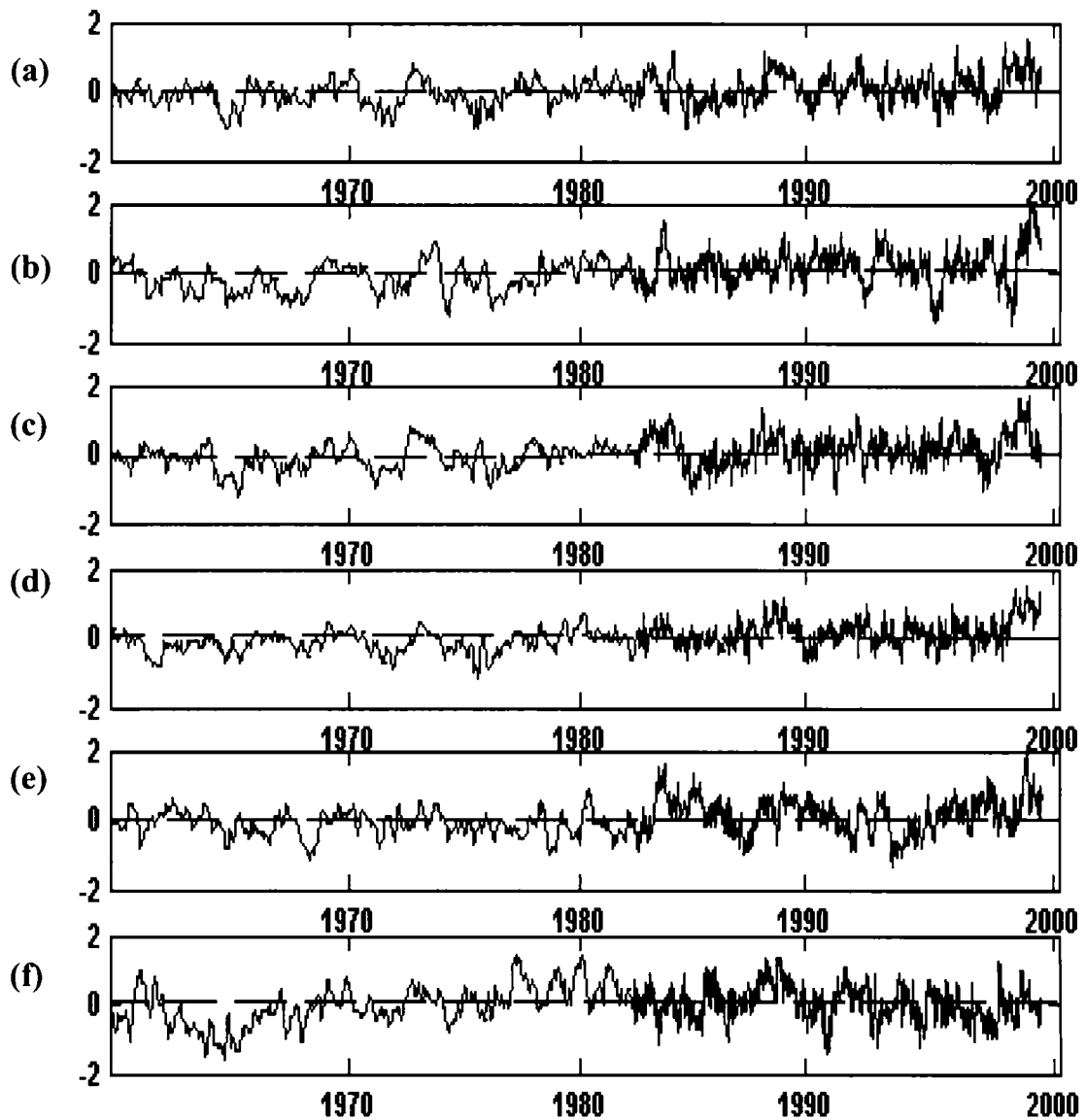


Fig 4.2 Timeseries of SST anomalies (5day averaged) for 1960-1998 (a) Arabian sea (b) eastern EIO, (c) western EIO, (d) Bay of Bengal, (e) eastern SIO and (f) western SIO

Over the Eastern EIO (EEIO) as shown in Fig. 4.2(b) SSTA is negative till 1980. In 1984-85, 1994-95 and 1997-98 the anomaly values are comparatively more positive ($1-2^{\circ}\text{C}$) indicating sea surface warming.

Fig. 4.2 (c) is the time series at the Western EIO location which shows more cooling during 1964-1965 and 1972-1973. During the first two decades of the dataset 1972-73 recorded as warming at this location. In 1980-1990 decade,

warming in 1983-1984 and 1985-1986 are indicated. Then SSTA values in 1997-1998 shows highly positive.

In Bay of Bengal (BB), Fig. 4.2 (d) the SST exhibited negative values from climatological mean during 1960-70. In 1989-90 and 1997-98 significant positive anomalies are seen. At the Eastern SIO (ESIO) the SST deviations from the 40 year climatological 5 day mean in Fig 4.2 (e), is predominant in 1968-69 and 1978-80 negatively. During 1982-94, warming of sea surface and cooling repeated alternatively for 2-3 years. Then a clear warming trend is seen during 1990-98.

The Fig. 4.2 (f) represents the time series of 5-day SSTA at the western SIO (WSIO) location. It shows that SST deviates drastically from the climatological mean. The warming and cooling episodes are stronger and prolongs for more period. At all these selected locations cooling is recorded during 1964-65, 1970-71 and 1975-76.

After 1980 the negative anomalies are not so pronounced for any location in the same time frame. The positive anomalies are seen during 1969, 1972-1973, 1983-1984, 1987-1988, 1992-1993 and 1997-1998. The amplitude of positive anomalies has comparatively high values in 1997-1998 except at ESIO. Similar is the case with 1972 and 1984. From this time series data at these locations, it can be concluded that different locations experiences variable thermal signatures and the trend is different.

The climatological 5 day mean for Jan- Dec is presented in Fig 4.3. It can be seen that the climatological average of SST at each location varies so differently than the other location. The difference can be noticed for amplitude as well as the phase. Especially over western SIO the amplitudes are very low and the peak value reaches much before all other areas. Generally they all have one crest and trough except for Arabian Sea where it shows two crests. The variation in temperature is within 24-30⁰C for all locations except for WSIO where SST range is within 19.5-25 ⁰C only. The SST has the highest value at the WSIO during February 4th pentad and minimum value in August 3rd pentad. At the ESIO the maximum value is in March 1st pentad, but the lowest SST record is the same in August 3rd pentad. In April 3rd pentad SST over WEIO peaks and the trough's minimum is in the last pentad in July and the seasonal oscillation effects

can be seen. Like over Arabian Sea the seasonal effects can also be seen over BB and EEIO but with lesser magnitude.

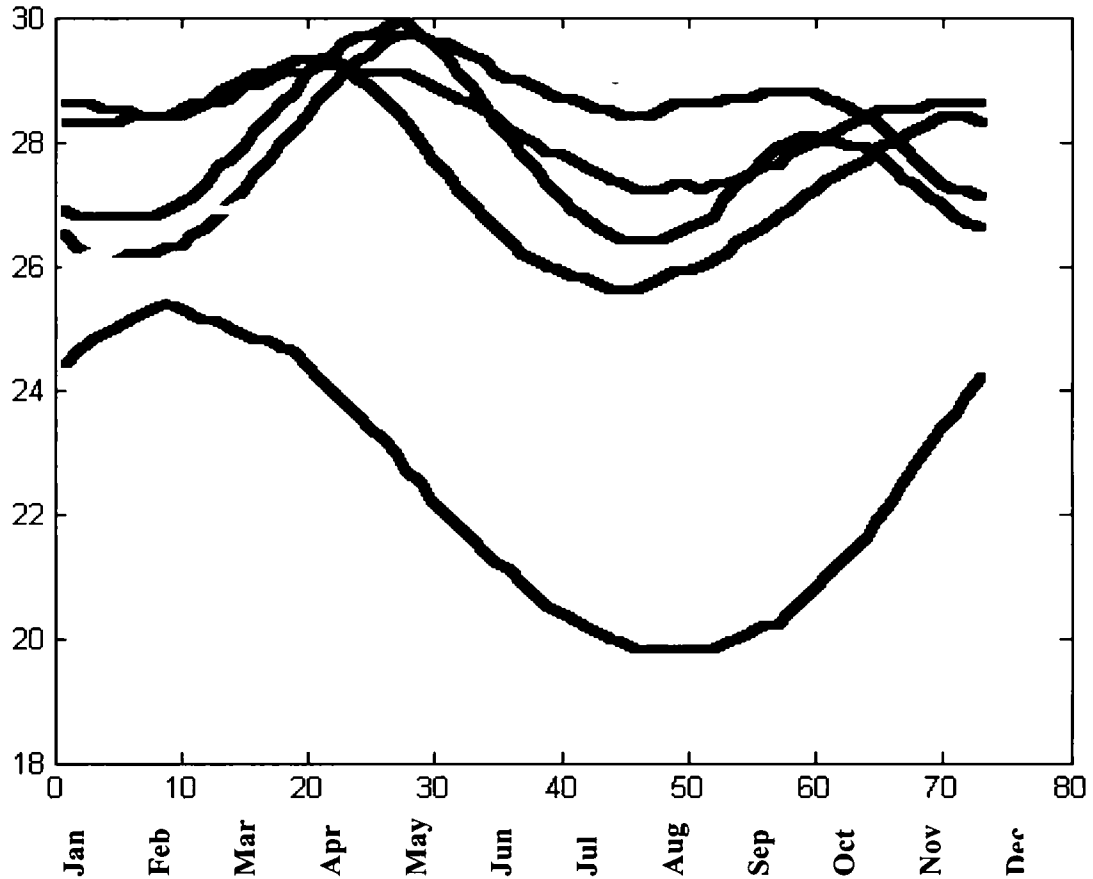


Fig 4.3 Climatological mean of 5 day averaged SST from 1960-1998 daily data of NCEP/NCAR for Arabian sea-red Eastern IO-green, western IO-black, Bay of Bengal-blue, , western SIO-magenta from top to bottom.

EEIO and BB peaks in May 1st pentad and reaches the lowest value in August 3rd pentad. It can also be seen that over tropical Indian Ocean, Arabian Sea SST behaves differently that it peaks in May 3rd pentad and lowers in August 1st pentad. The secondary peak occurs in October 1st pentad. Even though BB and AS response are almost the same in phase their amplitudes are different. The seasonal oscillations in Arabian Sea are very dominant and the peaks are significant. Similarly the WEIO and EEIO have a similar pattern, the

amplitude range is more for WEIO and a delay of 1 month is observed for EEIO. Generally phase effects are associated with latitude and amplitude variation with that of neighborhood. The sun's position river input and land locked sea are referred as the reasons for the surface signature differences over Bay of Bengal compared to Arabian Sea.

To estimate the frequency content in these time series Fourier spectral estimates are computed (Fig. 4.4), for SSTA over these six areas in TIO.

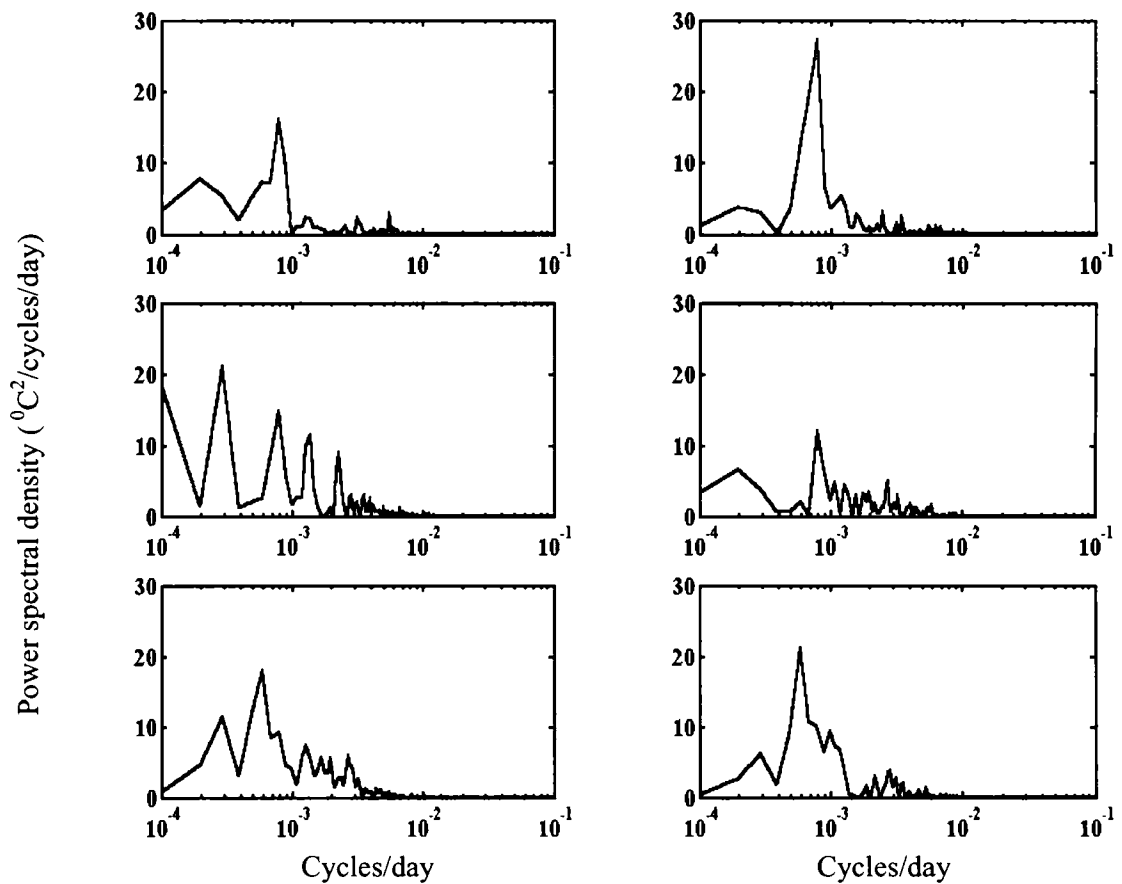


Fig 4.4 Spectra of the time series of five-day SST anomaly at the grid locations (a) Bay of Bengal, (b) Arabian Sea, (c) western SIO, (d) eastern SIO, (e) eastern EIO and (f) western EIO.

09064

Table 4.2

Frequency - period conversion table

Frequency Cycles/day	Period	Frequency Cycles/day	Period
$10^{-3.9}$	21.7 yr.	$10^{-2.9}$	2.17(yr)
$10^{-3.8}$	17.28 yr.	$10^{-2.8}$	1.7 yr.
$10^{-3.7}$	13.28 yr.	$10^{-2.7}$	1.37 yr.
$10^{-3.6}$	10.9 yr.	$10^{-2.6}$	1.09 yr.
$10^{-3.5}$	8.66 yr.	$10^{-2.5}$	316 days
$10^{-3.4}$	6.88 yr.	$10^{-2.4}$	251 days
$10^{-3.3}$	5.466 yr.	$10^{-2.3}$	199 days
$10^{-3.2}$	4.34 yr.	$10^{-2.2}$	158 days
$10^{-3.1}$	3.4 yr.	$10^{-2.1}$	125 days
$10^{-3.0}$	2.7 yr.	$10^{-2.0}$	100 days

Generally the spectrum peaks at 4.3 years and 21 years respectively. At the western SIO as shown in fig (c) the highest peak is at 17 years and the next at 4.3 years. Over EIO (Fig 4.4 (e) and (f)) the highest peak correspond to 6 year periodicity. To reveal the periodicity seen in Fig 4.4 the conversion table for easiness is given as table 4.2.

Now from this 39-year time series analysis, 5 day climatological values and the Fourier spectrum it is clear that the SST behaves differently over the study areas. The time evolution of the oscillatory behaviour of these SST anomalies is studied using Morlet wavelet.

Before going for the wavelet analysis, auto correlation of the respective time series have been computed to reveal the presence of any multi scale periodicities. The computed results are plotted in Fig 4.5.

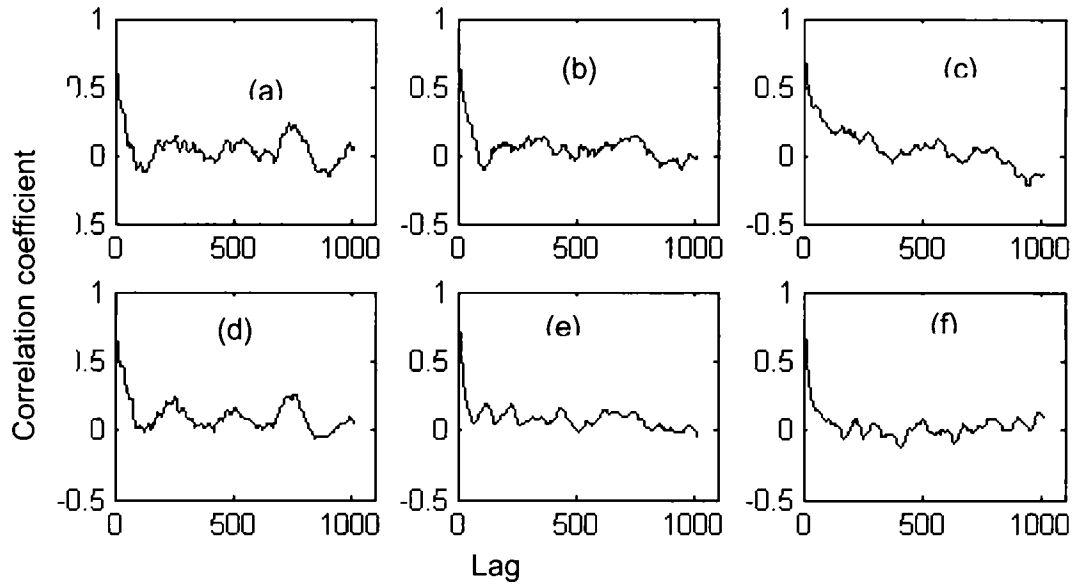


Fig 4.5 The autocorrelation coefficient of the time series of five-day SST anomaly at the grid locations (a) Bay of Bengal, (b) Arabian Sea, (c) western SIO, (d) eastern SIO, (e) eastern EIO and (f) western EIO.

This analysis shows that multi scale periodicities are present in SST anomaly over tropical Indian Ocean. Y axis represents the auto correlation coefficient. Values are plotted against lag. As the maximum scale which can be applied to wavelet analysis is only 1024 the maximum lag computed is restricted to this limit. The peak is generally around 700-850 which correspond to 9.5 -11.5 years. But at WEIO, EEIO and WSIO they are not so dominant.

4.3.1.2 Wavelet Analysis of Sea Surface Temperature Anomaly (SSTA)

Figures 4.6, 4.7 and 4.8 show the results of the wavelet analysis of the SSTA time series at the selected locations in TIO as shown in Fig 4.1. The modulus of wavelet transform (WT) is computed for the long scale (1024) up to 14 years and small scale (256) up to 640 days. They are presented in Fig 4.6 and Fig 4.7 respectively. As the oscillations with period less than a year is not clearly seen by these two sets, from SSTA for the recent three years (1996-98) of SSTA is analysed up to a maximum scale limit of 320 days and presented in Fig 4.8. The corresponding Wavelet analysis on these SSTA time series reveal a changing time evolution pattern for these regions in Tropical Indian Ocean.

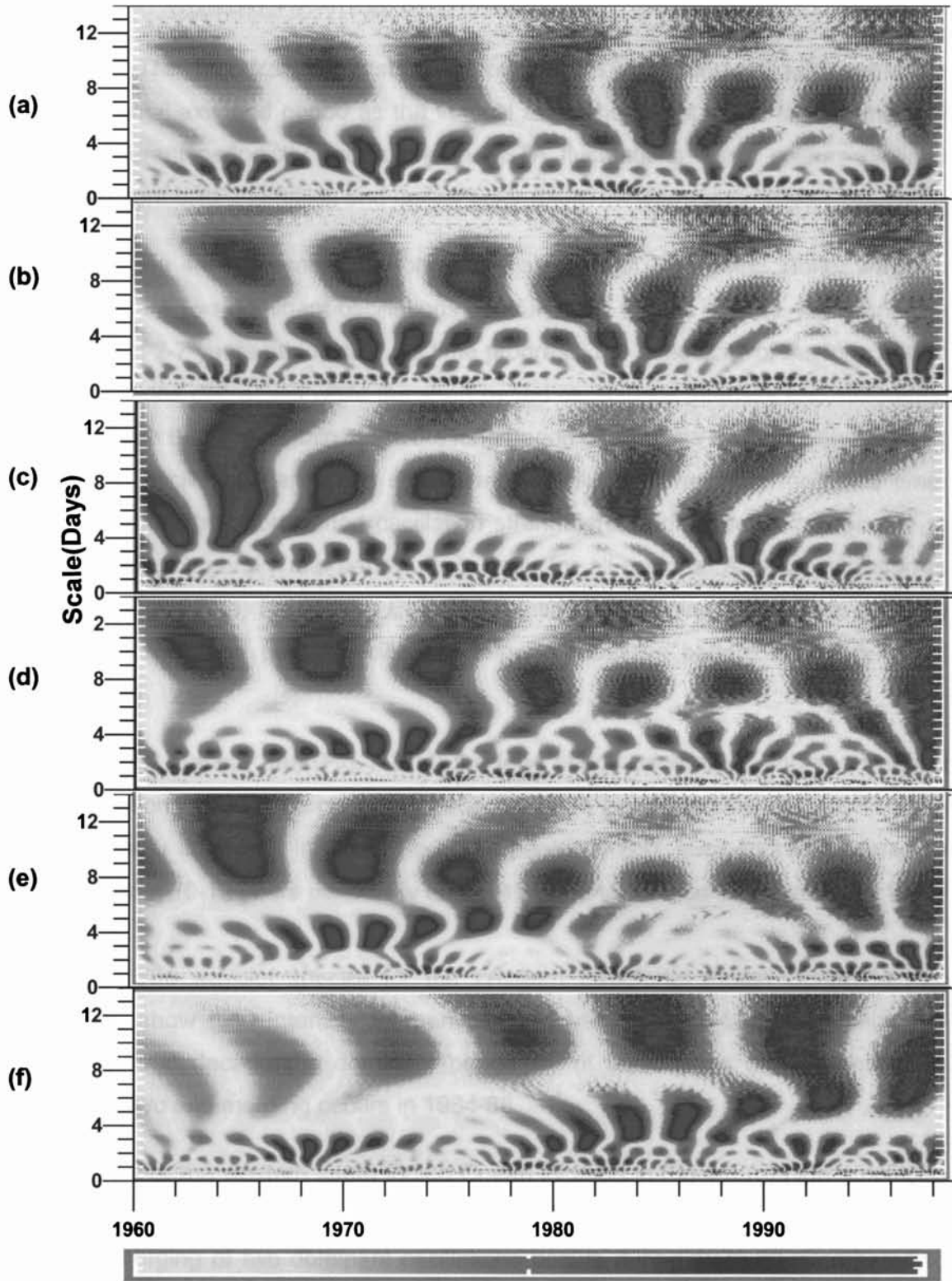


Fig:-4.6 Wavelet amplitude for the monthly SSTA(⁰C) time series (1960-98)
(a)Arabian Sea (b) western Equatorial IO (c) Western SIO (d)Bay of Bengal (e) Eastern EIO (f)Eastern SIO

The time-frequency structure of the SSTA is shown, with years on horizontal axis and period as the vertical axis. The colors stand for the intensity of different periodicity oscillations in SSTA fluctuations. Light colours (yellow) represent cold anomalies and darker colors (blue) for warm anomalies.

Fig 4.6 represents the long scale analysis of SST using Morlet wavelet. There are two dominant oscillations seen in SST. One is at 6-14 years and the other of 2-7 years periodicity. As time progress, the periodicity of the long period oscillations decreases while the short period oscillations intensify and increases. It is seen that at a certain stage the long period oscillations merges with the short period oscillations and then short period oscillations vanishes for some time. Thereafter the short period oscillation strengthens and its periodicity seems to increase. Generally this behaviour is seen for all regions. A clear indication is seen Fig. 4.6 (e) for eastern EIO. But the time of merging varies from place to place. The short period oscillations show a repetitive pattern for every 10-12 years.

In Arabian Sea (Fig. 4.6(a)) the long period oscillations and short period oscillations in SST merge during 1984-86. Short period oscillations in SST have maximum amplitude in this region. The period of SST fluctuations appeared to shift from 10-12 years periodicity during 1960-80 to 3-6 years periodicity in 1980-98.

The wavelet spectra for the Western Equatorial Indian Ocean in Fig. 4.6(b) show high intensity for periods 7-14 years and 2-4 years. During the 1988-1998 decade the dominant periodicity of fluctuations are different than these two and merging occurs in 1984-86.

For the western south Indian Ocean location in Fig 4.6 (c) high amplitude in wavelet transform are seen mainly of 3-14 year periodicity during 1963-65. The merging of two dominant oscillations occurs during 1978-80. Compared to other 5 locations, the amplitude is generally less during the last decade. As the time progress cascading of short period oscillations between the long period oscillations is clearly seen at this location.

For Bay of Bengal (Fig 4.6(d)) there is a concentration of wavelet power mainly of 8-14 years, 6-8 years and 2-4 years in scale. At the end of the time

series merging of periodicities are observed. The 8-14 year fluctuations are seen during 1962 - 65, 1967 - 70 and 1974-76.

The most significant oscillation in eastern equatorial IO is the 7-14 year periodicity oscillations seen during 1963 - 65. The fluctuations in 7-14 year periodicity are dominant during the first half of the time series.

For the eastern south Indian Ocean in Fig 4.6(f), the intensity of wavelet transform increases progressively for the long period fluctuations. The two dominant modes and their merging during 1994-96 are clearly visible. During 1980-98, the intensity of the oscillations show that these periodicities are dominant in SST fluctuations.

Fig 4.7 depicts the results of Morlet wavelet analysis of the 5-day SST anomaly data at different areas over Indian Ocean up to a scale of 256 which correspond to 1280 days (3.5 years). The oscillations with more than 450 days periodicity are predominant generally. These fluctuations appear for about 2 years with a gap of 1 year. The intensity of these oscillations peaks up more over Bay of Bengal and eastern SIO. This period of oscillation has a lull in 1975 - 1990 over eastern EIO (Fig. 4.7(e)). Over a period of 18-20 years, the wide band periodicity oscillations shift to small band high period oscillations with period of 2.5 year (912 days) and above. During 1965-75 they are significant irrespective of the location.

Over Arabian Sea as seen in Fig 4.7(a) high amplitude in wavelet spectra of SSTA is seen with 320-1280 days periodicity. They are significant during the first 15 years of dataset. It is seen that the periodicity shifts to the higher end (more than 750 days) progressively and then move to long period oscillations again.

For the western equatorial Indian Ocean location in Fig 4.7(b) fluctuation in SST are mainly of 640 -1280 days during 1968-74, 1980-1984 and 1996-98. The fluctuations with period of 320-640 and 640-1280 days are the dominant modes over WSIO. The shift of periodicity from 640-1280 days to more than 1000 days appears at the beginning of 1961 -1964. The small scale periodicity in this scale range is seen during 1960 - 1965, 1975 - 80 and 1990 - 1995. Even though they are not so predominant, their presence can be noted continuously in

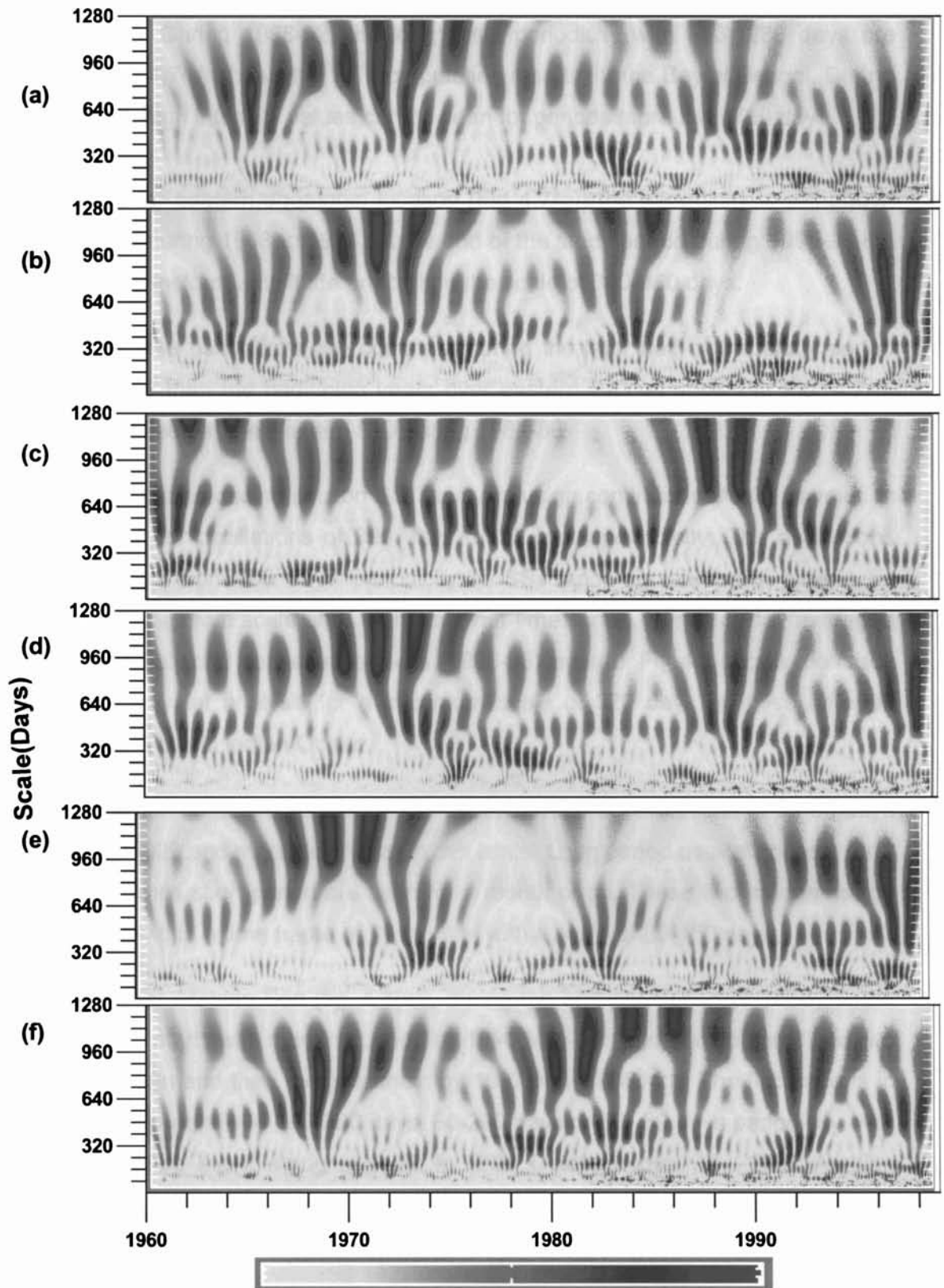


Fig:-4.7 Wavelet amplitude for the monthly SSTA($^{\circ}$ C) time series (1960-98)
(a)Arabian Sea (b) western Equatorial IO (c) Western SIO (d)Bay of Bengal (e)
Eastern EIO (f)Eastern SIO

975-1985. During 1988-92, the long scale periodicity with 640-1280 days are seen. Fig 4.7(d) shows the WT computation results for the Bay of Bengal. During 1970-74, high intensity values can be seen for periods more than 750 days.

Over eastern equatorial location (Fig 4.7(e)) the periodicity is still above 950 days during 1968 to 1974. At the end of the study period during 1995-98 the wavelet transform amplitude are high in the scale of 300-960 days.

These oscillations are dominant during the later half of the study period 1975-1998 than the beginning years over eastern SIO as shown in Fig. 4.7(f). They are seen at the western SIO during 1984-86.

In the preceding section SST analysis using continuous Morlet wavelet is discussed for oscillations of 300 days to 14 years periodicity. The oscillations with lesser than 300 days periodicity in SST anomaly are better visible by presenting up to a scale of 64 with a shorter time series. Hence 5- day averaged SST anomaly of 3 consecutive years (1996-98) is used. Fig 4.8 shows the result of SST wavelet analysis for a maximum scale of 320 days of these different areas in Tropical Indian Ocean.

It can be observed that two dominant modes of oscillations of 30-60 days and 200 -320 and more days exist in this scale. Long period oscillation lasts for 3 months while short period are seen for a month or so. These two modes merge together within a time frame of 18 months with a scale of 30-150 days.

Over Arabian Sea (fig. 4.8(a)), during the analysis period of 1996-98, the oscillation starts with merging period by 1996 May-Jun and decomposed into two by 1997 Jun and then merges again by 1997 Nov-1998Jan. The fluctuations in SST falls generally in 160-320 days, 60-200 days or 30- 80 days periodicity over WEIO. Here the merging appears in 1997 October-November. Over Arabian Sea and WEIO, the small period oscillations of 20-40 days are also seen continuously.

The merging of these two modes is clearly indicated in Fig. 4.8(c) by 1997 February - April for WSIO. When they appear separately the small period fluctuations have shorter periodicity compared to other areas. During the end of this data series these modes of fluctuations are not significant.

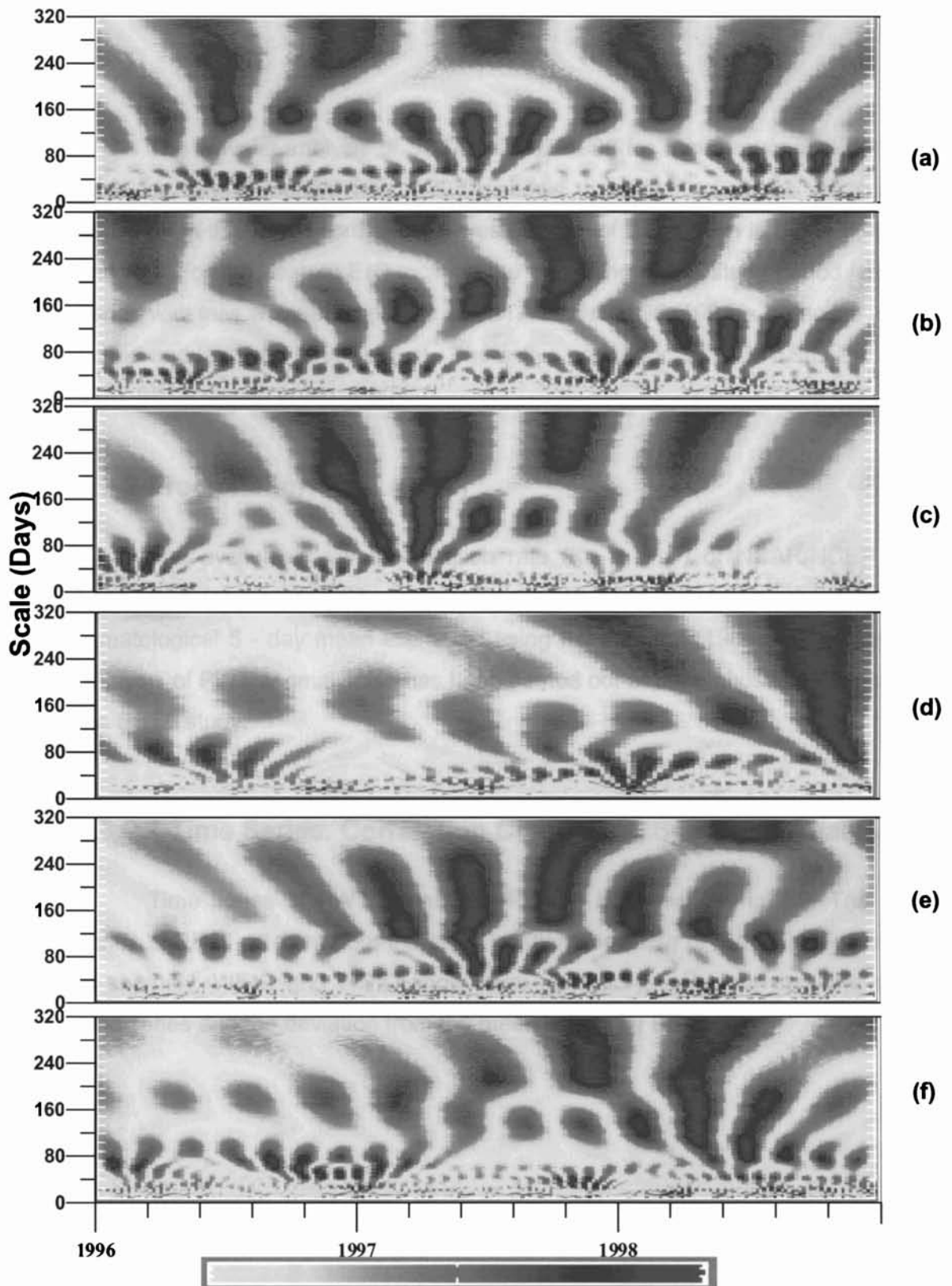


Fig:-4.8 Wavelet amplitude for the monthly SSTA($^{\circ}$ C) time series (1996-98)
 (a)Arabian Sea (b) western Equatorial IO (c) Western SIO (d)Bay of Bengal (e)
 Eastern EIO (f)Eastern SIO

The wavelet analysis of SSTA of 1996-1998 for a maximum scale of 320 days for Bay of Bengal (Fig. 4.8(d)) shows that the fluctuations are not so dominant in this range compared to western part of IO as seen in Fig. 4.8(a), (b) and (c). For the eastern EIO location the beginning of the study period is a lull period with less wavelet amplitude in SSTA till Oct 1996. 1997 is an active warm period and lasts till 1998 August. The active period for SSTA in ESIO is during 1997-98 as shown in Fig. 4.8(f).

4.3.2 Precipitation Rate (PWT)

The available daily precipitation rate ($\text{Kg m}^{-2} \text{s}^{-1}$) of NCAR/NCEP has been used for the study. 5 - day anomaly has been computed by subtracting climatological 5 - day mean estimated using full data set (1960-1998). Wavelet Analysis of PWT anomaly also has been carried out at the 6 chosen locations for the SSTA study.

4.3.2.1 Time Series, Correlation Coefficient, Spectrum Analysis

Time series of PWT anomalies (PWTA) is shown in Fig 4.9. The time series of BB is different from the other locations because of the amplitude range in anomaly. WEIO and WSIO show more oscillatory behaviour than the other time series and the deviation from the mean is less for EEIO.

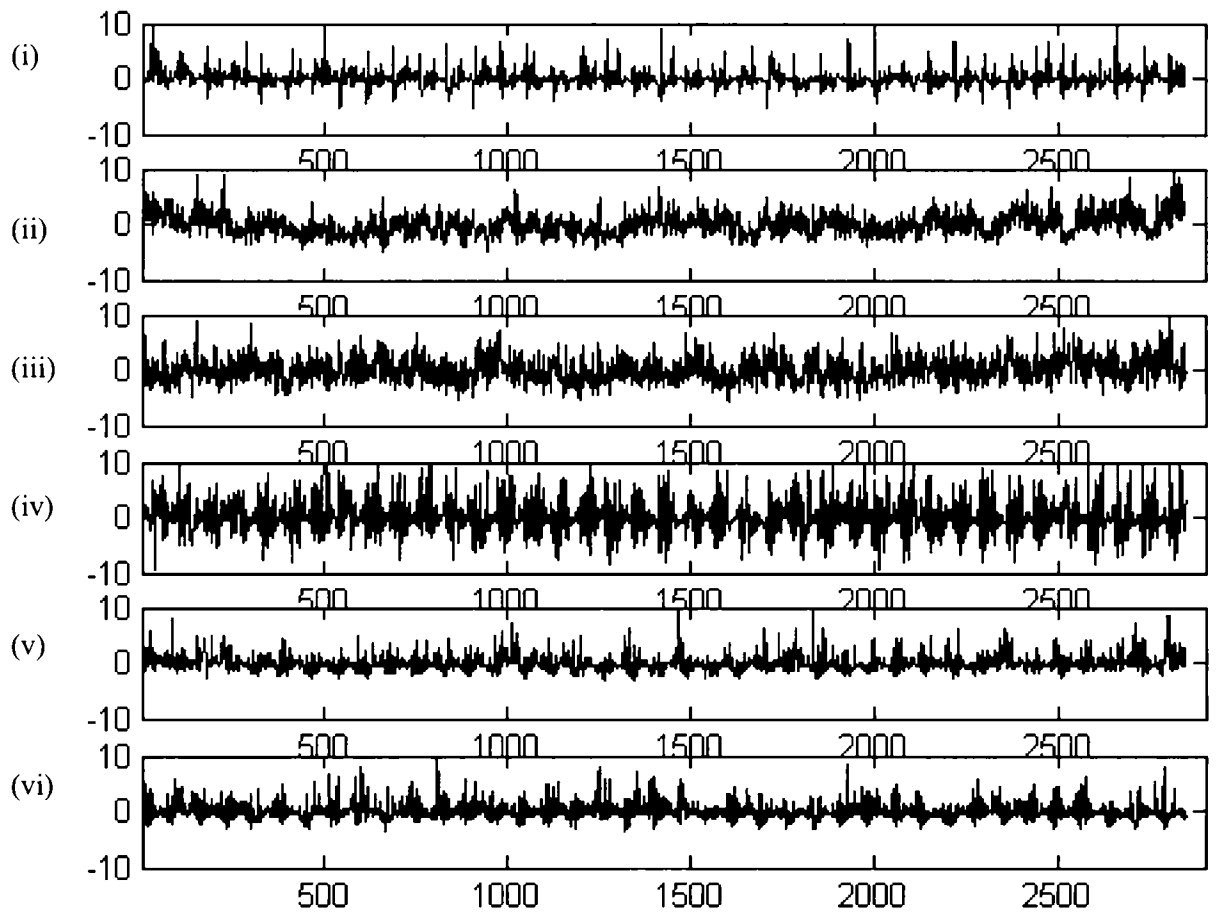


Fig 4.9 Time series of PWT ($\text{Kg m}^{-2} \text{s}^{-1}$) anomalies (5day averaged) for 1960-1998 (i) Arabian sea (ii) Eastern EIO, (iii)western EIO, (iv) Bay of Bengal, (v) eastern SIO and (vi) western SIO from top to bottom

To study the correlation between PWTA at these spatial locations, cross correlation coefficient of the time series is computed for all combination and presented in table 4.3.

Table 4.3

Correlation coefficient 5-day PWTA

From the table 4.3 it is seen that the significant correlation of PWTA is seen only between AS and BB, EEIO and WSIO. The PWTA of WSIO and WEIO

Correlation Coefficient	AS	WEIO	WSIO	BB	EEIO	WSIO
AS	1	0.040	0.008	0.116	-0.041	0.009
WEIO	0.040	1	-0.158	-0.054	-0.039	0.001
WSIO	0.008	-0.158	1	-0.042	-0.005	-0.002
BB	0.116	-0.054	-0.042	1	-0.040	-0.005
EEIO	-0.041	-0.039	-0.005	-0.040	1	0.186
WSIO	0.009	0.001	-0.002	-0.005	0.186	1

are negatively correlated. The spectrum of these PWTA time series shows that high frequency oscillations are predominant in PWT anomaly (PWTA) and only the short period spectrum is presented (Fig 4.10).

Here again the short period oscillations over BB Fig 4.10 (a) is different from other grid locations.

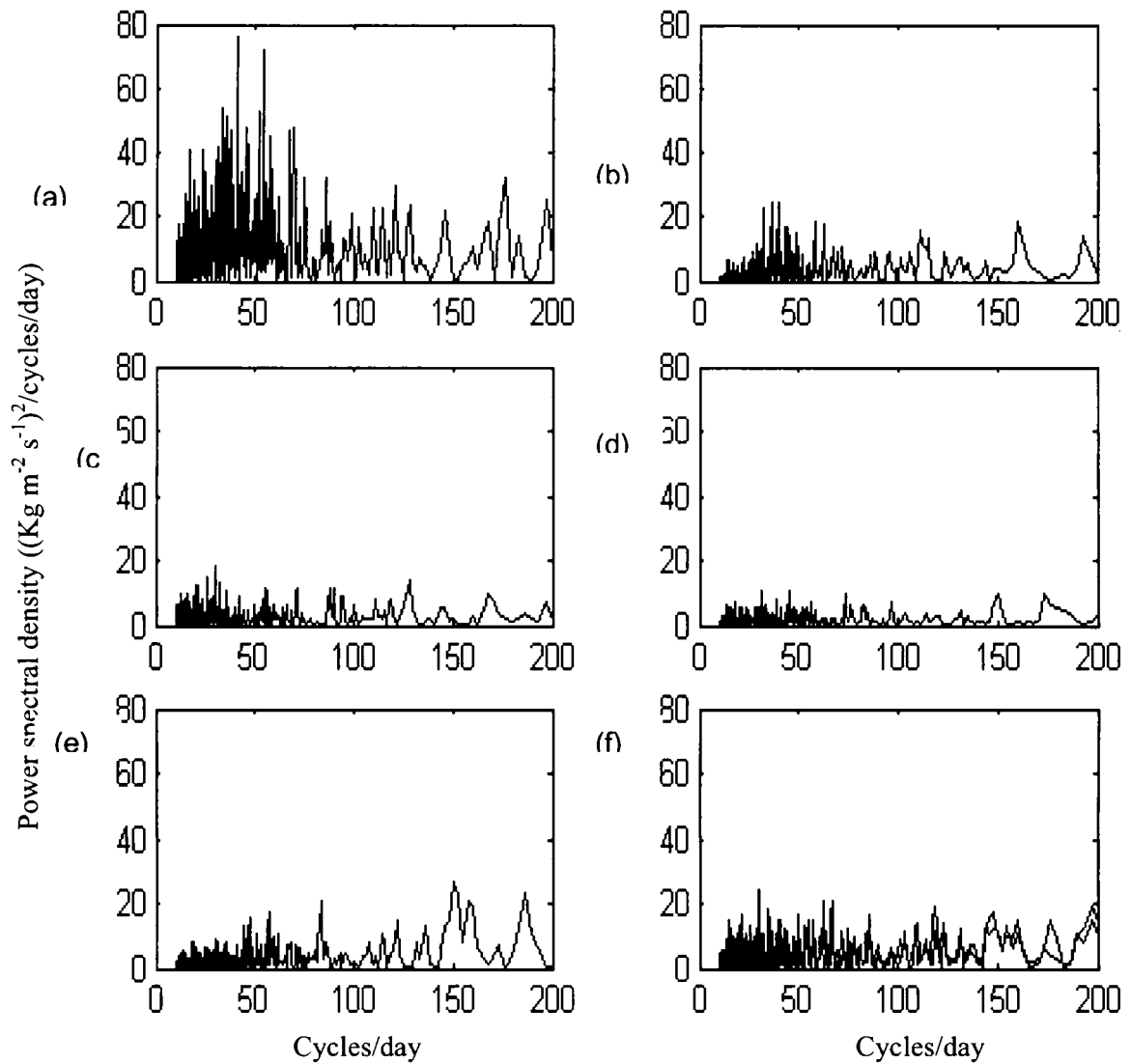


Fig 4.10 The fourier spectra of the time series of five-day PWT anomaly over (a) Bay of Bengal, (b)Arabian Sea, (c)western SIO, (d)eastern SIO, (e) eastern EIO and (f) western EIO. The abscissa is period

The autocorrelation estimates of these time series once again confirms that the PWTA contain more of short period oscillations as the higher lags confines to a value zero (figure not presented).

4.3.2.3 Wavelet Analysis of Precipitation Rate Anomaly (PWTA)

The wavelet analysis using Morlet wavelet has been carried out for precipitable water rate anomaly (PWTA) as similar to SSTA.

The long period oscillations of up to 14 years periodicity as noticed in SST are not so pronounced in PWT. The periodicity shows little higher amplitudes in WT in this range for EEIO compared to other parts of Indian Ocean. As the WT computation shows predominant oscillations for a scale of 64 days only those results are presented.

Generally, two dominant modes of oscillations are seen in wavelet analysis of 5-day anomaly of precipitable water rate with a maximum scale of 320 days, one with long period of 160-320 days and another with short period of 20-120 days.

During 1997-1998 precipitation rate fluctuations of 30-120 days period are significant over WEIO, WSIO and BB (Fig. 4.11 (b), (c) and (d)). Precipitation rate exhibits multiple periodicities over WEIO and WSIO. The intensity of WT of PWTA time series is generally less over EEIO as shown in Fig. 4.11(e).

Merging of these two oscillations are seen over Arabian Sea (Fig 4.11 (a)) in 1996 April-June and eastern SIO (Fig. 4.11(f)) during 1998 Apr-Jun. During the merging period short period oscillation increase in periodicity and prolong for long duration. In the case of long period oscillations their presence is reduced during merging period. According to Indian Meteorological Department, Indian summer monsoon rainfall (ISMR) was normal during 1996-98 and El Nino conditions prevailed in 1997-98. Such consistency of periodicity in oscillations can be seen only over WEIO, if these are the periodicities responsible for the precipitation rate fluctuations.

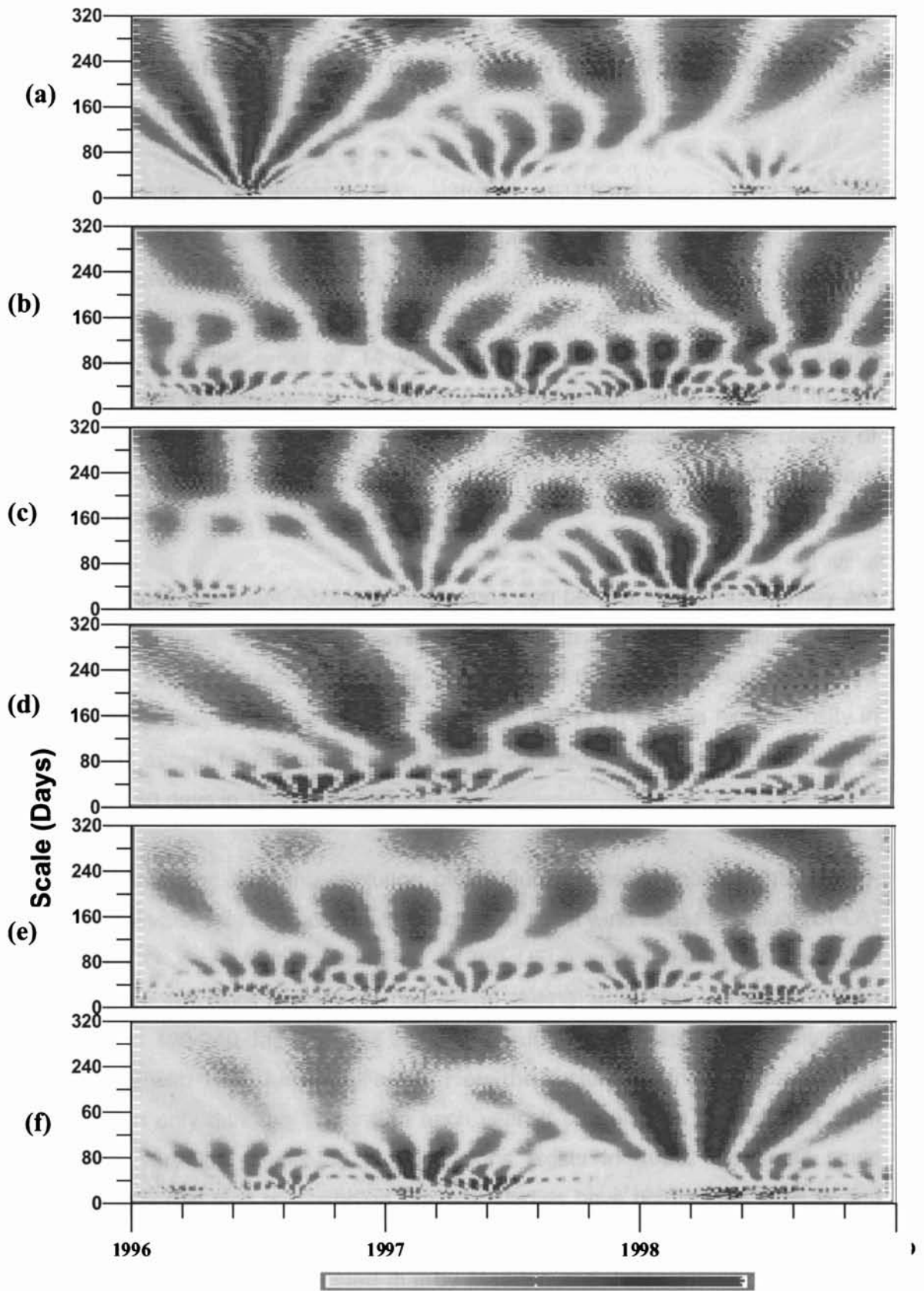


Fig:-4.11 Wavelet amplitude for the monthly PWTAs($\text{Kgm}^{-2}\text{s}^{-1}$) time series (1996-98)
 (a)Arabian Sea (b) western Equatorial IO (c) Western SIO (d)Bay of Bengal (e)
 Eastern EIO (f)Eastern SIO

4.3.3 Wavelet Analysis of Zonal Wind Stress Component Anomaly (UFLA)

Similar to SSTA and PWTA wavelet analysis have been carried out for 5 day anomaly of zonal (UFLA) and meridional (VFLA) wind stress components. The frequency analysis on UFLA and VFLA shows a number of peaks. Hence no clear indication of which one is dominant and so not presented. The long period oscillations of the order of 14 years are not so significant in wind stress components as observed in SSTA. And the maximum period obtained in WT computation is 3-6 years over SIO which is also not dominant. The results of UFLA wavelet analysis for a maximum scale of 64 correspond to 320 days are presented in Fig 4.12 and Fig 4.13.

Three dominant modes of oscillations can be seen in Fig 4.12. They are with 30-60 days, 60-100 days and with more than 120 days periodicity. In the case of UFLA as shown in Fig. 4.12, either one of these three modes is present or at times they all merge together. Generally WT of UFLA has high intensity in 1996-97 except for AS, and there is a shift of periodicity from below 180 days to above 180 days in 1998 over EIO.

Analysing the time evolution of the fluctuations, it appears that spatio-temporal variability even occurs in the case of zonal wind stress anomaly (UFLA) within TIO. Over Arabian Sea Fig. 4.12(a) UFLA within 1996-1997, has high amplitude in longer periods (30-320 days) during 1997 May - June and then shifted to 100-240 days by 1998 January. By June 1998 again fluctuations show similarity with 1997 June amplitudes. Here the fluctuations in 30-80 days range are seen only during May-June of each year. It can also be noticed that even though very low amplitude in fluctuations exists in 1996, the small scale periodicity can also be observed. Several studies have pointed out (Mysak and Mertz, 1984) this low frequency (40-60 day period) variability from winds over Arabian Sea. It was suggested that by Madden and Julian (1972), the oceanic oscillations were being forced by the 40- 50 day oscillations of the tropical atmosphere. This is also reported by Schott (1983) from current meter data from the ship measurements.

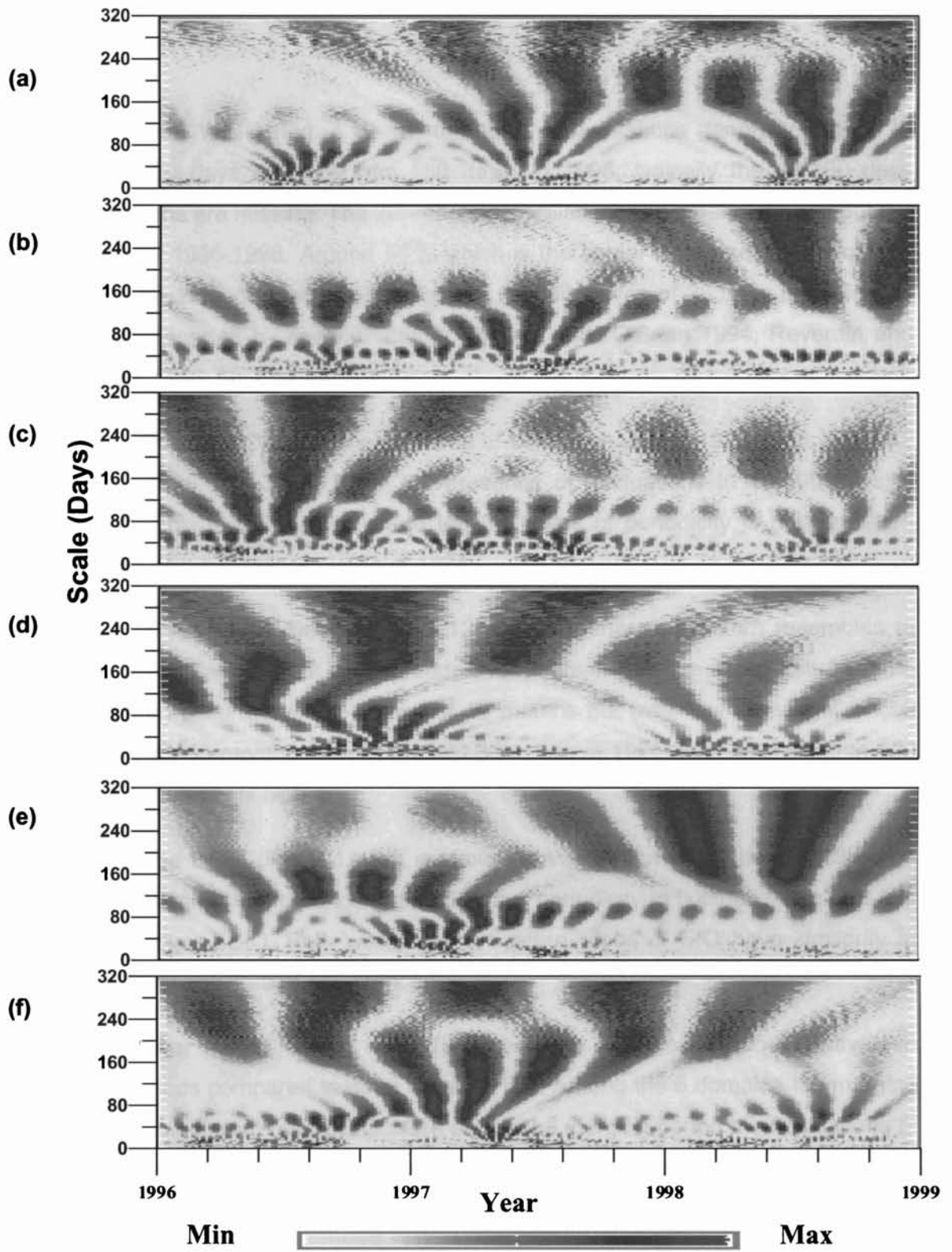


Fig:-4.12 Wavelet amplitude for the monthly UFLA(Nm^{-2}) time series (1996-98)
(a)Arabian Sea **(b)** western Equatorial IO **(c)** Western SIO **(d)**Bay of Bengal
(e) Eastern EIO **(f)**Eastern SIO

Over WEIO (Fig. 4.12 (b)) the scale of oscillations generally confine to either 180 days or more than 100 days. In 1998, typically the 40-100 days fluctuations are missing. The 20 - 40 days oscillations are present throughout the period of 1996-1998. Around 55°E which is the center of the selected location, the dominance of mixed Rossby-gravity (Yanai) waves of 26 days periodicity is already reported by several authors (Meyers and O'Brien 1994; Reverdin and Luyten, 1986; Mc Phaden, 1982).

Over WSIO the dominant mode of oscillation during 1996-1998 (Fig 4.12 (c)) is 1996 May-June. Here, the presence of fluctuations in 40-100 days is typical. This is the region, where the 3-5 years of periodicity is noticed when applied with a maximum scale of 1024.

Over Bay of Bengal (Fig. 4.12 (d)) the generated pattern resembles to that of Arabian Sea but widespread. Over Arabian Sea the same pattern (time evolution) occurred within a span of 18 months but over Bay of Bengal it took more than 30 months. During the last 3 months of 1996, fluctuations within 120 days periodicity is high.

The EEIO (Fig. 4.12 (e)) is similar to WEIO, but 20-40 days oscillations are not seen. The presence of 60-100 days periodicity in fluctuations in UFLA is regular over EEIO. Both western and eastern areas of EIO have similarity in periodicity and time of occurrence.

Over the ESIO (Fig. 4.12 (f)) fluctuations are occurred comparatively in long periods compared to other areas in TIO. Among the 6 domains the merging pattern is different over ESIO. Here during the merging period the fluctuations of short period (40-180 days in 1997 March-April) are also dominant. In other areas during the merging period the fluctuations shifted to longer periods of more than 180 days.

4.3.4 Wavelet Analysis of Meridional Wind Stress Component Anomaly (VFLA)

The wavelet analysis results of 5-day anomaly of meridional wind stress component using Morlet as the basis is presented in Fig 4.13.

Over Arabian Sea (Fig. 4.13 (a)) the dominant modes of fluctuations in meridional wind stress component (VFL) and their pattern is similar to that of the zonal wind stress anomaly in Fig 4.12 (a). The fluctuations in 100-120 days in 1996 and 80-100 days in 1997-1998 are more significant in meridional component compared to zonal component of wind stress.

Fig. 4.13 (b) is similar to Fig. 4.12(b) of WEIO. In the case of VFL the shift of periodicity in 1998 is not so significant that the small scale oscillations are also with less amplitude are seen.

The meridional wind stress fluctuations of this periodicity are less in 1998 over WSIO. But as in Fig. 4.13(c), the amplitudes are little higher. Even though the time evolution pattern looks similar to that of UFL, a delay of 3-5 months is observed.

In the case of Bay of Bengal as seen in Fig. 4.13(d), the intensity of WT shows high values in 1998. Over EEIO longer period oscillations in VFL (Fig. 4.13(e)) are quite less compared to UFL.

The presence of 20-100 days of oscillations can be seen in Fig 4.13(f) which is for eastern SIO. The time evolution of VFL seems to be similar during the merging period in 1997. But in the case of UFL over the same region one more dominant periodicity is noticed in 40-200 days scale.

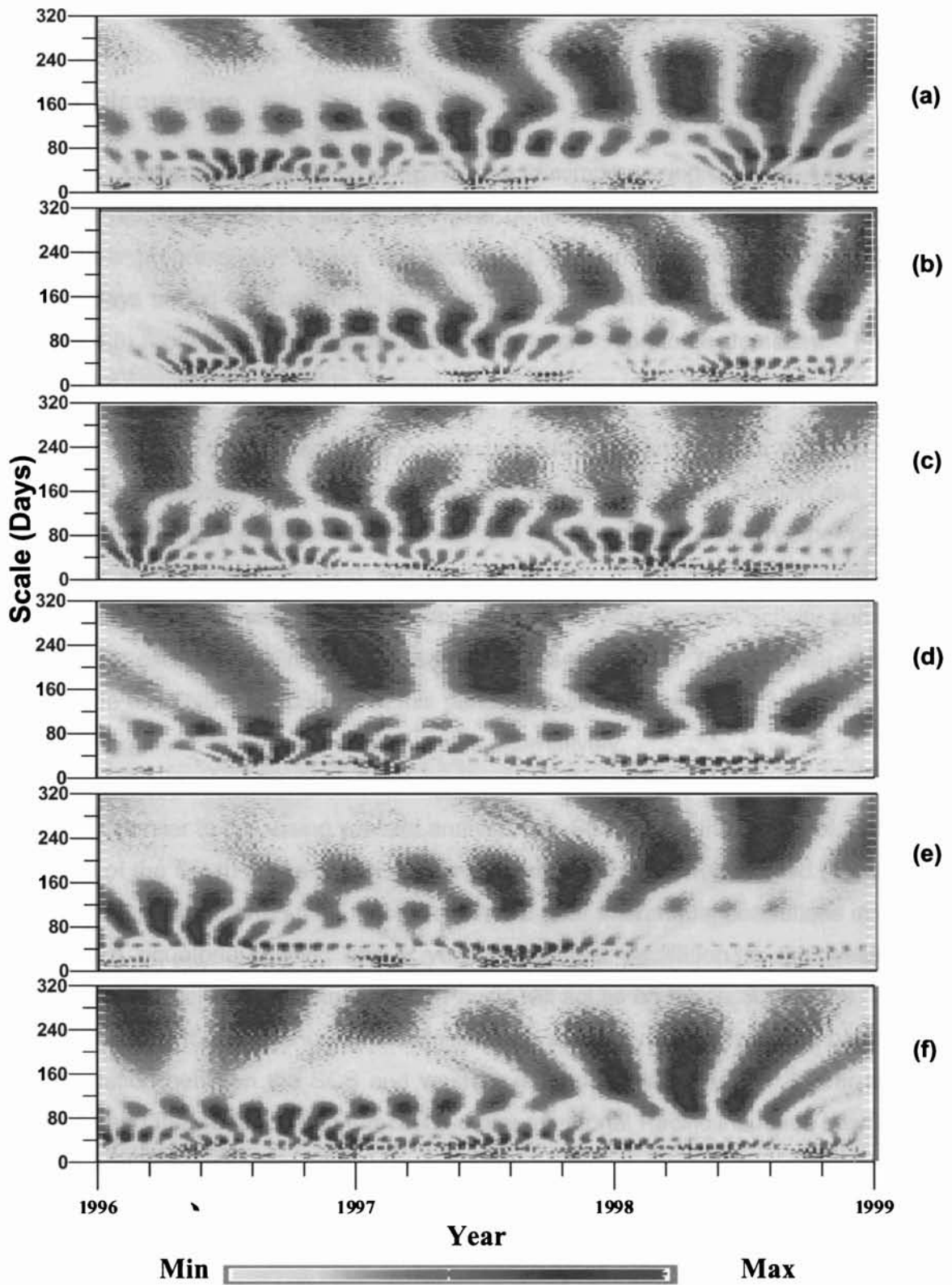


Fig:-4.14 The modulus of the wavelet transforms VFLA (Nm^{-2}) (a)Arabian Sea (b) western EIO (c) Western SIO (d)Bay of Bengal (e) Eastern EIO (f) eastern SIO

4.4 Discussion

Generally the analysis of SSTA for a maximum periodicity (Fig. 4.6) of 14 years resulted with 6-14 year and 2-7 year periodicity with a merging period of 5-10 year progressively. In the next scale (Fig. 4.7) analysis 700-1280 and 320-640 days period fluctuations have been reflected. From the small scale analysis (Fig 4.8) more than 160 days and 60-100 days are seen to be dominant. . From Fourier spectra the energy is concentrated in 4.3 year in timescale.

Among the studied locations, western SIO begins this warm episode and with lag in eastern EIO, Bay of Bengal and western EIO then Arabian sea and eastern SIO. At the eastern SIO location the specific pattern seen in other areas is not strong during the first half of the data viz., 1960-80. The long period oscillations (7-14 year) in SST are reported with 11 year Sunspot activity and the decadal oscillations (Fris_Christensen and Lassen, 1991). The 3-7 year period include the ENSO periodicity. In this periodicity we can see about 3 to 4 year of warming and 2 to 1 year of cold episodes alternatively.

Similar to this, using wavelet analysis the SST during the period of 1982 - 1999 of the South China Sea (SCS) and equatorial Pacific was studied (Jiwei et al., 2000) and reported that there are 4 and 8 year interannual oscillations in the eastern equatorial Pacific and 8 year interannual oscillation in the western equatorial Pacific. The change in the Pacific will act as on the SCS, and the SCS will respond to the change in the Pacific with a 5 – 8 months lag. The positive correlation between the SCS and western equatorial Pacific in the 8 year time scale and the evidence that the SSTA of the equatorial Pacific influence the SST of the SCS is presented.

The fluctuations of 2-7 year periodicity obtained from wavelet analysis also can fall into the category. In an analysis of observational data for 1952-92 Klein et al (1999) reported that surface heat flux anomalies explain the ENSO induced basin wide warming over most of the TIO but identified the western tropical SIO as an exception suggesting that some yet unidentified mechanisms are at work there. Xie et al (2002) reported that much of SST variability in the western SIO is not locally forced but instead due to oceanic Rossby waves that propagate from the east. Their study discussed ENSO as the major forcing for

these Rossby waves and that they interact with the atmosphere after reaching the western Indian Ocean. Such a subsurface effect on SST in the WSIO is explained by the simultaneous presence of upwelling and shallow thermocline.

In this study over TIO also the merging period of different scale of oscillations are reflected, hence during this time scale the corresponding periods differ. The increase of timescale of ENSO by about 10 months from 40 months before the late 1970s to 48-52 months after that is reported by Wang and Wang, (1996), Setoh and Imawaki (1999).

Setoh and Imawaki (1999) reported that the ENSO signal has inter decadal variations using SST and wind stress using 1950-1997 dataset over Pacific. They used wavelet and EOF techniques and estimated time scale of about 40 months before late 1970s and 48-52 months after that. In our analysis for periods of multiple years (Fig 4.6) also it can be seen that there is a small shift from 2-4 years to 3-5 years after 1980.

The Southern Oscillation also exhibits noticeable changes in its amplitude. It was most energetic during 1970-1992, but became weak during 1960s. The weak period is dominated by quasi-biennial oscillation. Excessively strong cold phases of the El Niño-Southern Oscillation cycle enhance annual variation of SST in the equatorial eastern and central Pacific. The enhancement, however, appears to be modulated by an interdecadal variation.

From the small scale analysis with 1996-98 dataset, Bay of Bengal condition is some what similar to eastern EIO. Here at the beginning the wavelet transform amplitudes are little higher than the eastern EIO. The scales of oscillations appear to be almost similar at the same time frame. At the eastern SIO location again at the beginning during 1996 WT amplitude are weak. Western SIO is similar to Arabian Sea with lag of say 3 months.

Spatial and temporal variation of Legeckis waves (Legeckis, 1987) was reported by Meyers & O'Brien (1994) using wavelet analysis over EIO using 2 year SST data at 53°E and 56°E at 3°N latitude. Within these two years WT amplitude as well as the frequency significantly vary. The oscillations in this periodicity are observed EIO and over Arabian Sea.

The effect of remotely forced mid latitude Rossby waves on the Somali Current was explored by Anderson and Rowlands (1976). Later Brandt et al (2002) reported westward propagation with 38-45 days for the different seasons. The generation and persistence of Great Whirl in south western Arabian Sea is interpreted as the intra seasonal fluctuations generated locally in the system. The WT amplitudes are high in 30-100 days periods over Arabian Sea and WEIO compared to other regions. This may be connected to the local generation mechanism for these waves.

4.5 Conclusion

The wavelet analysis of SST, wind stress and precipitable water anomalies over different regions of the Indian Ocean revealed oscillations of different periodicities ranging from few days to few years. The maximum scale of wavelet analysis possible using this dataset is limited to 14 years.

There are two dominant oscillations seen in SST, one in 6-14 years and the other in 2-4 years periodicity. As time progress, the periodicity of the long period oscillations decreases while the short period oscillations intensify and increases. It is seen that at a certain stage the long period oscillations merges with the short period oscillations and then short period oscillations, vanishes for some time. Thereafter the short period oscillation strengthens and its periodicity seems to increase. Generally this behaviour is seen for all regions. But the time of merging varies from place to place. The short period oscillations of 2-4 years show a repetitive pattern for every 10-12 years.

The analysis for a maximum period 1280 days (3.5 years) shows oscillations with more than 450 days periodicity as generally predominant. These fluctuations appear for about 2 years with a gap of 1 year. Over a period of 18-20 years, the wide band periodicity oscillations shift to small band high period oscillations with period of 2.5 year (912 days) and above. During 1965-75 they are significant irrespective of the location.

To understand the variations in short periodicity the data of 1996-98 is used. It can be observed that two dominant modes of oscillations of 30-80 days

and 200 -320 and more days (annual) exist in this scale. Long period oscillation lasts for 3 months while short period are seen for a month or so. These two modes merge together within a time frame of 18 months with a scale of 30-150 days.

Unlike the SSTA field the precipitation rate and wind stress components do not exhibit long period fluctuations. The precipitation field showed fluctuations of 30-120 days and annual period. The zonal and meridional wind stress components exhibited periodicities of 30-60 days, 60-100 days, semiannual and annual periodicities. The 30-60 day oscillations could be associated with intra seasonal oscillation attributed by Madden and Julian (1972).

Comparing SSTA and PWTA for the small scale, it is seen that SST and PWT evolution (warming and excess of PWT) occurs at the same time for western TIO (AS and WEIO) and SIO (WSIO and ESIO) but not in EEIO and Bay of Bengal.

Propagating Disturbances

In chapters 3 and 4 the spatio-temporal variability of the SST, u-stress, v-stress and precipitable water rate over tropical Indian Ocean is examined based on EOF analysis and Wavelet analysis. Even though the dominance of variability and the frequency content of these fields are revealed by using these techniques, their movement with space and time could not be well understood. To reveal the propagating nature of their variability, longitude-time (called Hovmöller diagram) sections of SSTA is extracted for analysis and the results are included in this chapter. The slowly moving thermal anomalies that have the propagation characteristics of baroclinic Rossby waves and Kelvin waves are analysed in this chapter.

5.1 Planetary Waves

Planetary waves are propagating perturbations in the layered structure of the ocean as the structure adjusts to the disturbance of isopycnal surfaces. Oceanic planetary waves such as Kelvin waves or Rossby waves are of great importance for ocean circulation and climate. They transport momentum and information across the main oceanic basins, affect currents and delay the effects of climatic anomalies such as El Nino (Graham et al 1990; Frankignoul, 1985).

An eastward wind-stress forcing produces equator-ward mass transport in both hemispheres, acting to increase locally the depth of the warm water layer near the equator, and decrease it locally farther poleward in either hemisphere. The mass surplus near the equator then begins to disperse eastward as a so-called (downwelling) Kelvin wave, and the mass-deficit areas begin to propagate westward as so-called (upwelling) Rossby waves (upwelling and downwelling refer to the wave tendencies either to shallow or deepen the warm water layer).

If the Coriolis parameter is allowed to change with latitude then Rossby waves are generated. Rossby waves have a westward phase velocity. When a long Rossby wave impacts on the western boundary it reflects as short Rossby waves. The short Rossby waves attenuate quickly, so that energy tends to collect along the western boundary.

The principle from which planetary waves arise is the conservation of potential vorticity when a parcel of fluid is displaced in N-S direction on the surface of earth. Since the restoring force is proportional to the displacement the result is a sinusoidal signal, an intriguing property of which is that the propagation is westward although the displacements are meridional (Schott and Stommel 1978).

Kelvin and Rossby waves have different propagation speeds (and directions) because of their different latitudinal structure, once again owing to the important effect of the Coriolis force, which is strongly latitude-dependent. Rossby waves are dispersive and travel westward at a speed fixed by the environment and independent of the wave number or orientation of the waves

(Hill et al., 2000). Kelvin waves travel at the speed of a gravity wave. Kelvin waves are observed in the ocean along coastlines. Kelvin waves propagate with the boundary on the right in the Northern Hemisphere (on the left in the Southern Hemisphere). Disturbances symmetric on the equator generate an equatorially trapped Kelvin wave. The amplitude of the Kelvin wave decreases exponentially with distance from the boundary.

5.2 Observations of Oceanic Planetary Waves

Following the first identification of the Rossby wave mechanism (Rossby, 1939), the basic theory of Rossby wave propagation has become well established. From the analysis of model results and observations, White et al (1998) has demonstrated that the Rossby waves coupled to the atmosphere by the thermal feedback between the ocean atmosphere and their resulting phase speed may be influenced by the local spatial gradients of the SST field. The phase speed modification includes a meridional component. Masumoto and Meyers (1998) observed inter annual Rossby waves with periods ranging from 3 to 5 years in the tropical Indian Ocean from 6° to 14° S for 10 years from 1984 to 1993 in anomalous depth of the 20° C isotherm. Perigaud and Delecluse (1993) observed interannual Rossby waves with periods ranging from 3 to 4 years in the Indian Ocean near 15° S using 5 years data from 1985 to 1989 in anomalous sea level height using Geosat altimeter data. One of the characteristic features of the Northern Indian Ocean is the large scale, low frequency forcing associated with the monsoons which generate Rossby and Kelvin waves along the equator. Recently evidence of propagating signal with speeds consistent with those of planetary waves has been found in filtered longitude/time plots of phytoplankton chlorophyll concentration from ocean colour radiometers (Cipollini et al., 2001). Similar Rossby waves are observed in Pacific Ocean (White et al., 1998; White, 2000). The lack of transition in phase difference from the tropics to the extra tropics separated the Indian Ocean from the Pacific Ocean.

Several attempts have been made to study the propagating nature of oceanographic features based on models and observations. Most of the modeling studies on large scale oscillations between ocean and atmosphere rely on theoretical models of Rossby wave propagation and comparison between

theory and observations still shows discrepancies. The studies generally confine to some longitudinal sections or latitudinal sections concentrating on the scales of the objective of that study. Thus for modeling and forecasting of climate variations such as ENSO, having a more complete definition of how Rossby wave vary across the ocean, in both space and time, would be valuable.

The objective of the present chapter is to analyse the propagating nature of the surface thermal signatures in different climate conditions across the Indian Ocean (Kessler, 1990; Van Woert and Price, 1993). The propagating Rossby and Kelvin wave in the Indian Ocean is already reported. The Kelvin waves are long gravity waves which propagate along the coast or along the equator, and always in the direction to keep the coast on the right in the northern hemisphere. In the open ocean the low frequency adjustment is made via Rossby waves these long waves propagate westward. The principle of using SST as an indicator of Rossby waves is well established (Kessler, 1990; Van Woert and Price, 1993). As already the period and the presence are well established, the nature of these waves across the Indian Ocean in 39 years (1960-1998) is studied in this chapter

5.3 Data

For the present study daily SST from the NCEP/ NCAR for 1960 to 1998 is used. In order to isolate possible SST signature of planetary waves from the regular variability of seasonal cycle the SST anomaly distributions for each month were evaluated by subtracting a climatic mean SST field for each month of the year. The average of each year is computed. The longitude- time sections are taken along 25°S , 15°S , at equator and 15°N . 15°N section is separately plotted for Arabian Sea and Bay of Bengal.

To reveal the propagation along equator TOPEX/POSEIDON ten day anomaly of Sea Surface Height (SSH) has been used. Zonal averages are used for each section. The details of the spatial average at these locations are given as a table 5.1 and shown in Fig 5.1

Table 5.1

Spatial section Details

Section	Latitude/Longitude coverage
15°N longitude – time (Arabian Sea)	12°N - 17°N
15°N longitude – time (Bay of Bengal)	12°N - 17°N
Equator	3°S - 3°N
25°S longitude – time	23°S - 28°S

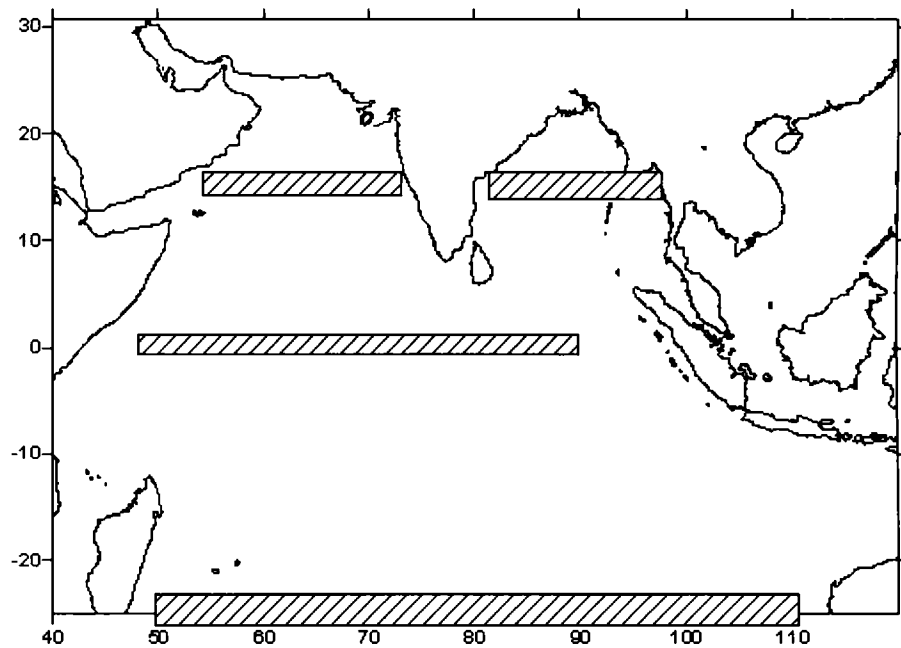


Fig. 5.1 Area selected for study

By plotting the 39 years of monthly SST anomaly values in a single graph could not reveal any pattern as it is very much packed, the data set divided into two as 1960-1979 and 1980-1998.

5.4 Results

5.4.1 NCEP/NCAR Sea Surface Temperature

The simulation of interannual Rossby waves in a time-longitude diagram of interannual pycnocline depth anomalies along 13°S by Masumoto and Meyers (1998) led them to hypothesize that observed Rossby waves at this latitude derived from anomalous wind stress curl forcing by the overlying atmosphere. Here we examine time-longitude diagrams of interannual SST anomalies used to trace the westward propagation over each time sequence one of 20 years 1960-1979 and the other of 19 years of 1980-1998. Representative time-longitude diagrams of annual SST anomalies at 25°S , equator and 15°N in the Indian Ocean display westward phase propagation. From Fig 5.2 to 5.4 warming nature during 1980 - 1998 compared to 1960 - 1979 is well indicated. The tendency for westward propagation of SST anomalies is clearly seen from Arabian Sea (Fig 5.2 (a) and Fig 5.4(a)) and South Indian Ocean (SIO) plots (Fig 5.3 (b) and Fig 5.5(b)). Neither in Bay of Bengal nor in Equator region meridional movement is directly seen. But over Arabian Sea slow speeds are indicated compared to SIO. Even though 20 years of SSTA are plotted together the first appearance of respective anomalies on the eastern part of the basin can be traced easily.

The phase speed variation of free Rossby waves and interannual coupled Rossby waves are reported. The interannual coupled Rossby waves in the TIO (White, 2000) propagated westward much slower than free waves (Killworth et al 1997) and slower than forced Rossby waves simulated in numerical ocean models by Masumoto and Meyers (1998). White (2000) reported that in extratropics near 26°S the coupled and free wave speeds are nearly the same. From the meridional profile of the observed phase speed from 10°S to 26°S of TIO, estimated using 1993 - 1998 SST and mean surface wind of NCEP and sea level height of TOPEX/altimeter (White, 2000) it is seen that there is much smaller reduction in speed with latitude than for free waves. Applying Complex EO (CEOF) analysis White, (2000) found that coupled Rossby waves were superimposed upon a standing wave in the Indian Ocean and magnitudes were

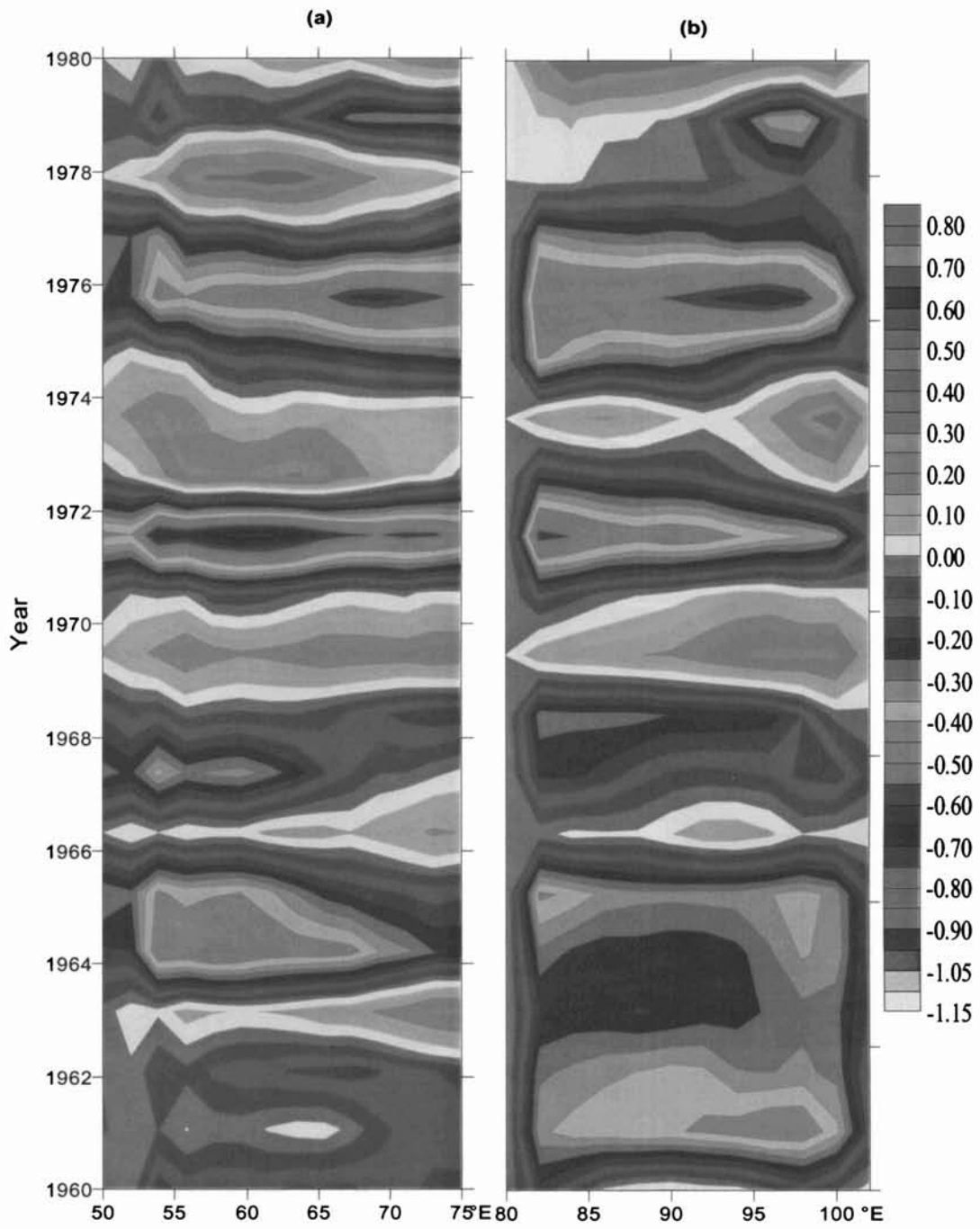
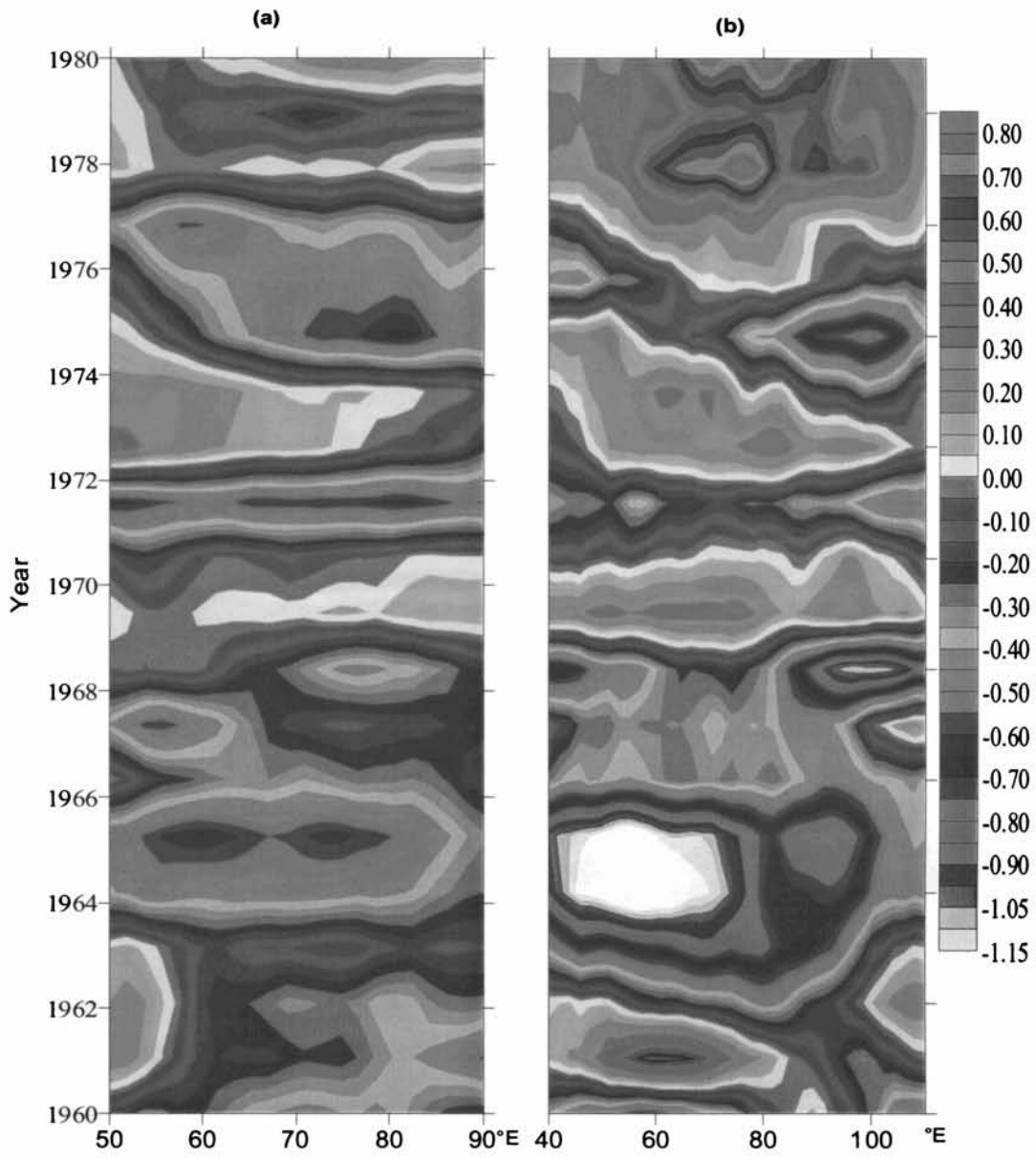


Fig 5.2 Time longitude diagram for interannual SSTA [°C]
 (a) at 15°N AS and (b) 15°N BB for 20 years from 1960-1979



**Fig 5.3 Time longitude diagram for interannual SSTA [°C]
 (a) Equator and (b) at 25°S for 20 years from 1960-1979**

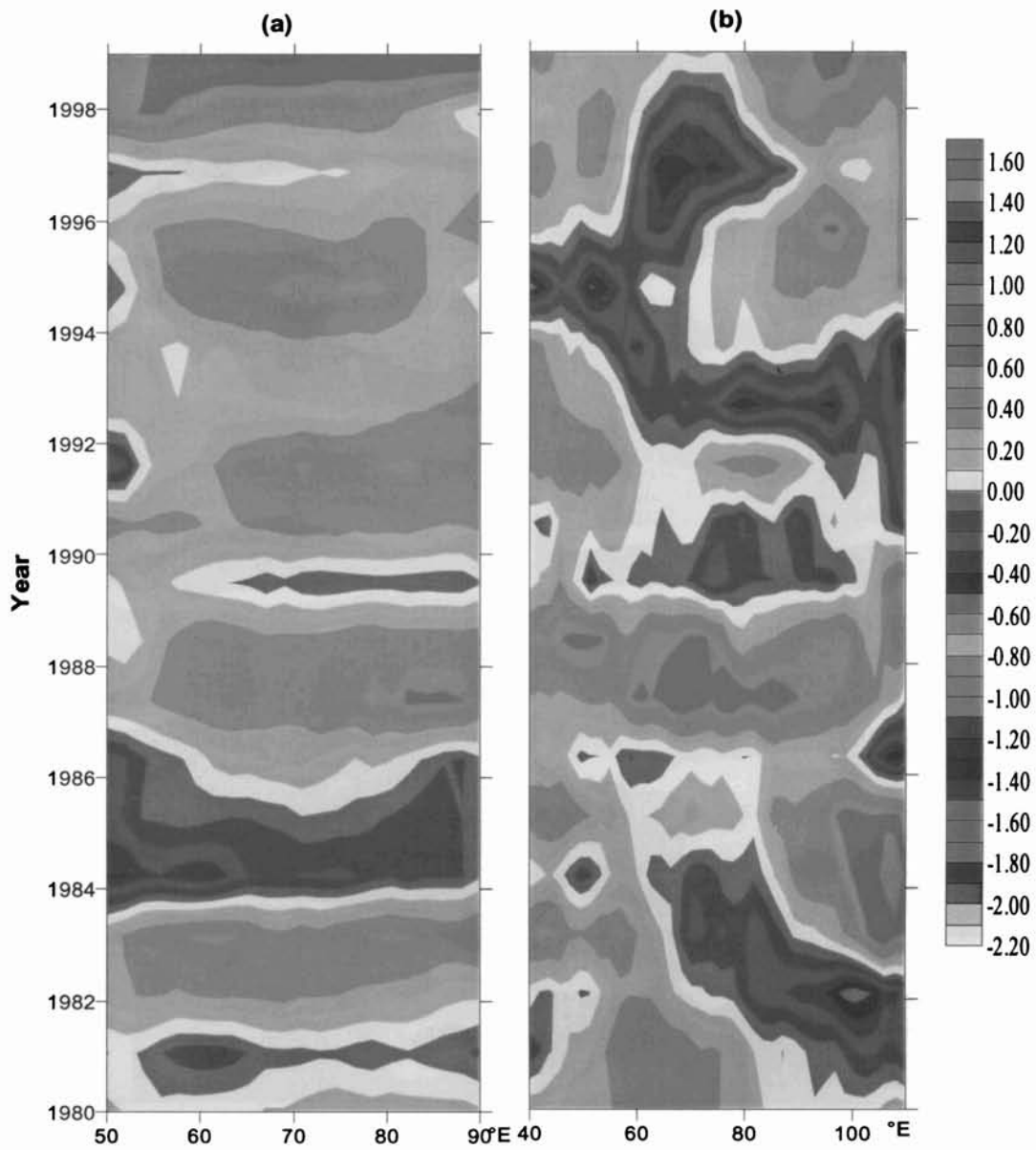


Fig 5.4 Time longitude diagram for interannual SSTA [°C]
 (a) Equator and (b) at 25°S for 19 years from 1980-1998

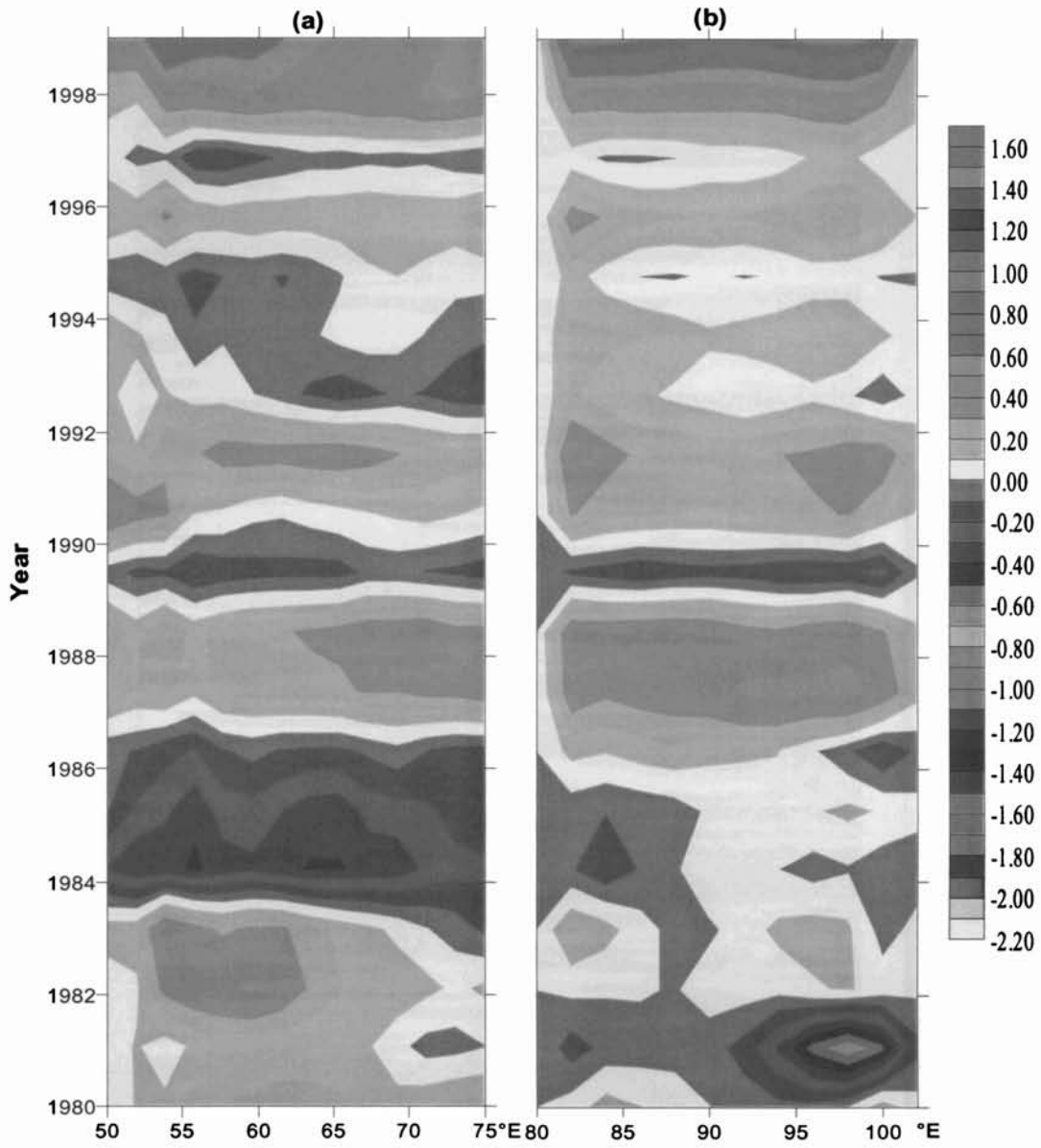


Fig 5.3 Time longitude diagram for interannual SSTA [°C]
 (a) at 15°N AS and (b) 15°N BB for 19 years from 1980-1998

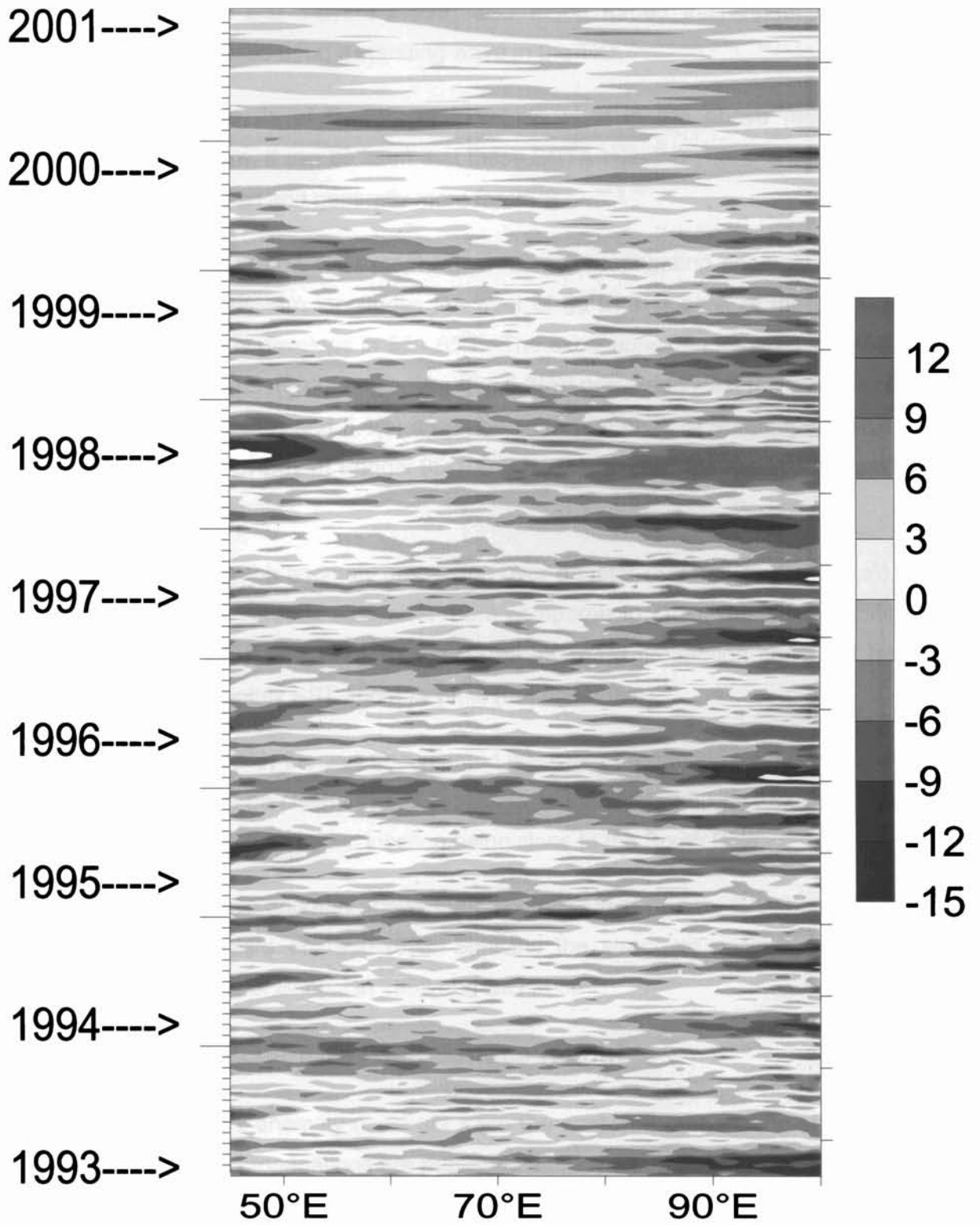


Fig 5.6 Time longitude diagram for monthly sea level height anomaly (cm) along equator

only half as large using 29 years (1970-98) dataset of SST and mean surface wind. Masumoto and Meyers (1998) also found forced interannual Rossby waves superimposed upon a standing wave in the TIO.

Analysis of these time-longitude plots in the above mentioned published literature, it can be seen that these SSTA take 2-3 years to propagate across Indian ocean and generally more for 25°S.

In Fig 5.2(a) and 5.4 except (a), westward propagating anomaly can be traced over the western longitudes i.e., west of 60°E. The peak of the positive anomaly generally develops in 55 - 65°E. The exceptions can be seen in 1963, 1966 and 1988. The maximum cooling (Fig 5.2(a)) occurred in last few months of 1971. From Fig 5.2(b) and 5.4(b) it can be seen that peak of anomaly appears towards the east of Bay of Bengal 95-100°E. In this exceptions are in 1971 and 1975 for cold anomaly.

Comparing the anomaly propagation over equator (Fig. 5.3(a) and 5.5(a)), it appears that it spreads east west more compared to other studied locations exceptions in 1961 and 1973. The reported eastward propagation could not be revealed from monthly SST anomaly plots (not presented).

But over 25°S, the well documented westward propagation for 2-5 years in SST anomaly can be clearly traced especially to the west of 80°E. SST anomaly shows the peak values at this location being close to the South Pole.

The negative anomaly shows the peak value in 1965 over SIO along 60°E out of the 39 years of 1960-1998. Similarly the strongest positive anomaly occurred over Bay of Bengal in 1998 and SIO at 80°E.

5.4.2 TOPEX/POSEIDON Sea Surface Height

As the SST anomaly could not trace the eastward propagating signature directly and such propagations are published already along equator and analysis has been carried out using the 10 day anomaly values of SSH of TOPEX/POSEIDON. From the available SSH of 1993 to 2001 time -longitude

plots are made to analyse the propagation characteristics near equator and presented in Fig. 5.6.

It can be seen clearly that every year in Feb-Apr period such propagation of positive SSH anomaly occurs in Tropical Indian Ocean along equator. These are eastward propagating waves and within a period of 3 months they reach the eastern part.

5.5 Conclusion

The westward and eastward propagation of disturbance in the tropical Indian Ocean is analysed using NCEP/NCAR SST and TOPEX/POSEIDON SSH. Westward propagation of SST anomalies are observed with slow speeds along 25°S compared to them in Arabian Sea. The propagation is more towards the western Indian Ocean. The eastward propagation is traced from SSH plots especially during Feb-Apr.

Conclusion

Some aspects of spatio-temporal variability of sea surface temperature, precipitation rate and wind stress are studied in this thesis using NCEP/NCAR reanalysis dataset over tropical Indian Ocean. Major results of the study are presented as follows.

The tropical Indian Ocean exhibits a variety of unique features in spatial and temporal scales of variability. Sea surface temperature is the basic thermodynamic field affected by such periodicity. The variability of sea surface temperature with time and space are analysed using different techniques.

Using EOF analysis the leading standing oscillation in sea surface temperature, precipitation rate and wind stress are analysed. First mode of EOF analysis in SST indicated positive loading in almost the Indian Ocean with higher values in the Arabian Sea, equatorial and southwestern and central Indian Ocean and lower values in the Bay of Bengal and eastern Indian Ocean. The second EOF mode shows positive loadings in the southwestern and southern regions of

the Indian Ocean while strong negative loadings are seen in the eastern and northern equatorial Indian Ocean. The Bay of Bengal is characterized by moderate negative loading while marginal negative loading is noticed in the Arabian Sea. The third mode of EOF showed strong negative loadings over western Arabian Sea, eastern equatorial Indian Ocean and south western Indian Ocean while strong positive loading is confined to the southeastern regions of the Indian Ocean. They respectively account for 29%, 12% and 9% of the variance. Frequency analysis of the time series of the first of these three modes showed periodicity of 2.7 years, 500 days and 10 years, respectively. Hence the first EOF mode can be identified as ENSO mode and third with decadal oscillations.

The El Nino occurred in 1965 - 1966, 1969 - 1970, 1972 - 1973, 1976 - 1977, 1982 - 1983, 1986 - 87 and 1997 - 98 within the study period. The significant warming in the Indian Ocean took place in 1969, 1973, 1977, 1979, 1983, 1987, 1991 and 1998. Out of these, except 1979 and 1991, the warming of the Indian Ocean is in-phase with the occurrence of El Nino. Incidentally during the El Nino of 1965-1966 and 1992-93 cooling instead of warming took place in the Indian Ocean, which indicate the influence of other forcing mechanisms in regulating SST in the first EOF mode. However, presently it is not clear the mechanism which offset the influence of El Nino in these years. The first EOF mode showed significant cooling of the Indian Ocean during 1964-65, 1968, 1971, 1974-76, 1988 and modulate cooling during the early 1990's. The cooling during this period either coincided with La Nina or preceded El Nino except in the early 1990's. The warming in the Indian Ocean during 1998 was abnormally high where the first and third modes of EOF contributed warming.

The first, second and third EOF mode of precipitation rate explain 6%, 5% and 4% of the variability respectively indicating that the variance in PWT in the Indian Ocean affected by a number of factors. The first mode indicates strong positive loadings in the eastern Indian Ocean south of equator and Bay of Bengal whereas negative loadings are seen on central and western Indian Ocean. The maximum positive loadings in EOF2 of precipitation rate are observed in the central Indian Ocean south of the equator whereas negative loadings are

observed in the Bay of Bengal, Arabian Sea and western equatorial Indian Ocean. The EOF3 of precipitation rate anomaly shows that positive loadings north of 5°S covering north Indian Ocean except the eastern part of Bay of Bengal and negative loading to the South Indian Ocean areas. The frequency analysis of respective time series shows major peaks at 500 days in EOF1 and one year in EOF2. Analysis of the EOF2 time coefficient of precipitation rate shows that it has similarity to Indian rainfall to a certain extent and the differences can be due to land - ocean differences.

The first mode of EOF of zonal wind stress shows positive loadings in the southern Indian Ocean while negative loadings most of other regions of Indian Ocean. The second mode of EOF shows maximum positive loadings in the south central Indian Ocean, and weak negative/positive loadings in the Arabian sea and Bay of Bengal. This spatial loading pattern looks similar to EOF2 mode of precipitation rate. The third mode shows negative loading concentrated on the southwestern Indian Ocean. The loading pattern is such a way that both sides of the positive loading in the southeast to northwest direction is covered with negative pattern. They explain 12%, 10% and 6% of the total variance. The frequency analysis of EOF1 and EOF2 time series indicates a periodicity of one year suggesting annual variance.

First mode of meridional wind stress accounts for 12% and EOF2 accounts for 10% of variability. The first and second EOF mode shows negative loadings only at the southern Indian Ocean of the studied area while positive loadings most of other regions of Indian Ocean. The third mode shows negative loading concentrated on the southwestern Indian Ocean. Generally, the loading pattern are such a way that it increases towards southern hemisphere without much differences in between. The frequency analysis of EOF1 and EOF2 time series indicates a periodicity of one year suggesting annual variance.

Analysis of spatial and temporal variability of different oscillations in Indian Ocean with their respective variances is explained in EOF analysis. In wavelet analysis using the 5 day anomaly of these fields the presence of these multi scale

oscillations upto 14 years is discussed. Different regions of the Indian Ocean revealed the coexistences of these oscillations with periodicities ranging from few days to few years and it is found that the time evolution is different.

The dominant oscillations in SST are seen in 6-14 years, 2-4 years, 200 - 320 days (annual) and 30-60 days periodicity. As time progress, the periodicity of the long period oscillations decreases while the short period oscillations intensify and increases. It is seen that at a certain stage the long period oscillations merges with the short period oscillations and then short period oscillations, vanishes for some time. Thereafter the short period oscillation strengthens and its periodicity seems to increase. This behaviour is seen for all regions. But the time of merging varies from place to place. The short period oscillations of 2-4 years show a repetitive pattern for every 10-12 years.

The analysis for a maximum period 1280 days (3.5 years) shows oscillations with more than 450 days periodicity as generally predominant. These fluctuations appear for about 2 years with a gap of 1 year. Over a period of 18-20 years, the wide band periodicity oscillations shift to small band high period oscillations with period of 2.5 year (912 days) and above. During 1965-75 they are significant irrespective of the location.

To understand the variations in short periodicity the data of 1996-98 is used. It can be observed that two dominant modes of oscillations of 30-80 days and 200 -320 and more days (annual) exist in this scale. Long period oscillation lasts for 3 months while short period are seen for a month or so. These two modes merge together within a time frame of 18 months with a scale of 30-150 days.

Unlike the SSTA field the precipitation rate and wind stress components do not exhibit long period fluctuations. The precipitation field showed fluctuations of 30-120 days and annual period. The zonal and meridional wind stress components exhibited periodicities of 30-60 days, 60-100 days, semi-annual and annual periodicities. The 30-60 day oscillations could be associated with intraseasonal oscillation attributed by Madden and Julian (1972).

Comparing sea surface temperature anomaly and precipitable water anomaly for the small scale, it is seen that SST and PWT evolution (warming and excess of PWT) occurs at the same time for western tropical Indian Ocean (Arabian Sea and western equatorial Indian Ocean) and Southern Indian Ocean (western south Indian Ocean and Eastern Indian Ocean) but not in equatorial eastern Indian Ocean and Bay of Bengal.

Both in the EOF and wavelet analysis SST shows the effect of decadal oscillation, 11 year sunspot cycle and effects of ElNino.

To study the propagating nature of these variability Håmøller diagrams are plotted. The propagation of the SST anomaly has been analysed at 25°S, equator and 15°N. The propagation of planetary waves are traced and the difference with decades have been studied. The propagation of these anomalies is found to be different with location. The anomalous warming in Indian Ocean in 1984, 1987 and 1997-98 are clearly indicated by these time-longitude plots. Warming tendency of the TIO within this 40 year period is revealed visibly from these time-longitude plots.

References

- Ajaymohan, R. S. and B. N. Goswami, 2000: A common spatial mode for intra-seasonal and inter-annual variation and predictability of the Indian summer monsoon. *Curr. Science*, **79**, 1106-1111.
- Anderson, D. L. T. and P. B. Rowlands, 1976: The Somali Current response to the monsoon: the relative importance of local and remote forcing, *J. Mar. Res.*, **34**, 395-417.
- Barnett, T. P., 1983: Interaction of the Monsoon and Pacific trade wind system at interannual time scales. Part I: The equatorial zone. *Month. Weath. Rev.*, **111**, 756-773.
- Bauer, S., G. L. Hitchcock and D. B. Olson, 1991: Influence of monsoonally-forced Ekman dynamics upon surface-layer depth and plankton biomass distribution in the Arabian Sea, *Deep Sea Res.*, **38**, 531-553.
- Behera, S. K. and T. Yamagata, 2003: Impact of the Indian Ocean dipole on the Southern Oscillation, *J. Met. Soc. Jap.*, **81**, 169-177.
- Blanc. J. L., 1996: The role of the Indian Ocean in the Global Climate System: Interannual hydro-climatic variability and ENSO in the Indian Ocean. *WMO/TD-No.788; WCASP-39*.
- Brandt, P., L. Stommel, F. Schott, J. Fischer, M. Dengler and D. Quadfasel, 2002: Annual Rossby waves in the Arabian sea from TOPEX/POSEIDON altimeter and insitu data, *Deep Sea Res.*, **49**, 1197-1210.
- Cadet, D. L. and B. C. Diehl, 1984: Interannual Variability of Surface Fields over the Indian Ocean during Recent Decades. *Month. Weath. Rev.*, **112**, 1921-1935.
- Chambers, D. P., B. D. Tapley and R. H. Stewart, 1999: Anomalous warming in the Indian Ocean coincident with El Nino. *J. Geophys. Res.*, **104**, 3035-3047.
- Cipollini, P., D. Cromwell, P. G. Challenor and S. Raffaglio, 2001: Rossby waves detected in global ocean colour data. *Geophys. Res. Letters*, **28**, 323-326.
- Colborn, J. G., 1975: Thermal structure of the Indian Ocean, IIOE Monographs No.2, East West Centre Press Honolulu, 173.
- Dai, A and T. M. L. Wigley, 2000: Global patterns of ENSO-induced precipitation, *Geophys. Res. Let.*, **27**, 1283-1286.

- Dai, A., T. M. L. Wigley, B. A. Boville, J. T. Kiehl and D. L. E. Buja, 2001: Climates of the 20th and 21st centuries simulated by the NCAR Climate System Model. *J. Climate*, **14**, 485-519.
- Daubechies, I. 1990: Ten lectures on wavelets, SIAM Press, Philadelphia.
- Deser, C. and M. L. Blackmon, 1993: Surface Climate Variations over the North Atlantic Ocean during Winter : 1900-1989. *J. Climate*, **6**, 1743-1753
- Drosdowsky, W., 1993: Potential predictability of winter rainfall over southern and eastern Australia using Indian Ocean sea surface temperature anomalies. *Aust. Met. Mag.*, **42**, 1-6.
- Düing, W. and F. Schott, 1978: Measurements in the source current of the Somali Current during monsoon reversal. *J. Phys. Oceanogr.*, **8**, 278-289.
- Düing, W. and A. Leetma., 1980: Arabian Sea cooling, a preliminary heat budget. *J. Phys. Oceanogr.*, **10**, 307-312.
- Evans, R. H. and O. B. Brown, 1981: Propagation of thermal fronts in the Somali current system, *Deep Sea Res.*, **28**, 521-527.
- Frankignoul, C. 1985: Sea surface temperature anomalies, planetary waves and air-sea feed back in the middle latitudes. *Rev. Geophys.*, **23**, 357-390
- Fris_Christensen, E. and K. Lassen, 1991: Length of the solar cycle an indication of solar activity closely associated with climate, *Science*, **254**, 698-700.
- Godfrey, J.S., A. G. Alexiou, D. M. Ilahude, M. E. Legler, J. P. McCreary, Jr., G.A. Meyers, K. Mizuno, R. R. Rao, S. R. Shetye, J. H. Toole and S. Wacongne, 1995: The role of the Indian Ocean in the global climate system : Recommendations regarding the global ocean observing system. *Report of the Ocean Observing System Development Panel, Texas A&M University, College Station., TX, USA.* 89.
- Goswamy, B. N. and D. Sengupta, 2003: A Note on the Deficiency of NCEP / NCAR Reanalysis Surface winds over the Equatorial Indian Ocean. *J. Geophys. Res.*, **108**, 3124.
- Graham N. E., W. B. White and A. P. Sierra 1990: Low frequency ocean-atmosphere onteractions in the tropical Pacific, *in Air-Sea Interaction in the Tropical Western Pacific*, C. Jiping and J. Yaung(ed.) China Ocean Press, Beijing, 457-484,

- Gu, D. and S. G. H. Philander, 1995: Secular change of annual and interannual variability in the tropics during the past century, *J. Climate.*, **8**, 864-876.
- Haddad, Z. S. J. P. Meagher, R.F. Adler, E.A. Smith, E. Im and S. L. Durden, 2004: TRMM and the global interannual variability of rain over the past five decades. Combined Preprints CD-ROM, 84th AMS Annual Meeting. Paper P3.8 in 15th Symp. on Global Change and Climate Variations, 11-15 January 2004, Seattle, WA, 11.
- Hastenrath, S. and L. Greisher, 1991: The monsoonal current regimes of the tropical Indian Ocean, observed surface flow fields and their geo-strophic wind-driven components. *J. Geophys. Res.*, **96**, 12619-12633.
- Hastenrath, S. and L. Greisher, 1993: The monsoonal heat-budget of the hydrosphere-atmosphere system in the Indian Ocean sector. *J. Geophys. Res.*, **98**, 6869-6881.
- Haugen, V E., O. M. Johnson and G. Evensen, 2002: Indian Ocean; validation of the Miami Isopycnic coordinate ocean model and ENSO events during 1958-1998, *J. Geophys. Res.*, **107**, 3048
- Hill, K. L., I. S. Robinson and P. Cipollini, 2000, Observations of Rossby wave characteristics from satellite-derived global sea surface temperature, *J. Geophys. Res.*, **105**, 21,927-21,945
- Hsiung, J. and R. E. Nowell, 1983, The Principal non-seasonal modes of variation of Global Sea Surface Temperature, *J. Phys. Oceanogr.*, **13**, 1957-1967
- Jensen, T. G., 1991: Modeling the seasonal undercurrents in the Somali current system. *J. Geophys. Res.*, **96**, 22151-22167.
- Jiwei, T., X. U. Jinshan and W. E. I. Enbo, 2000: The wavelet analysis of satellite sea surface temperature in the South China Sea and the Pacific Ocean. *Chinese Science Bulletin*, **45**, 2187-2192.
- Kalnay, E., M. Kanamitsu, R. Kistler, W. Collins, D. Deaven, L. Gandin, M. Iredell, S. Saha, G. White, J. Woolen, Y. Zhu, M. Chelliah, W. Ebisuzaki, W. Higgins, J. Janowiak, K. C. Mo, C. Ropelewski, J. Wang, A. Leetma, R. Reynolds, R. Jenne and D. Joseph, 1996: The NCEP/NCAR 40-year reanalysis project. *Bullet. Amer. Meteorol. Soc.*, **77**, 437-471
- Kapala, A. K., Born and H. Flohn, 1994: Monsoon anomaly or an El Nino event at the equatorial Indian Ocean?, Casterspheric rains

1961/62 in East Africa and their teleconnections, Proc. Int. Con. On Monsoon variability and prediction, WMO, 119-126.

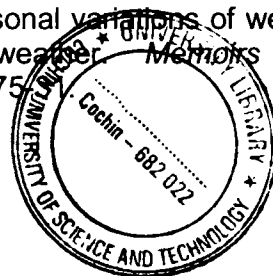
- Kawamura, R. A., 1994: A rotated EOF analysis of the global SST variability with annual inter decadal scale. *J. Phys. Oceanogr.*, **24**, 707-715.
- Kessler, W. S. 1990, Can Reflected Extra-Equatorial Waves Drive ENSO?, *J. Phys. Oceanogr.*, **21**, 444-452
- Killworth, P. D., D. B. Chelton, and R. A. DeSzoek, 1997: The speed of observed and theoretical long extratropical planetary waves. *J. Phys. Oceanogr.*, **27**, 1946–1966.
- Klein S. A. B. J. Soden and N. C. Lau, 1999: Remote sea surface temperature variations during ENSO; Evidence for a tropical atmospheric bridge, *J. Climate*, **12**, 917-932.
- Knox, R. A., 1986: The Indian Ocean: interaction with the monsoon, Monsoons. J. S. Fein and P. L. Stephens, Eds., Wiley – Interscience, 365-398.
- Krishnamurti, T. N., H. S. Bedi and M. Subramaniam, 1989: The Summer Monsoon of 1987, *J. Climate*, **2**, 321–340.
- Lagerloef, G. S. E. and R. L. Bernstein, 1988: Empirical orthogonal function function analysis of AVHRR surface temperature patterns in Santa Barbara Channel. *J. Geophys. Res.*, **93**, 6863-6873.
- Lau, K. M. and S. Shen, 1988: On the dynamics of intra-seasonal oscillations and ENSO. *J. Atmos. Sci.*, **45**, 1781-1797.
- Lau, K. M. and H. Weng, 1995: Climate signal detection using wavelet transform: How to mke a time series sing. *Bull. Amer. Met. Soc.*, **76**, 2391-2402.
- Legates, D. R. and C. J. Willimott, 1990: Mean, seasonal and special variability in gauge corrected global precipitation, *Int. J. Climat.*, **10**, 111-127.
- Legeckis, R., 1987: Observation of a western boundary current in the Bay of Bengal. *J. Geophys. Res.*, **92**, 12 974-12 978.
- Levitus, S., 1984: Annual cycle of temperature and heat storage in the world ocean. *J Phy. Ocean.*, **14**, 727-746.
- Lie, H. J. and M. Endoh, 1991: Seasonal and interannual variability in temperature of the upper layer of the northwest Pacific, 1964–1983. *J. Phys. Oceanogr.*, **21**, 385–397

- Liu, P. C., 1994: Wavelet spectrum analysis and ocean wind waves, wavelets in geophysics. E. Foufoula-Georgiou and P. Kumar., Eds., *Academic Press*, 151-166.
- Liu Z. and B. Huang, 2000: Causes of the warming trend of the tropical Pacific Ocean. *Geophys. Res. Let.*, **27**, 1935-1938.
- Loschnigg, J. and P. J. Webster, 2000: A coupled ocean atmosphere system of SST modulation for the Indian Ocean. *J. Climate*, **13**, 3342-3360.
- Madden, R. A. and P. R. Julian, 1972: Description of global scale circulation in the tropics with a 40-50 day period. *J. Atmos. Sci.*, **43**, 3138-3158.
- Madden, R. A. and P. R. Julian, 1994: Observations of the 40-50 day tropical oscillation - a review. *Month. Weath. Rev.*, **122**, 814-837.
- Mantua, N. J., 2001: The Pacific Decadal Oscillation. *In: Encyclopedia of Global Environmental Change*, John Wiley & Sons, Inc
- Masumoto, Y. and G. Meyers, 1998: Forced Rossby waves in the southern tropical Indian Ocean. *J. Geophys. Res.*, **103**, 27589-27602.
- McCreary, J. P., H. S. Lee and D. B. Enfield, 1989: The response of the coastal ocean to strong offshore winds: with application to circulations in the Gulfs of Tehuantepec and Papagayo. *J. Mar. Res.*, **47**, 81-109.
- McCreary, J. P. and P. K. Kundu, 1989: A numerical investigation of sea surface variability in the Arabian sea, *J. Geophys. Res.*, **94**, 16097 - 16114.
- McCreary, J. P., P. K. Kundu and R. L. Molinari, 1993 : A numerical investigation of dynamics, thermodynamics and mixed-layer processes in the Indian Ocean, *Prog. in Ocean.*, **31,3**, 181-3,244.
- Mc Creary, J. P., W. Han, D. Shankar and S. R. Shetye, 1996 : Dynamics of the east India Coastal Current. 2. Numerical solutions. *J. Geophys. Res.*, **101**, 13 993-14 000.
- Mc Phaden, M. I., 1982; Variability in the central equatorial Indian Ocean, I, *Ocean dynamics, J. Mar. Res.*, **40**, 157-176.
- Mc Phaden, M. I., F. Bahr, Y. du Penhoat, E. Firing, S. P. Hayes, P. P. Niiler, P. L. Richardson and J. M. Toole, 1992: The response of the western equatorial Pacific Ocean to westerly wind burst during

- November 1989 to January 1990, *J. Geophys. Res.*, **97**, 14 289–14 303.
- Meehl, G. A., 1994 : Coupled land-ocean-atmosphere processes and South Asian Monsoon variability. *Science*. Vol. 265, p. 263-267. *J. Geophys. Res.*, **101**. 15 033-15 049.
- Meyers, G., 1996 : Variation of the Indonesian through flow and the El Niño-Southern Oscillation. *J. Geophys. Res.*, **101**, 12 255-12 263.
- Meyers, S. D. and J. J. O'Brien, 1994: Spatial and temporal 26-day SST variations in the equatorial Indian Ocean using wavelet analysis, *Geophys. Res. Lett.*, **21**, 777-780.
- Meyers, S. D., B. G. Kelly and J. J. O'Brien, 1993: An introduction to wavelet analysis in oceanography and meteorology: with application to the dispersion of Yanai waves. *Month. Weath. Rev.*, **121**, 2858-2866.
- Mizoguchi, K I., Meyers, S. D., Basu, S. and J. J. O'brien, 1999: Multi- and quasi-decadal variations of sea surface temperature in the North Atlantic, *J. Phys. Oceanogr.* , **29**, 3133-3144
- Morrow, R., and F. Birol, 1997: Variability in the south-east Indian Ocean from altimetry - forcing mechanisms for the Leeuwin Current. *J. Geophys. Res.*, **103**, 18 529-18 544.
- Murtugudde, R., J. McCreary and A. Busalacchi, 2000: Oceanic processes associated with anomalous events in the Indian Ocean. *J. Geophys. Res.*, **105** , 3295-3306.
- Mysak, L. A. and G. J. Mertz, 1984: A 40 to 60 day oscillation in the source region of the Somali current during 1976. *J. Geophys. Res.*, **89**, 711-715.
- Nicholls, N., 1987: The use of canonical correlation to study teleconnections. *Month. Weath. Rev.*, **115**, 393-399.
- Nitta, T. and S. Yamada, 1989: Recent Warming of tropical sea surface temperature and its relationship to the Northern Hemisphere circulation. *J. Met. Soc. Jap.*, **67**, 375 – 383.
- Palmer, T. N. and D. A. Mansfield, 1984: Response of two atmospheric general circulation models to sea-surface temperature anomalies in the tropical east and west Pacific. *Nature*, **310**, 483-485.
- Parker D. E. and C. K. Folland, 1988, The nature climatic variability, *Met. Mag.* **117**, 201-210.

- Perigaud, C. and P. Delecluse, 1993: Interannual Sea Level Variations in the Tropical Indian Ocean from Geosat and Shallow Water Simulations. *J. Phy. Ocean.* , **23**, 1916–1934.
- Potemara, J. T., M. E. Luther and J. O'Brien, 1991: The seasonal circulation of the upper ocean in the Bay of Bengal. *J. Geophys. Res.* ,**96**, 12 667-12 683.
- Rapelewski, C. F. and M. S. Halpert, 1987, Global and regional scale precipitation patterns associated with El Nino / Southern Oscillation., *Month. Weath. Rev.* **115**, 1606-1627.
- Rapelewski, C. F. and M. S. Halpert, 1989, Precipitation pattern associated with high index phase of the southern oscillation., *J. Cimate*, **2**, 268-284.
- Rao, K. G. and B. N. Goswami, 1988: Interannual Variations of Sea Surface Temperature over the Arabian Sea and the Indian Monsoon. *A New Perspective. Month. Weath. Rev.*, **116**, 558-568.
- Reason, C. J. C. and H. M. Mulenga, 1999: Interannual displacements of convection and surface circulation over the equatorial India Ocean. *Int. J. Climat.*, **19**, 4651-1673.
- Reverdin, G. and J. Luyten, 1986 : Near-surface meanders in the equatorial Indian Ocean. *J. Phys. Oceanogr.*, **16**, 1088-1100.
- Rioul, O. and M. Vetterli. 1991: Wavelets and signal processing. *IEEE Signal processing magazine*, 14-38.
- Rossby, C. G. 1939 (*cross reference*): Relations between variations in the intensity of the zonal circulation of the atmosphere and the displacements of the semi-permanent centers of action, *J. Mar. Res.*, **2**, 38-55.
- Saji N. H., B. N. Goswami, P. N. Vinayachandran, and T. Yamagata, 1999: A dipole mode in the tropical Indian Ocean, *Nature.*, **401**, 360-363.
- Saji, N. H. and T. Yamagata, 2003: Structure of SST and surface wind variability during Indian Ocean Dipole mode events: COADS observations, *J. Climate*, **16**, 2735-2750.
- Schott, F., 1983: Monsoon response of the Somali Current and associated upwelling. *Prog. Ocean.*, **12**, 357-382.
- Schott, F. and H. Stommel, 1978: Beta spirals and absolute velocities in different oceans. *Deep Sea Res.*, **25**, 961-1010

- Schott, F. J., U. Fischer and D. Quadfasel, 1997: Summer monsoon response of the northern Somali current, *Geophys. Res. Lett.*, **24**, 2565 – 2568.
- Setoh, T. and S. Imawaki, 1999: Interdecadal variations of ENSO signals and annual cycles revealed by wavelet analysis. *J. Ocean.*, **55**, 385-394.
- Shankar, D., J. P. McCreary, W. Han and S. R. Shetye, 1996: Dynamics of the East India Coastal Current. 1. Analytic solutions forced by interior Ekman pumping and local alongshore winds. *J. Geophys. Res.*, **101**, 13 975-13 991..
- Shetye, S., A. Gouveia, D. Shankar, S. Shenoi, P. Vinayachandran, D. Sundar, G. Michael, and G. Nampoothiri, 1996: Hydrography and circulation in the western Bay of Bengal during the Northeast monsoon. *J. Geophys. Res.*, **101**, 114011-14025.
- Soman, M. K. and J. Slingo, 1997: Sensitivity of the Asian summer monsoon to aspects of sea surface temperature anomalies in the tropical Pacific Ocean. *Q. J. R. Met. Soc.*, **124**, 1985-2004.
- Sterl, A., 2001: On the impact of gap filling algorithms on variability patterns of reconstructed oceanic surface fields. *Geophys. Res. Lett.* **28**, 2473-2476.
- Torrence, C. and G. P. Compo, 1998: A practical guide to wavelet analysis. *Bull. Amer. Met. Soc.*, **79**, 61-78.
- Tourre, Y. M. and W. B. White, 1995 : ENSO signals in global upper-ocean temperature. *J. Phys. Oceanogr.*, **25**, 1317-1332.
- Tsai, P. T. H., J. O'Brien and M. E. Luther, 1992: The 26-day oscillation observed in the satellite sea surface temperature measurements in the equatorial western Indian Ocean. *J. Geophys. Res.*, **97**, 9605-9618.
- Van Woert, M. L. and J. M. Price, 1993, Geosat and Advanced Very High Resolution Radiometer observations of oceanic planetary waves adjacent to the Hawaiian islands, *J. Geophys. Res.*, **98**, 14619-14631.
- Wacongne. S. and Pacanowski, 1996: Seasonal heat transport in the tropical Indian ocean, *J. Phys. Oceanogr.*, **26**, 2666-2699.
- Walker, G. T., 1923: Correlation in seasonal variations of weather VIII A preliminary study of world weather. *Memoirs of Indian Meteorological Department*, **24**, 75



G9064

- Wang, B. and Y. Wang, 1996: Temporal structure of the southern oscillation as revealed by waveform and wavelet analysis. *J. Climate.*, **9**, 1586-1598.
- Webster, P. J., 1994: The role of hydrological process in ocean atmosphere interactions. *Rev. Geophys.*, **32**, 427-476.
- Webster, P. J. and S. Yang, 1992: Monsoon and ENSO: Selectively interactive systems. *Q. J. R. Met. Soc.*, **118**, 877-926.
- Webster, P. J., A. M. Moore and J. P. Loschnigg, R. R Leben, 1999: Coupled ocean-atmosphere dynamics in the Indian Ocean during 1997-98. *Nature.*, **401**, 356-360.
- Weisberg, R. H. and T. J. Weingartner, 1988: Instability Waves in the equatorial Atlantic Ocean. *J. Phys. Oceanogr.*, **18**, 1641-1657
- Weng, H. and K. M. Lau, 1994: Wavelets, period doubling, and time frequency localisation with application to organisation of convection over tropical western Pacific. *J. Atmos. Sci.*, **51**, 2523-2541.
- White W. B., S. C. Chen and R. Peterson, 1998: The Antarctic Circumpolar Wave: A beta-effect in ocean-atmosphere coupling over the Southern Ocean. *J. Phys. Oceanogr.*, **28**, 2345-2361.
- White, W. B., 2000: Coupled Rossby Waves in the Indian Ocean on Interannual Timescales. *J. Phys. Oceanogr.*, **30**, 2972-2988.
- Xie S. P., H. Annamalai, F. A. Schott and J. P. Mc Creary, 2002: Structure and mechanisms of south Indian ocean climate variability, *J. Climat.*, **15**, 864-874.
- Yasunari, T., 1985: Zonally propagating modes of the global east-west circulation associated with the Southern Oscillation. *J. Met. Soc. of Jap.*, **63**, 1013-1029.
- Yu L. S. and M. M. Rienecker, 1999: Mechanisms for the Indian Ocean warming during the 1997-98 El Nino. *Geophys. Res. Lett.*, **26** 735-738.
- Zhang, Y. I., 1996: An Observational study of atmosphere-ocean interaction in the northern ocean on interannual and inter decadal time-scales. *Ph. D. Dissertation. Univ. of Washington, Seattle, WA.*, 162.

